

**Mechanisms of inhibition and neuronal integration for signal
processing in the primary auditory cortex of the Mongolian
gerbil (*Meriones unguiculatus*)**

Dissertation
der Fakultät für Biologie
der Ludwig-Maximilian-Universität München

vorgelegt von
Elisabeth Foeller

München, im Oktober 2001

1. Gutachter: Prof. Dr. M. Kössl

2. Gutachter: Prof. Dr. G. Neuweiler

eingereicht am: 9.10.01

Tag der mündlichen Prüfung: 27.11.01

Abbreviations	5
1 Summary	6
Zusammenfassung	9
2 Introduction	13
2.1 Functional organization of the auditory cortex	13
2.2 Inhibition in the auditory cortex.....	18
2.3 Comodulation masking release: A psychoacoustic phenomenon which enables animals to detect acoustic signals in background noise	20
2.4 Aims of this study	24
3 Methods	25
3.1 Neurophysiology.....	25
3.1.1 Surgical procedure	25
3.1.2 Microiontophoresis of pharmac.....	26
3.1.3 Neuronal frequency tuning: acoustic stimulation and recording procedures	26
3.1.4 Analysis of tuning curve data.....	28
3.1.5 Comodulation masking release: acoustic stimulation and recording procedures	29
3.1.6 Comodulation masking release: Data analysis.....	32
3.2 Immunocytochemistry.....	34
4 Results	36
4.1 Extent of diffusion of bicuculline in the auditory cortex	36
4.2 General effects of bicuculline	37
4.3 Influence of bicuculline on receptive fields of single and multi units	38
4.4 GABAergic involvement in two-tone masking.....	42
4.5 Influence of bicuculline on the tuning sharpness.....	42
4.6 Effects of bicuculline across different cortical layers	44

Contents

4.6.1 Latency of single units	45
4.6.2 Change of tuning caused by GABA _A blockade.....	46
4.6.3 Paradoxical effects of bicuculline and silent neurons.....	48
4.6.4 Immunocytochemistry	51
4.7 Blockade of GABA_A receptors induces late responses	54
4.8 A neural correlate of comodulation masking release in the auditory cortex of the gerbil.....	58
4.8.1 Responses to unmodulated and comodulated noise	58
4.8.2 Detection thresholds for test tones masked by unmodulated and comodulated noise.....	59
4.8.3 Release from masking in relation to envelope locking	63
4.8.4 Blockade of GABA _A receptors does not influence the amount of masking release.....	65
5 Discussion	68
5.1 Methodological consideration.....	68
5.2 Comparison of pharmacological blocking of GABA with other studies	68
5.3 Effect of pharmacological blocking of GABA compared with two-tone masking in the auditory cortex	70
5.4 Is there a layer-specific strength of inhibition?	71
5.5 Potential functional role of silent neurons in the auditory cortex.....	73
5.6 Late responses	74
5.7 A neural correlate of comodulation masking release	75
5.7.1 Comparison of behavioral and neural masking release	76
5.7.2 Possible neural mechanisms contributing to CMR in the gerbil primary auditory cortex	76
5.8 Outlook and open questions	80
6 References	82
7 Danksagung.....	92
8 Lebenslauf	93

Abbreviations

A1	primary auditory cortex
AAF	anterior auditory field
BIC	(-) bicuculline-methiodide
BF	best frequency
CMR	comodulation masking release
GABA	γ -aminobutyric acid
MGB	medial geniculate body of the thalamus
PSTH	peri-stimulus time histogram

1 Summary

A. A fundamental property of hearing is the decomposition of complex sounds into perceptually distinct frequency components. Each receptor cell in the cochlea and most centrally located neurons respond only to a limited range of frequencies. The individual frequency channels are spatially organized on the cortical surface. This consistent topographical pattern provides a framework for the investigation of other functional organization principles, e.g., the functional properties of neurons in the six cortical layers and the responsiveness of neurons to complex sounds. The frequency specific features of inhibition should play an important role in shaping a neuron's response to complex behaviorally relevant stimuli.

Physiological and immunocytochemical evidence indicates a layer-dependent organization of inhibitory circuits in the neocortex. To investigate the contribution of GABAergic inhibition to frequency tuning in the different cortical layers, single and multi units were recorded in near-radial penetrations before and during iontophoretic application of the GABA_A-receptor antagonist bicuculline in the auditory cortex of the lightly anaesthetized gerbil (*Meriones unguiculatus*). Bicuculline generally increased the spontaneous neuronal activity and enhanced and prolonged onset responses to sound. Application of bicuculline often resulted in a shift of the most sensitive frequency of the neurons' receptive fields and a decrease of threshold (5.5 dB). A broadening of the frequency tuning evident by lower Q_{40dB} values was observed in 63% of the units. In units with several peaks in their tuning curve or clearly separated response areas, bicuculline application removed inhibitory gaps in the receptive fields and created single-peaked tuning curves. The influence of bicuculline on the receptive field size was not significantly layer-specific but tended to be most pronounced in layers V and VI. In layer VI, "silent" neurons were frequently found that responded to sound only when GABAergic inhibition was antagonized. From the analysis of postembedding GABA immunocytochemistry, the proportion of GABAergic neurons was found to be maximal in layers I and V, and the number of GABAergic perisomatic puncta (axon terminals) on cell somata peaked in layer V.

The influence of bicuculline was compared with the effects of two-tone suppression. It was found that in some units, the effects of suppression could be partially mediated by intracortical GABAergic inhibition.

In some units in layers IV, V, and VI, additionally to the initial excitatory activity in response to stimulus onset, a second, long-lasting excitatory response occurred several hundred milliseconds after the stimulus. This late response was not dependent on stimulus duration and could be enhanced or elicited by GABA_A blockade. The fact that several, rhythmically occurring late responses were elicited by the application of bicuculline suggests that recurrent excitatory networks can become entrained by small modifications of inhibition.

B. In the natural environment, acoustic signals like animals' communication sound or human speech is often masked by background noise. Amplitude fluctuations are often superimposed upon environmental sounds on their path of transmission which can lead to a distinct temporal structure of the sound. Furthermore, many natural background sounds are often temporally structured. Vertebrates have evolved mechanisms to exploit amplitude modulations in background noise to improve signal detection. Psychophysical and behavioral experiments have shown that amplitude-modulated background noise (comodulated noise) is less effective as a masker than unmodulated noise bands of the same bandwidth, a phenomenon called comodulation masking release (CMR). This phenomenon has been extensively studied in human psychoacoustics. However, the underlying neural mechanisms are still debated. Animal models in which a direct comparison of the neuronal response and the behaviorally measured performance is possible could increase our understanding of the underlying mechanisms. CMR could be demonstrated behaviorally and neurophysiologically in a songbird, however, models for mammals are still lacking. In behavioral experiments, Kittel et al. (2000) demonstrated CMR in the gerbil. In the present study, using acoustic stimuli that were identical with those of a behavioral experiment, a neural correlate of CMR was described in the auditory cortex of the gerbil and compared with the behavioral data.

In this study of neural mechanisms of masking release in the primary auditory cortex of the anaesthetized gerbil, I determined neural detection thresholds for

1 Summary

200-ms test tones presented in a background of band-pass amplitude modulated (50 Hz) noise maskers of different bandwidth (between 50 and 3200 Hz). Neural release from masking caused by comodulated band-pass noise was evident at the level of the gerbil's primary auditory cortex. On average, the largest masking release (median 6.9 dB) was found for a masker bandwidth of 3200 Hz. This is less than the median masking release of 15.7 dB observed in the behavioral study in the gerbil. For most masker bandwidths, however, a small fraction of the neurons exhibited a masking release that was close to or even larger than the behavioral masking release. The observation that the release from masking increased as a function of the masker bandwidth indicates that spectral components remote from the signal frequency enhance the signal detection. However, there was no correlation between the neurons' filter bandwidths and the amount of masking release. Thus, neuronal masking release in the gerbil primary auditory cortex could be attributed to both signal-masker interactions across different frequency channels and also to mechanisms that act within a single frequency channel. The gerbil appears to be a suitable animal model for additional studies comparing behavioral and physiological performance in the same species. These studies could increase our understanding of the perceptual mechanisms that are useful for the analysis of auditory scenes.

Zusammenfassung

A. Eine grundlegende Aufgabe des Hörsystems besteht darin, den Frequenzgehalt komplexer Geräusche zu analysieren. Jede Sinneszelle in der Hörschnecke (Cochlea) und die meisten Neurone im zentralen Hörsystem antworten nur auf einen bestimmten Frequenzbereich. Diese individuellen Frequenzkanäle sind auf der Kortexoberfläche räumlich geordnet repräsentiert (Topographie). Das topographische Muster des Hörkortex bietet die Möglichkeit, andere funktionelle Organisationsprinzipien des Kortex, wie beispielsweise die funktionellen Eigenschaften von Neuronen in den sechs kortikalen Schichten oder die Antworteigenschaften von Neuronen auf komplexe akustische Reize, zu untersuchen. Frequenzspezifische hemmende neuronale Mechanismen sollten eine entscheidende Rolle bei der Modulation der neuronalen Antworten auf komplexe verhaltensrelevante akustische Reize spielen.

Erkenntnisse aus physiologischen und immunocytochemischen Studien deuten auf eine schichtenspezifische Organisation der inhibitorischen neuronalen Schaltkreise im Neokortex hin. In der vorliegenden Studie wurde der Einfluss von GABA_A-Rezeptor Inhibition auf die Frequenzabstimmung der Neurone in den sechs Kortexschichten untersucht. Dazu wurden im Hörkortex von leicht betäubten Wüstenrennmäusen (*Meriones unguiculatus*) Einzel- und Mehrzelleableitungen in Elektrodenpenetrationen senkrecht zur Kortexoberfläche durchgeführt. Die Antworteigenschaften der Neurone wurden vor und während der iontophoretischen Applikation des GABA_A-Rezeptorantagonists Bicucullin gemessen.

Ein Vergleich der neuronalen Antworteigenschaften vor und während der Blockierung der GABA_A-Rezeptoren zeigte, dass Bicucullin zu einer Erhöhung der spontanen neuronalen Aktivität und zu einer länger andauernden neuronalen Aktivität in Antwort auf den akustischen Reiz führte. Die Blockierung von GABA_A-Rezeptoren resultierte oftmals in einer Verschiebung der besten Frequenz (die Frequenz für die das Neuron am sensitivsten ist) und in einer Abnahme der Schwelle an der besten Frequenz (5.5 dB). Eine Abnahme der

Zusammenfassung

Q_{40dB} -Werte und damit eine Verbreiterung der rezeptiven Felder wurde in 63% der Neurone beobachtet. In Neuronen mit vielgipfligen Abstimmkurven oder mit mehreren separaten Antwortbereichen wurden inhibitorische Bereiche aufgehoben was zu eingipfligen Abstimmkurven führte. In einigen Neuronen konnte exemplarisch die Auswirkung intrakortikaler Inhibition mit den Effekten von Zwei-Ton-Maskierung verglichen werden. Es wurde festgestellt, dass in einzelnen Neuronen intrakortikale GABAerge Inhibition ausreicht, um einen Grossteil der Maskierungseffekte zu erklären.

Ein signifikanter Unterschied im Einfluss der GABA_A-Rezeptorblockierung in Neuronen verschiedener Kortexschichten war nicht festzustellen. Jedoch wurde eine Tendenz zu stärkerem inhibitorischen Einfluss in den tiefen Schichten V und VI beobachtet. In Schicht VI wurden „silent“ Neurone gefunden, die nur unter Blockierung der GABAergen Inhibition auf Reintöne antworteten. Die immunocytochemischen Färbungen zeigten, dass der Prozentsatz der GABAergen Neurone in den Schichten I und V maximal war. Des Weiteren war die Zahl der GABAergen Axonterminalien auf Neurone in der Schicht V am höchsten. Dies deutet darauf hin, dass die kortikalen Ausgangsneurone einer besonderen Kontrolle durch GABAerge inhibitorische Prozesse unterliegen.

In Neuronen in den Schichten IV, V, und VI wurde zusätzlich zu der exzitatorischen Antwort auf den Beginn des akustischen Reizes eine zweite exzitatorische, langandauernde Antwort beobachtet, die mehrere Hundert Millisekunden nach dem akustischen Reiz auftrat. Diese späte Antwort war unabhängig von der Reizdauer und konnte durch eine Blockierung der GABA_A-Rezeptoren verstärkt oder sogar ausgelöst werden. Mittels GABA_A-Rezeptorblockierung konnten auch rhythmisch auftretende späte Antworten induziert werden. Dies deutet an, dass geringe Veränderungen in der neuronalen Inhibition exzitatorische neuronale Netzwerkschleifen anregen können.

B. Im zweiten Teil dieser Arbeit wird ein neuronales Korrelat eines psychoakustischen Phänomens im Hörkortex der Wüstenrennmaus beschrieben. Die Wahrnehmung von akustischen Signalen in der Umwelt erfolgt immer vor dem Hintergrund von Störgeräuschen. Akustisch relevante Signale wie z.B. Kommunikationslaute von Tieren oder die menschliche Sprache werden meist von Hintergrundgeräuschen maskiert. Aufgrund von

atmosphärischen Turbulenzen werden natürlichen Geräuschen auf ihrem Übertragungsweg oft Amplitudenmodulationen aufgeprägt. Außerdem sind viele natürliche Hintergrundgeräusche zeitlich strukturiert, z.B. ein Vogelchor in der Dämmerung oder das Stimmengewirr von Menschen in einem Restaurant. Das Hörsystem der Vertebraten hat Mechanismen entwickelt, die zu einer Verbesserung der Signaldetektion in störenden Hintergrundgeräuschen führen.

Psychoakustische Experimente am Menschen und Verhaltensversuche mit Tieren konnten zeigen, dass amplitudenmodulierte Hintergrundgeräusche ein Signal weniger effektiv maskieren als ein unmoduliertes Hintergrundgeräusch derselben spektralen Bandbreite. Dieses Phänomen wird als „comodulation masking release“ (CMR) bezeichnet. Ins Deutsche übertragen bedeutet dieser Begriff soviel wie „verminderte Maskierung durch kohärente Modulation“. In psychoakustischen Untersuchungen beim Menschen ist CMR detailliert untersucht, die zugrundeliegenden neuronalen Mechanismen werden jedoch noch kontrovers diskutiert. Zu einem besseren Verständnis der beteiligten Mechanismen können Tiermodelle beitragen, bei denen ein direkter Vergleich der neuronalen Antworten von Tieren mit der im Verhalten gemessenen Leistung derselben Spezies möglich ist. Auf Verhaltensebene und neuronal konnte CMR bisher beim Vogel Star nachgewiesen werden, für Säugetiere fehlen jedoch bisher Modelle. In einer Verhaltensstudie konnten Kittel et al. (2000) CMR bei der Wüstenrennmaus nachweisen. In der vorliegenden Arbeit wurden zu den Verhaltensversuchen identische akustische Reize verwendet, um ein neuronales Korrelat von CMR im Hörkortex der Wüstenrennmaus zu beschreiben und mit den Verhaltensdaten zu vergleichen.

Hierzu wurden Testsignale (Reintöne der Dauer 200 ms) in Bandpass-Rauschen (Bandbreiten zwischen 50 und 3200 Hz) geboten. Das Bandpass-Rauschen war entweder unmoduliert oder mit einem Tiefpass-Rauschen (0-50 Hz) amplitudenmoduliert (comoduliertes Rauschen). Neuronale Wahrnehmungsschwellen der Testsignale wurden in unmoduliertem und comoduliertem Rauschen bestimmt. Eine Abnahme der Signalmaskierung durch das comodulierte Rauschen konnte auf der Ebene des Hörkortex gezeigt werden. Das größte CMR wurde für eine Rauschbandbreite von 3200 Hz gefunden (Medianwert 6.9 dB). Dies ist zwar geringer als der in den Verhaltensversuchen

Zusammenfassung

gefundene Medianwert von 15.7 dB, für die meisten Maskierbandbreiten zeigte jedoch ein Teil der Neurone ein dem Verhalten vergleichbares oder sogar größeres CMR. Das neuronale CMR war umso ausgeprägter je größer die Bandbreite des maskierenden Rauschens war. Dies zeigt, dass spektrale Komponenten außerhalb des Signalfilters die Signalentdeckung verstärken. Eine Korrelation zwischen der Filterbandbreite der Neurone und dem Ausmaß des CMR konnte jedoch nicht festgestellt werden. Ein Vergleich des CMR vor und während der Blockierung der GABAergen Inhibition ergab keine signifikanten Unterschiede. Aus diesen Ergebnissen kann gefolgert werden, dass das neuronale CMR im Hörkortex der Wüstenrennmaus sowohl durch Verrechnungen zwischen mehreren auditorischen Filtern als auch durch Signal-Maskierer-Interaktionen innerhalb eines Filters bedingt wird. Mit dem Nachweis des neuronalen CMR wurde die Wüstenrennmaus als geeigneter Modellorganismus für weiterführende Studien etabliert, in denen die Verhaltensleistung mit der neuronalen Leistung in derselben Spezies untersucht werden kann. Diese Studien könnten zum genaueren Verständnis der Wahrnehmungsmechanismen bei der Analyse von auditorischen Bildern dienen.

2 Introduction

2.1 Functional organization of the auditory cortex

The auditory system, composed of the ear and the auditory pathways of the brain, enables us to recognize the frequency composition of a sound and to detect the sound source. Recognition of a sound pattern is based on the analysis of spectral, temporal and intensity information. The auditory sensory epithelium, the cochlea, reveals a tonotopic organization such that high frequencies are represented at the cochlear base and low frequencies are represented at the apex. In every mammalian species investigated to date, the topography of the cochlea is maintained in its representation within the primary auditory cortex (for review: Clarey et al. 1992). While the principal processing of sound is performed in the cochlea, higher tasks in sound analysis require integration of neuronal information by both excitatory and inhibitory mechanisms which takes place along the auditory pathway. For example, the ability to localize sound requires binaural neuronal interaction in the auditory brainstem. For the perception and the processing of complex acoustic signals like speech a correct functioning of the auditory cortex is indispensable.

In mammals, the auditory cortex is composed of several fields that can be distinguished by their cytoarchitecture, their neuronal connections and by the physiological characteristics of their neurons (for review: Winer 1992). In the last years, the Mongolian gerbil (*Meriones unguiculatus*) has become a valuable laboratory animal for acoustic research particularly because of its high sensitivity to low frequencies (Ryan 1976; Faulstich and Kössl 2000), similar to that of humans, and the easily accessible cochlea and central auditory structures. In addition, this rodent is robust and easy to breed. Recently, the topographic organization and the neuronal connections of the auditory cortex of the gerbil were intensively studied (Scheich et al. 1993; Thomas et al. 1993; Budinger et al. 2000a,b; Budinger and Scheich 2001). In the gerbil, the auditory cortex is composed of at least 7 auditory fields (Fig. 1). At least four of those fields are tonotopically organized. In the largest field, namely the primary

2 Introduction

auditory field (A1) with its dorsal subfield, high frequencies are located rostrally and low frequencies are represented caudally. Rostral to A1, the anterior auditory field (AAF) shows a mirror-imaged tonotopic organization. Neurons located in these core fields are characterized by their narrow frequency tuning and short latencies in response to pure tone signals. At the caudal end of A1, two tonotopically organized fields, namely the dorsoposterior and the ventroposterior field, have low-frequency borders with A1 and with each other. Neurons located in fields surrounding A1 and AAF are usually more broadly tuned and their response to sound exhibits prolonged latencies.

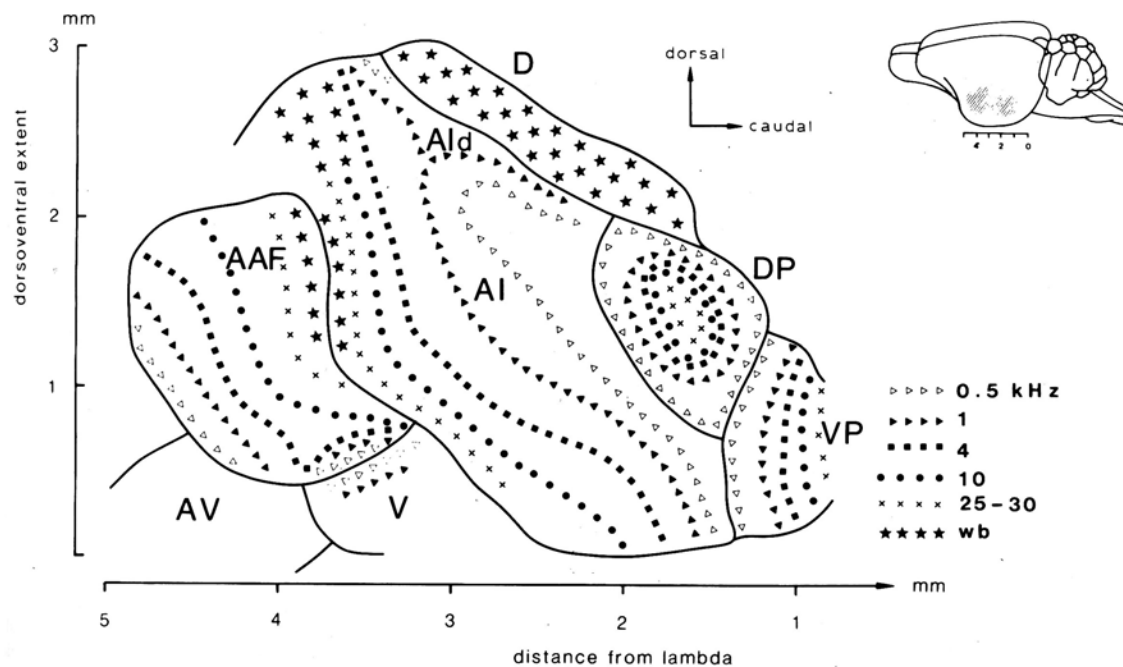


Figure 1 Electrophysiological map of the auditory cortex of the Mongolian gerbil showing the frequency representation within the fields A1 (primary auditory field with its dorsal subfield A1d), AAF (anterior auditory field), DP (dorsoposterior field), VP (ventroposterior field), AV (anteroventral field), V (ventral field), VM (ventromedial field), and D (dorsal field). Note the tonotopic organization of A1: low frequencies are represented caudally and high frequencies are located rostrally. wb, wideband. (From Thomas et al. 1993).

Neurons along a path perpendicular to the cortical surface often share similar response characteristics and these properties vary systematically across the cortical surface. Columnar organization is a common feature of cortical architecture (Mountcastle 1997). In the visual cortex, systems of columns are well documented for ocular dominance, orientation selectivity, and spatial frequency. In the auditory cortex, there is ample information about topographic

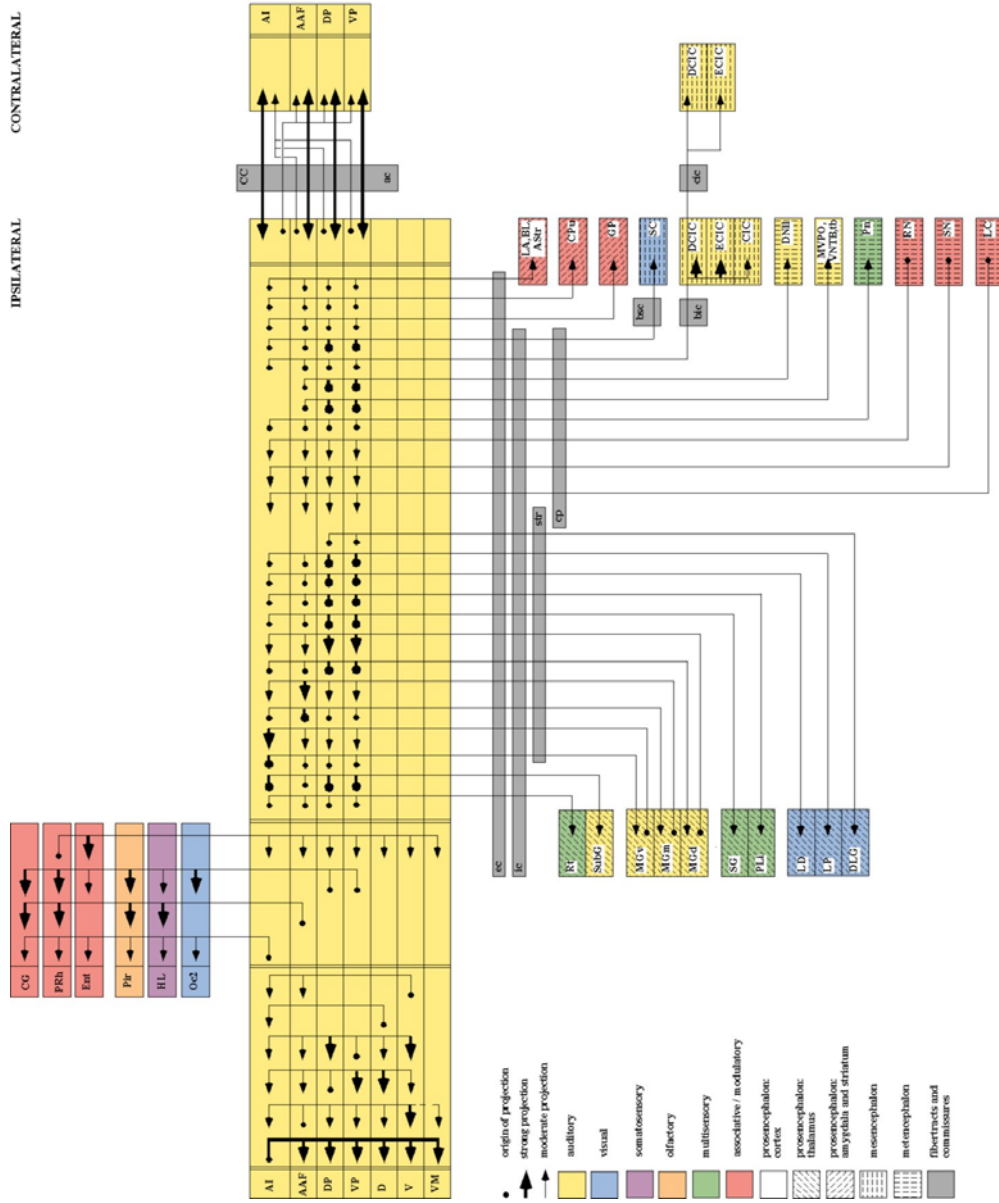
organization in the form of tonotopic frequency gradients (e.g., cat: Merzenich et al. 1975; mustached bat: Suga and Jen 1976; owl monkey: Imig et al. 1977; albino rat: Sally and Kelly 1988; gerbil: Thomas et al. 1993) or binaural maps (e.g., Imig and Adrian 1977; Phillips and Irvine 1983). Figure 2 gives an illustration of the extensive connectivity of A1 and shows that the auditory cortex is characterized by the presence of multiple local and long-range connections. Most of them are organized in recurrent feedback loops. The main input in the auditory cortex is provided by the excitatory input from the medial geniculate body of the thalamus (MGB), mainly from its ventral division, to the primary auditory cortex A1. AAF receives a parallel afferent pathway from the medial MGB.

The neocortex consists of six layers that can be individually identified because of their specific neuronal cell types and their specific corticocortical and subcortical connections. Local cortical circuits, corticocortical connections and descending connections to subcortical structures are all layer-specific. Signals from the MGB target on layer IV stellate cells, then propagate to the superficial layers I, II, and III, and finally to the deeper layers V and VI (e.g., Barth and Di 1990). Large pyramidal cells in layer V mainly provide the descending output to e.g., the MGB, inferior colliculus and to nuclei of other sensory modalities. Layer VI pyramidal cells mainly project to the contralateral auditory cortex. Both the thalamocortical afferents and the corticocortical projection neurons are excitatory. Hence, modulation of cortical information processing by inhibitory mechanism is exclusively mediated by local inhibitory interneurons. One might hypothesize that neurons in all six layers at a certain rostrocaudal location (i.e., within one cortical column) in the gerbil auditory cortex would show similar responses to sound. To investigate basic responses of acoustic neurons to sound, pure tones at different frequencies and intensities are presented. From the neuron's activity in response to these stimuli, a receptive field (tuning curve) can be computed that gives a measure of the frequency tuning of the neuron. The smaller the tuning curve bandwidth, the higher the tuning sharpness. The peak of the tuning curve is the frequency which a neuron is most sensitive to, i.e., to which it responds at lowest tone intensities (best frequency, BF). Indeed, neurons recorded during perpendicular penetrations and, hence, within a single

2 Introduction

column, exhibit similar best frequencies (Oonishi and Katsuki 1965; Abeles and Goldstein 1970; Sugimoto et al. 1997; Shen et al. 1999). However, there is still discrepancy regarding the functional organization of tuning sharpness within a single column. On the level of single neuron recordings, Oonishi and Katsuki (1965) reported that, with increasing cortical depth, the sharpness of tuning curves of cat auditory cortex neurons within a single column increased. They suggested an integrative mechanism from deeper layers to the superficial layers such that the frequency information of several neurons in deeper layers is projected to superficial layers and combined in the response area of a single neuron in these layers. In contrast, Volkov and Galazjuk (1991) found that tuning sharpness decreased with cortical depth. Furthermore, no statistically significant evidence for a layer-dependent sharpness of tuning was observed by Abeles and Goldstein (1970). No change of tuning with recording depth was reported for the mouse auditory cortex (Shen et al. 1999). Sugimoto et al. (1997) found increased tuning sharpness in layers III and IV of the gerbil primary auditory cortex and concluded that the laminar differences of the receptive field size were mainly determined by the highly specific afferent input in A1. A possible explanation for these divergent results may be found in the fact that receptive field size is determined by intracortical inhibition, which could vary considerably depending on the stimulation procedure and anaesthesia.

Figure 2 Diagram of corticocortical and subcortical connections of the Mongolian gerbil's auditory cortex. Connections were established by the anterograde and retrograde transport of biocytin. Additional connections probably exist (personal communication, E. Budinger). AAF, anterior auditory field; ac, anterior commissure; A1, primary auditory field; AStr, amygdalostratial transition area; bic, brachium of the inferior colliculus; BL, basolateral amygdaloid nucleus; bsc, brachium of the superior colliculus; CC, corpus callosum; CG, cingulate cortex; cic, commissure of the inferior colliculus; CIC, central nucleus of the inferior colliculus; cp, cerebral peduncle; CPu, caudate putamen; D, dorsal auditory field; DCIC, dorsal cortex of the inferior colliculus; DLG, dorsal lateral geniculate nucleus; DNLL, dorsal nucleus of the lateral lemniscus; DP, dorsoposterior auditory field; ec, external capsule; ECIC, external cortex of the inferior colliculus; Ent, entorhinal cortex; GP, globus pallidus; HL, hindlimb area of somatosensory cortex; ic, internal capsule; LA, lateral amygdaloid nucleus; LC, locus ceruleus; LD, laterodorsal thalamic nucleus; LP, lateral posterior thalamic nucleus; MGd, medial geniculate body, dorsal division; MGm, medial geniculate body, medial division; MGv, medial geniculate body, ventral division; MVPO, medioventral periolivary nucleus; Oc, occipital cortex (Oc2: secondary visual areas); Pir, piriform cortex; PLi, posterior limitans thalamic nucleus; Pn, pontine nuclei; PRh, perirhinal cortex; RN, raphe nucleus; Rt, reticular thalamic nucleus; SC, superior colliculus; SG, supragenulate nucleus; SN, substantia nigra; str, superior thalamic radiation; SubG, subgenulate nucleus; tb, trapezoid body; V, ventral auditory field; VM, ventromedial auditory field; VNTB, ventral nucleus of the trapezoid body; VP, ventroposterior auditory field. (Figure kindly provided by E. Budinger, see also: Proceedings of the 4th meeting of the German Neuroscience Society 2001).



2 Introduction

Layer-dependent differences in tuning sharpness could be a consequence of either specific thalamocortical input or of layer-specific intracortical inhibition. Laminar differences in the geometry of dendritic trees (e.g., Mitani et al. 1985) and neuronal connections (e.g., Prieto et al. 1994a,b) might indicate a possible difference in the integration of excitatory and inhibitory inputs in specific layers.

2.2 Inhibition in the auditory cortex

Neurons containing γ -aminobutyric acid (GABA, structural formula: $^-OOC-CH_2-CH_2-CH_2-NH_3^+$, Fig. 3) and GABA receptors are conspicuous elements of cortical organization (review for the auditory cortex: Winer 1992). GABA is synthesized from glutamic acid in a reaction catalyzed by the enzyme, L-glutamic acid decarboxylase, and broken down to succinate by the mitochondrial enzyme GABA transaminase. Released GABA binds to several receptor types. The binding induces either a direct opening of ion channels or

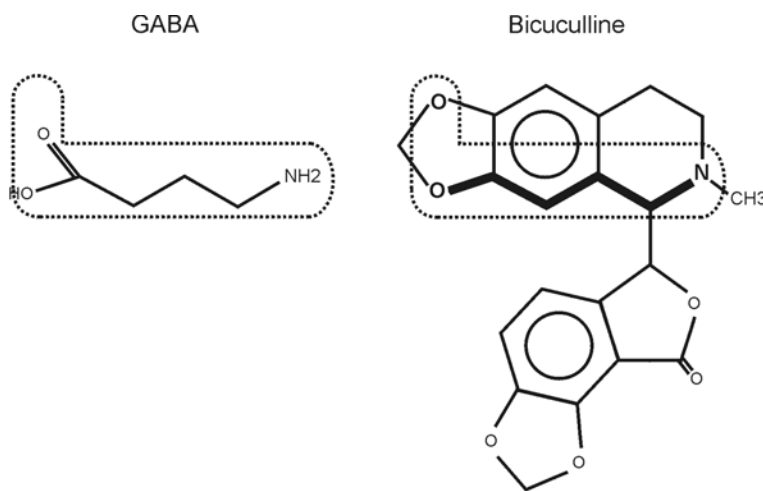


Figure 3 The molecular structure of the inhibitory transmitter GABA and the GABA_A-receptor antagonist bicuculline. Note that bicuculline contains a GABA-like moiety (area marked by the dashed line).

metabolic mechanisms which involve the formation of second messengers. The function of the ionotropic GABA_A receptor channel in the adult vertebrate central nervous system is to mediate fast inhibitory synaptic transmission. The binding of two GABA molecules results in a rapid and transient increase in permeability to chloride ions and hence, a hyperpolarisation of the neuron. The convulsant alkaloid bicuculline (BIC), extracted from *Corydalis* species, blocks the hyperpolarizing effect of GABA. The molecular structure shows that GABA is isosteric with a GABA-like moiety in the BIC molecule, suggesting a competitive interaction of

GABA and BIC on the GABA_A receptor (Fig. 3). BIC is selective for the GABA_A receptor and therefore serves as a good tool to identify GABA_A responses. GABA also acts via receptors coupled to G-proteins called GABA_B receptors and via ionotropic GABA_C receptors.

In immunocytochemical studies of the cat auditory cortex, GABAergic neurons and axon terminals were identified and localized (Prieto et al. 1994a,b) and a layer-specific distribution of the percentage of GABA-immunopositive cells and axon terminals was observed. GABAergic neurons serve to regulate overall cortical excitability and neuronal population synchronization (e.g., Avoli et al. 1994; Tamás et al. 2000) and are involved in shaping neuronal receptive fields and response profiles. For example, GABAergic inhibition controls the orientation selectivity of neurons in the visual cortex (e.g., Sillito 1984; Crook et al. 1998), and the receptive field size of neurons in the somatosensory cortex (cat: Dykes et al. 1984; rat: Kyriazi et al. 1996; raccoon: Tremere et al. 2001).

Several studies investigated the influence of inhibition in the auditory cortex using forward or simultaneous masking (e.g., Shamma et al. 1993; Calford and Semple 1995; Brosch and Schreiner 1997; Sutter et al. 1999). In these experiments, the suppressive influence of masker tones of different frequencies on a fixed probe tone at a given frequency within the cells' excitatory response area was measured. The masker was presented either at the same time (simultaneous) or prior to (forward) the probe tone. The origin of the inhibition seen in these masking studies was unclear since the investigated cortical neuron received excitatory afferents whose response characteristics were already shaped by excitation and inhibition in lower stages of the auditory pathway. In addition, mechanical suppression in the cochlea could contribute to the masking effects measured at the cortical level.

Several studies have looked directly at the effects of GABA inhibition on the response features of auditory cortical cells to complex auditory stimuli. In the bird auditory cortex, GABA-mediated inhibition increases neuronal selectivity to natural sounds and sharpens frequency tuning (Müller and Scheich 1987, 1988). Horikawa et al. (1996) showed that optically recorded excitatory bands are surrounded by GABA-mediated inhibitory areas in the guinea-pig auditory cortex. Recently, Wang et al. (2000) demonstrated that removal of GABA-

mediated inhibition results in lower threshold, an increase in neuronal discharge activity, and a broadening of excitatory receptive fields in the chinchilla A1. In the gerbil, there are massive effects of GABA_A antagonists on overall neuronal activity in the auditory cortex as viewed by deoxyglucose mapping (Richter et al. 1999). Schulze and Langner (1999) investigated the influence of blocking GABA-mediated inhibition on the response of A1 neurons in the gerbil and concluded that GABA sharpens neuronal amplitude-modulation tuning.

2.3 Comodulation masking release: A psychoacoustic phenomenon which enables animals to detect acoustic signals in background noise

Because background noise is ubiquitous in humans' and animals' natural environment, its masking effects on acoustic signals, e.g. speech, frequently limits their communication. Background noise often exhibits temporal patterns (Richards and Wiley 1980; Langemann and Klump 1994; Nelken et al. 1999). Environmental sounds transmitted over a distance show considerable fluctuations in amplitude that are correlated in different spectral ranges. Furthermore, many natural sound sources generate temporally structured signals, e.g., birds singing in a dawn chorus or a group of humans chatting (Klump and Nieder 2001). Animals have evolved mechanisms to make use of fluctuations in background noise. For example, there is evidence that speech perception is improved in fluctuating background noise (e.g., Fastl 1993; Festen 1993). In psychoacoustical studies, these mechanisms were investigated in experiments that presented signals in amplitude-modulated maskers. The absolute signal amplitude is one important factor that determines the detection of the signal. However, the level and the spectral and temporal characteristics of the background noise are other major components of the detectability of acoustic signals. Psychophysical and behavioral experiments have shown that amplitude-modulated background noise is less effective as a masker than unmodulated noise bands of the same bandwidth, a phenomenon called "comodulation masking release" (CMR) (Hall et al. 1984; Moore 1992).

Simplified, the cochlea can be viewed as an alignment of band-pass filters which is preserved throughout the auditory system. In psychoacoustics, these filters are called auditory filters (Fletcher 1940). In Fletcher's (1940) model, the information of a particular filter tuned to the frequency of the signal is used for its detection. For the detection of a pure tone, only the signal to noise ratio within the filter band of the respective auditory filter is essential. Masker energy outside the filter centered on the signal frequency does not influence the detectability of the signal. For CMR, it has been proposed that the auditory system not only relies on the output of a single auditory filter but additionally makes use of the coherent amplitude modulations of the masker by analyzing the envelope patterns of several auditory filters (see below).

The classical paradigm for demonstrating CMR was pioneered by Hall et al. (1984). They used two types of maskers; one was a band-limited random noise, which had irregular fluctuations in amplitude and the fluctuations were independent in different frequency regions. The other was a band-limited random noise which was modulated in amplitude by a noise which was low-pass filtered at 50 Hz. This modulation resulted in fluctuations in the amplitude of the noise which were correlated in different frequency regions. In other words, the magnitudes of all frequencies change coherently. This across-frequency coherence was called "comodulation" by Hall et al. (1984). In the psychoacoustic experiment, Hall et al. (1984) found, that the detection threshold of a masked pure tone signal at 1 kHz was dependent on the type and the bandwidth of the masker. For the random noise, the signal detection threshold increased with increasing masker bandwidth up to about a bandwidth of 100-200 Hz (which corresponds to the bandwidth of one auditory filter) and then remained stable. For the modulated maskers, signal detection threshold also increased up to a bandwidth of about 100-200 Hz. Interestingly, for bandwidths greater than 100-200 Hz (which corresponds to more than one auditory filter) the signal detection threshold decreased as the masker bandwidth increased. The fact that the decrease in the signal detection threshold with increasing bandwidth only occurred when the masker was modulated suggests that fluctuations in the masker were critical, and that the fluctuations had to be correlated across frequency bands.

2 Introduction

There are two types of models how comodulated noise improves the ability to detect a signal in noise. One hypothesis is that across-frequency cues are required for the detectability of the signal. The signal is presented in one auditory filter and the masker is covering several auditory filters including the signal filter. The amplitude fluctuations of the coherently modulated masker create the same time pattern in all auditory filters involved. This results in a coherent output of these filters. Adding the signal, the time pattern of that auditory filter which is tuned to the signal frequency changes and the envelope at the signal frequency is different from the envelope at the flanking frequencies. The detection of the signal could be based on a comparison of the output of the signal frequency channel and the flanking channels. This mechanism was described by Buus (1985) and is similar to a model proposed by Durlach (1963) describing the improvement of signal detection when the signal and the masker are spatially separated (“equalization-cancellation”). The auditory system could first calculate and normalize the envelope amplitudes of all involved auditory filters (“equalization”) and then, subtract the envelope present in remote frequency channels from the signal channel (“cancellation”). Because of the coherent envelope fluctuations in the auditory channels, the filter which shows a changed envelope by adding the signal should be detectable. In addition, Buus (1985) proposed that coherent fluctuations of the masker envelope are used by frequency channels remote from the signal channel to inform the auditory system about periods of maximal signal detection. This is the case for minima in the envelope amplitude, therefore, selective listening at periods of minimum masker amplitude could maximize signal detection (“dip-listening model”).

Another model proposes within-channel cues: The temporal pattern of envelope fluctuations could be extracted within a single analysis channel of the auditory system (within-channel cues; Schooneveldt and Moore 1987, 1989). In this case, the signal would “fill” the amplitude minima of the masking noise, and the temporal pattern of amplitudes would change. The extraction of changes in the time pattern of the amplitude fluctuations could result in an improvement of the signal detectability within a single auditory filter.

CMR has been extensively investigated in humans (for review: Moore 1992), but the neural mechanisms underlying CMR are still debated and only a few studies have presented evidence of neural masking release in the auditory system of mammals (Mott et al. 1990; Henderson et al. 1999; Nelken et al. 1999; Pressnitzer et al. 2001). Until now, no model has been generally accepted. Recently, Pressnitzer et al. (2001) described physiological release from masking in the cochlear nucleus of the guinea-pig and proposed a neural circuit for CMR within the cochlear nucleus. A narrowband neuron that is sharply tuned to its best frequency and a wideband inhibitory neuron that integrates over a wide range of frequencies receive excitatory input from auditory nerve fibers. In addition, the narrowband neuron receives inhibitory input from the wideband neuron. The wideband neuron responds mainly to the modulation of the masker. Because of the inhibitory input from the wideband neuron, the narrowband neuron's response to the modulated masker is reduced, and, thus, signal detection is improved in the comodulated condition.

Nelken et al. (1999) used masking noise bands that were modulated with a 10 Hz sinusoidal. They observed that 63% of the neurons in the cat A1 modulated their firing rates coherently with the temporal envelope, i.e., peaks in the neurons' firing rate were found at an interval of 100 ms. This phenomenon is called "envelope locking". Adding the signal, the neurons' ability to follow the modulation was impaired. The amount of deterioration of envelope locking was dependent on the masker bandwidth and, hence, neurons were suggested to represent a neural correlate of comodulation masking release. However, until now, in the laboratory mammals used in these neurophysiological studies, a behavioural CMR has not been investigated.

In recent studies, CMR was demonstrated for the starling in behavioral and neurophysiological experiments (Klump and Langemann 1995; Klump et al. 1997; Klump and Nieder 2001; Langemann and Klump 2001; Nieder and Klump 2001). The authors suggest that rather than across-channel cues, the temporal patterns of masking are the major constituent of CMR. The auditory system of songbirds is more suited than that of mammals to encode temporal patterns of acoustic signals. Therefore, it seemed interesting to study the neuronal mechanisms underlying CMR in a laboratory mammal. In a behavioral study,

2 Introduction

Kittel et al. (2000) demonstrated CMR in the gerbil. The results were similar to human psychoacoustic data, thus providing an excellent animal model for studying the physiological correlate of CMR. Using the same stimulus paradigms as in the behavioral experiments, the present study demonstrates a physiological correlate of CMR in the primary auditory cortex of the gerbil. This is the first study which allows the direct comparison of neurophysiological CMR on the basis of single unit analysis to the behavioral CMR in the same mammalian species.

2.4 Aims of this study

The aim of the first part of this study was to examine the functional role of intracortical inhibition in frequency tuning of single and multi units in the gerbil primary auditory cortex by iontophoretic application of the GABA_A-receptor antagonist bicuculline and to investigate a possible layer-specific effect of inhibition on the frequency tuning. In the second part of this study, I searched for a neuronal correlate of comodulation masking release in the gerbil primary auditory cortex and investigated the functional role of inhibition on masking effects.

3 Methods

3.1 Neurophysiology

3.1.1 Surgical procedure

Experiments were performed on adult gerbils (*Meriones unguiculatus*) of both sexes (body weight between 50 and 90 g). For initial surgery, animals were anaesthetized with an intramuscular injection of a 10:1 mixture of ketamine (130 mg/kg) and xylazine (Rompun 2%, Bayer). During the experiments, light anaesthesia was maintained by a continuous infusion of the anaesthetic administered subcutaneously by a Harvard Apparatus Infusion Syringe Pump 22 (20-40 mg/kg/per hour). Light anaesthesia was monitored using the pedal-withdrawal reflex in regular intervals and observation of breathing patterns. The body temperature of the animals was maintained at 37°C by a heating pad. Recording sessions lasted up to 20 hours. After the experiments were completed, the animals were killed with an overdose of pentobarbital sodium. All experiments were conducted in a sound-shielded chamber.

The animal's head was fixed by a metal bar cemented on the skull with dental cement. The temporal muscle on the left hemisphere (right hemisphere in 4 animals) was retracted and the lateral cortex was exposed by a craniotomy. The overlying dura was incised and retracted, and the cortex was covered with either paraffin oil or physiological saline solution throughout the experiment. In each experiment, the location of the primary auditory cortex was determined by the position of the cortical vasculature (Thomas et al. 1993; Sugimoto et al. 1997) and by recordings of multi units or local field potentials at slightly different rostrocaudal positions and comparing the measured frequency gradient with a frequency map of the gerbil A1 (Thomas et al. 1993).

3.1.2 Microiontophoresis of pharmaca

"Piggyback" multibarrel electrodes (Havey and Caspary 1980) were used for recording and iontophoretic drug application. The tip of a 4-barrel glasspipette was broken to a total diameter of 8-15 μm . A single-barrel recording electrode was glued onto the multibarrel pipette such that its tip protruded about 5-15 μm beyond the tip of the multibarrel. One barrel of the multibarrel electrode was used for balancing currents and was filled with 1 M NaCl. The other 3 barrels were filled with the GABA_A-receptor antagonist bicuculline-methiodide (5 mM, pH 3, Sigma), GABA (0.5 M, pH 3.5, Sigma) or glutamate (1 M, pH 8, Sigma). A microiontophoresis system (S7061A, WPI) was used to generate and monitor ejection currents (BIC, GABA: 2 to 60 nA; glutamate: -5 to -10 nA) and retention currents (BIC, GABA: -8 to -15 nA, glutamate: 10 to 15 nA). The recording electrode was filled with 3 M KCl (resistance *in situ*: 3-10 M Ω). Using a piezo-microdrive, the piggyback electrode was lowered in a direction perpendicular to the cortical surface to record multi and single units in cortical layers I to VI. During near-radial penetrations, the recorded units could be assigned to cortical layers by means of cortical depth. The extents of the six auditory cortex layers were analyzed in two brains stained for Richardson blue and Nissl and were found to be comparable to data from Sugimoto et al. (1997): Layer I: 0-120 μm ; layer II: 120-210 μm ; layer III: 210-410 μm ; layer IV: 410-560 μm ; layer V: 560-850 μm ; layer VI: 850-1300 μm .

3.1.3 Neuronal frequency tuning: acoustic stimulation and recording procedures

For these experiments, 21 gerbils were used. The electrical signal from the recording electrode was amplified, band-pass filtered (0.3-3 kHz; Stanford SR650), and fed into a window discriminator (custom-made) which produced digital signals that were fed into a digital input of a Data Translation DT 2820 board (Fig. 4). Pure tone stimuli (50-100 ms duration, 4 ms rise/fall time) were generated by a synthesizer (HP 8904 A), gated with the D/A output signal of the Data Translation board, and fed through an attenuator (Jim Hartley, custom-made) into the calibrated loudspeaker (1/2" B&K 4133 microphone capsule). A

tube fixed on the speaker was tightly sealed into the auditory meatus. To obtain frequency response areas, pure tones of various frequencies and intensities (duration: 80-100 ms) were randomly presented with interpulse intervals of 400-500 ms. Each frequency-intensity combination was presented 10 times and corresponding neuronal responses were averaged. Twenty-four or 32 logarithmically spaced frequencies spanned 3-8 octaves centered on the approximate best frequency. Usually a 5-octave range was used which provided a 0.2-0.16-octave resolution between frequencies. Sound pressure levels covered a total range of 80 dB.

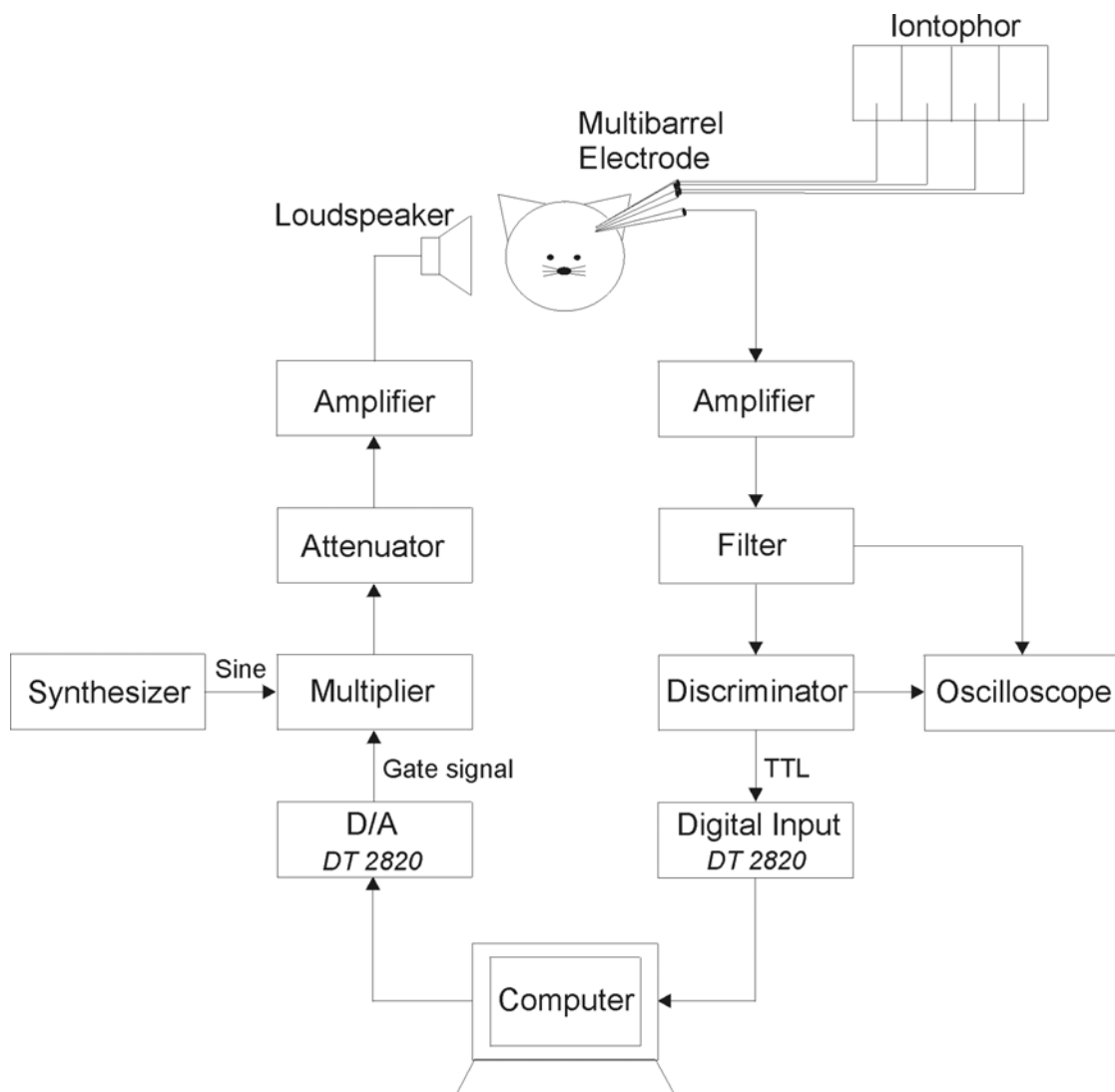


Figure 4 Schematic of the setup used in tuning curve experiments.

3.1.4 Analysis of tuning curve data

From the neuronal response obtained at the different frequency-intensity combinations, a software routine interpolated the positions of equal responses and calculated the receptive field of the neuron or the frequency tuning curve. In addition, the BF, the threshold at BF, and the $Q_{10\text{dB}}$ and $Q_{40\text{dB}}$ values (the best frequency of a neuron divided by the bandwidth of the tuning curve 10 dB or 40 dB above threshold) were calculated. To obtain comparable tuning curves under control and drug condition, a method similar to that of Sutter and Schreiner (1991) and Sutter et al. (1999) was used. The maximum driven spike rate and the spontaneous activity were included in the threshold criterion used for defining tuning curves because bicuculline usually increased both activity components. The response threshold was defined as 20% maximal stimulus-evoked onset discharge rate plus the spontaneous activity calculated in an equally long time window. The onset discharge rate was used because in the majority of the cells, the onset discharge was followed by an inhibitory period that considerably reduced the spike discharge rate during the stimulus duration. The onset time window was individually adjusted to each unit because latency and duration of the onset discharge rate varied among units, e.g., units exhibiting bursting activity showed prolonged onset discharge duration. Accordingly, the used measurement window varied between 20 and 30 ms. The spontaneous rate was calculated from the averaged spike rate measured during the whole record duration for at least 12 frequency-level combinations for which no obvious driven discharge rate was observed. For example, in Figure 8A the neuronal activity during the first eight frequency steps (1.7–3.7 kHz) at the two lowest levels (-10 and -5 dB SPL) was classified as "spontaneous" and used to derive the spontaneous activity value.

The first spike latency of single neurons which is defined as the latency of that spike in a peri-stimulus time histogram (PSTH) that occurs first after onset of the stimulus, was analyzed before and during BIC application. During BIC application, the threshold could change (see below). The latency was measured 10-20 dB above the actual threshold at BF. In 8 out of 57 neurons that could be measured before and during BIC application, the response was extremely variable before BIC application because of a low spike probability (<30%) and,

hence, the latency was unreliable. Because of the high response variability, these units were excluded from the analysis of a latency shift caused by BIC.

3.1.5 Comodulation masking release: acoustic stimulation and recording procedures

For comodulation masking experiments, 39 adult gerbils of both sexes were used. The electrical signal from the recording electrode was amplified, band-pass filtered (0.3-3 kHz; TDT PC1; Tucker-Davis Technologies, USA), sent to an A/D converter and stored on the computer (Fig. 5).

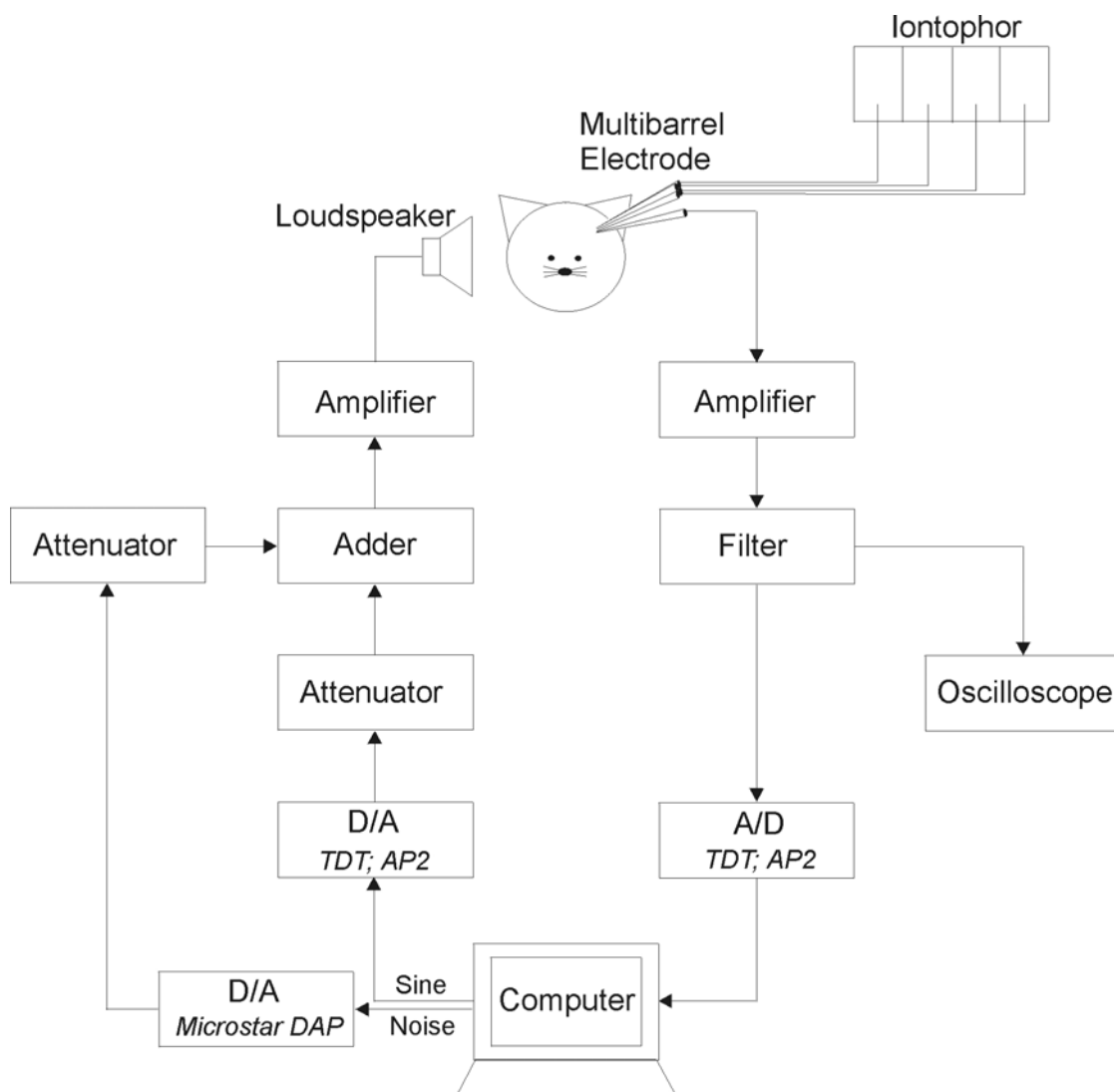


Figure 5 Schematic of the setup used in CMR experiments.

3 Methods

After a unit was isolated, its receptive field was measured using the setup for CMR experiments. Pure tone stimuli (80 ms duration, 5 ms rise/fall time) were produced at a sampling rate of 44.1 kHz by a computer board (AP2; TDT). The stimuli were fed into the loudspeaker (Canton XS) which was placed 20 cm away from the contralateral ear. The ipsilateral ear channel was plugged with wax to guarantee monaural stimulation. The loudspeaker was calibrated with a ¼" B&K 4135 microphone placed at the animals ear (using SigCal-software; TDT). The produced calibration curve was used by a signal generation software (SigGen; TDT) to generate pure tones of defined intensities. To obtain frequency response areas, pure tones of various frequencies and intensities were randomly presented with an interpulse interval of 400 ms. Each frequency-intensity combination was presented 2-10 times and corresponding neuronal responses were averaged (using Brainware; Jan Schnupp, TDT).

Files with pure tone stimuli (test tones) and noise maskers were produced by G. Klump. They were synthesized digitally by a Pentium II-PC at a sampling rate of 44.1 kHz. Band-limited noise maskers were generated by digital FIR-filtering (1024 points) of Gaussian white noise. To generate unmodulated maskers of a certain bandwidth, the Gaussian white noise was only band-pass filtered. To generate comodulated maskers, the Gaussian white noise was multiplied with a 50 Hz low-passed noise before being subjected to band-pass filtering. The masking noise had a bandwidth of 50, 200, 800, 1600, or 3200 Hz (Fig. 6A). All maskers had the same long-term acoustic energy. Each noise stimulus was calculated 5 times, only differing in the random seed for the time series of Gaussian amplitude values (stimulus variation type 1-5; see below). The noise spectrum level was measured using a ¼" B&K 4135 microphone connected to a calibrated microphone amplifier (B&K 2610), integrating over a time of several seconds. The noise spectrum level was 53 dB SPL/Hz at 0 dB attenuation. The spectrum level of the masking noise was set 5-20 dB above the neurons' threshold at BF. The presentation of the stimuli was controlled using TDT software (Brainware). The test tone (duration 200 ms, rate 1 per sec, rise/fall time 10 ms) at the neurons' BF was presented by a computer board (AP2; TDT). The masking noise was applied via a Microstar DAP 3200/415i DSP board.

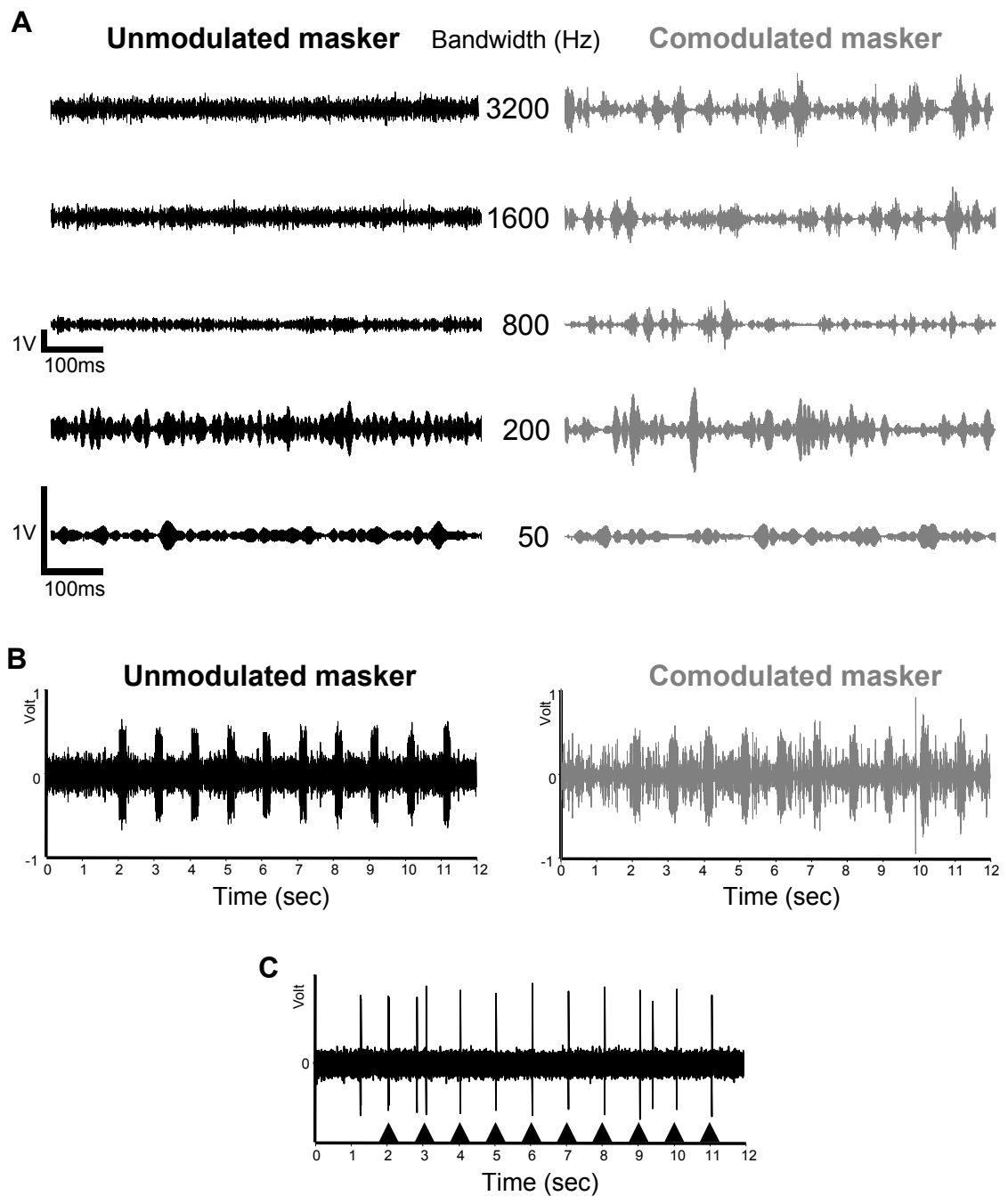


Figure 6 (A, B) Exemplary waveforms of the stimuli used in CMR experiments. **(A)** Oscillogram of 1 s time traces of noise with bandwidths of 3200 Hz, 1600 Hz, 800 Hz, 200 Hz, and 50 Hz. Center frequency is 2 kHz. To generate unmodulated maskers (black), Gaussian white noise was band-pass filtered. To generate comodulated maskers (grey), Gaussian white noise was multiplied with a 50 Hz low-passed noise (the modulator) prior to band-pass filtering. All maskers have the same spectrum level. A doubling of the noise bandwidth results in an increase in the overall intensity of 3 dB. Note the different y axes for maskers of bandwidths of 3200, 1600, 800 and 200, 50 Hz. Comodulation results in a distinct temporal structure of the envelope of the masking noise. The envelope fluctuations are correlated between different frequency bands that can be analyzed in separate frequency filters of the auditory system. **(B)** Ten presentations of a 200-ms tone (frequency of 2 kHz) are added to an unmodulated or comodulated masking noise of 200 Hz bandwidth (duration 12 s). **(C)** Example for a spike train recorded over 12 sec. In the first 2 seconds, only the masking noise was presented. Then, 10 tone signals were added (triangles). Note that the neuron responded consistently to tones.

3 Methods

The center frequency of the masking noise was equal to the BF and, hence, to the frequency of the test tone. The masking noise and the test tones were attenuated (PA4; TDT), added (SM3; TDT) and fed to the loudspeaker. The test tone was presented starting 2 sec after masker onset. Responses to 10 repetitions of the test tone were collected during a 12-sec time window of continuous presentation of the masker (Figs. 6B,C). Usually, the 12 sec of masking noise plus 10 test tones were presented twice to increase the number of test tone presentations (averages) to 20. The level of the test tone was varied from approximately the neuron's pure-tone threshold to approximately 60 dB above threshold in 5 dB increments. Each masking series consisted of the presentation of the test tone alone, followed by blocks of simultaneous presentation of the masker and test tone. Modulated and unmodulated maskers alternated, and between blocks with different test tone intensities, different variations of the same masker (type 1-5) were used to avoid a habituation of the neuron to the masker. In detail, the order of presentation of the maskers and test tone was the following: At the lowest test tone intensity, which was set approximately to the neuron's threshold at BF, a comodulated masker of type 1 was presented twice, then the unmodulated masker of type 1 was presented. At the next higher intensity of the test tone, comodulated masker of type 2 was presented, then the unmodulated masker of type 2 was presented and so on. Three to 5 different types of maskers were alternated.

3.1.6 Comodulation masking release: Data analysis

To analyze single units from multi unit recordings, spike sorting was performed using Tucker-Davis software (Brainware). Tuning curves of single units were analyzed as described above (see chapter 3.1.4). To analyze release from masking, a software routine (Testpoint, Keithley) was used to calculate peri-stimulus time histograms and rate-level functions of the onset discharge rate in response to the 10 or 20 presentations of the test tone during unmodulated and comodulated conditions, respectively (Fig. 7). The neuron's ability to encode the test tone is observed qualitatively as an increase in spikes in response to the test tone. From presentations of the test tone alone, a time window for the excitatory response was obtained (Fig. 7A). Dependent on the phasic or tonic

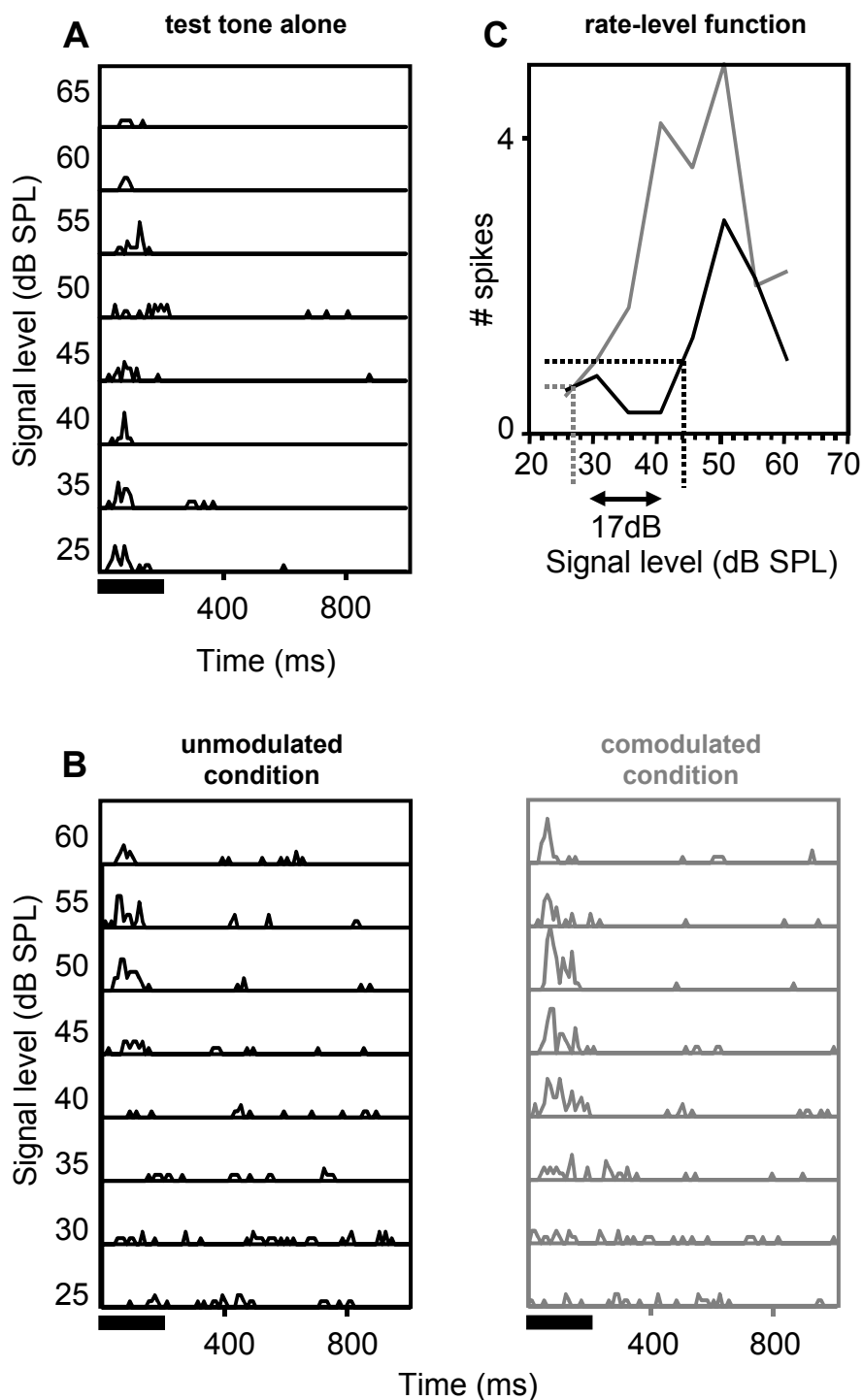


Figure 7 (A) Example for a PST-histogram for a signal presented alone. (B) Example for PST-histograms for signals masked by unmodulated (black) or comodulated (grey) noise. Each box represents the average of neural activity over 10 presentations of the test tone (signal; indicated by black bars) in noise for test tone intensities from 25 to 60 dB SPL. Neural activity in response to the signal was elicited at a lower signal level in the comodulated than in the unmodulated condition. (C) The corresponding rate-level functions. Dotted lines represent detection thresholds in the unmodulated (black) and comodulated (grey) condition. The difference in the signal detection between the comodulated and the unmodulated masking condition is 17 dB. The neuron's BF and, hence, the test tone frequency is 1.7 kHz. Noise bandwidth is 200 Hz. Noise spectrum level is 13 dB SPL/Hz and, thus, 5 dB above the neuron's pure tone threshold at BF (8 dB SPL). PSTH bin width is 10 ms. PSTH y axis is 1 spike.

3 Methods

character of the response the used time window for analysis of the units' activity during the presentation of the test tone varied between 30 and 200 ms. The response threshold indicating detection of the test tone in noise was defined as the mean spike rate observed while the masker alone was presented plus the standard deviation multiplied by a factor of 1.8. The release from masking was determined as the difference between the detection threshold of the test tone when masked with comodulated and with unmodulated noise of the same bandwidth. Therefore, positive values of the release from masking indicate a lower detection threshold for the signal masked by comodulated noise (Fig. 7C).

3.2 Immunocytochemistry

Two adult animals were deeply anaesthetized by intraperitoneal injection of a 10:1 mixture of ketamine (350 mg/kg) and xylazine (Rompun 2%, Bayer), then perfused through the heart at 4 ml/minute with saline (5 min) followed by a fixative (2.5% glutaraldehyde in 0.1 M phosphate buffer, 40 min). The brain was removed and postfixed overnight at 4°C. Frontal sections 200 µm thick and containing the primary auditory cortex (2-3 mm rostral of Lambda) were cut on a vibratome, osmicated, dehydrated, and embedded in epoxy resin (Durcupan). Alternating series of semithin sections (1 µm) were collected; one series was stained with Richardson blue and the other was used for GABA immunostaining. Immunocytochemistry basically followed the protocols given by Liu et al. (1989) and Kolston et al. (1992). The mounted sections were first placed in KOH in methanol/propylenoxid to remove the resin, followed by NaIO₄ to alleviate the masking effect of osmium. They were then preincubated in 10% normal goat serum (NGS) in 0.1 M phosphate-buffered saline (PBS) and subsequently incubated in the primary GABA antiserum (SFRI, France; diluted 1:10000 in PBS containing 2% NGS) overnight at 4°C. Sequential incubations were carried out in biotinylated goat anti-rabbit IgG (Sigma) diluted 1:200 in PBS containing 2% NGS, the avidin-biotin-peroxidase complex (Vectastain ABC kit; diluted 1:50 in PBS), and diaminobenzidine (DAB)/H₂O₂. Between each step, the sections were rinsed with PBS. After the final DAB step, the staining was silver-intensified (for details see: Vater 1995; Kemmer and Vater 1997).

The sections were washed in acetate buffer, dehydrated in ethanol, cleared in xylol, and coverslipped in DepeX (BDH Chemicals).

For quantitative analysis, immunostained sections and adjacent Richardson blue-stained sections were light microscopically analyzed with a Leitz Dialux 20 microscope to which an image processing system was attached. To determine the percentage of GABA-immunopositive neurons, cell counts were performed in semithin (1 μm) sections from two 200- μm -thick slabs. For each slab, three semithin sections with a 20 μm -interval between sections were studied. In each section two columns running from the pia to the white matter were analyzed from videoprints obtained with a magnification of $\times 400$. After establishing layer boundaries, all nucleated neuronal profiles were counted in 12 sample areas per layer (300 μm wide and 100 μm high; layer II: 300 μm wide and 75 μm high). To estimate the laminar distribution of GABAergic axon terminals, immunopositive puncta on cell somata were examined with an objective (N.A. 1.25, $\times 100$) under oil immersion. In layers I and IV, puncta on nonpyramidal cells and in layers II, III, V, and VI puncta on pyramidal cells were counted. Profiles were classified as puncta when they were either round or oval and did not resemble cross-sectioned dendrites or axons (Prieto et al. 1994b).

4 Results

4.1 Extent of diffusion of bicuculline in the auditory cortex

There are some difficulties in interpreting results obtained by iontophoretic application of pharmacologically active compounds (Hicks 1983), especially bicuculline. Its removal from the tissue appears to be dependent on diffusion rate, and in the present study, it could take as long as 20 minutes until the effect of BIC disappeared. Because of time constraints, a full recovery from the drug effect was not always achieved and, therefore, during a penetration through the cortex, BIC could accumulate. To gain insight into the extent of the diffusion and the time course of clearance of BIC within the cortical tissue, I applied BIC in one animal using single-barrel injection electrodes (tip diameter = 3 μm) separated several 100 μm from the recording pipette and measured the effect of the drug at different current levels. The influence of BIC at the recording site was tested in a multi unit in layer III and in four single units in layer V. A pure tone at the best frequency and 20 dB above threshold was presented (stimulus duration of 80 ms, interpulse interval of 800 ms). From responses to 40 presentations of this tone, the overall spike rate was calculated. This procedure was repeated 5 times during a time interval of 5 minutes. An average spike rate and the standard deviation were calculated from the 5 measurements. Then, BIC was applied at ejection currents of 10, 20, 30 and 40 nA. At each current level, the response rate was measured with the same measurement procedure as under predrug conditions and the drug was applied continuously while the units' response was recorded. If, at a given current level, there was no effect of BIC after 10 minutes of drug injection, the injection current was increased to the next higher level. BIC was considered to have a significant effect at a particular current level when the spike rate increased to a value of the mean spike rate plus two times the standard deviation measured during the control situation.

In layers III and V, an ejection current of 30 nA increased the spike rate of a cell that was 150 μm away from the injection site, while a 40 nA current increased spiking in a cell 350 μm from the BIC injection. At a distance of 400 μm , one unit was affected after 5 minutes at 40 nA, while another was not affected after 10 minutes. I conclude that for the ejection currents commonly applied in my experiments (10-40 nA), locally applied BIC can influence responses of neurons located at distances of up to approximately 400 μm . Long range effects of BIC caused by diffusion take several minutes. I recorded only from units that showed a fast effect to drug application. Therefore, local effects were measured and possibly - during the time course of the tuning curve measurement (13-17 min) - diffusion effects. I cannot rule out the possibility that those units that were recorded in a sequence and were spaced less than approximately 400 μm were under the influence of elevated levels of BIC. Thus, the net effect of BIC on a small network of cells was measured. To minimize such indirect effects of BIC, the drug was applied at the lowest effective ejection currents and a waiting period of at least 10 minutes was interspersed between data collection from different units.

4.2 General effects of bicuculline

88 multi units and 64 single units from 21 gerbils in 22 near-radial penetrations were recorded. The number of units recorded in a penetration varied between 3 and 14. The variability of BF with depth could be analyzed in 20 penetrations where units were recorded over a depth range of at least 600 μm . According to Sugimoto et al. (1997) and Merzenich et al. (1975), the variability of BF within each penetration was estimated using the fractional bandwidth, which is defined as the ratio of the difference of the maximum BF and minimum BF encountered to the minimum BF. Fourteen penetrations showed a fractional bandwidth of ≤ 1 (0.1-1.0) and were defined as exhibiting nearly constant BF with depth. In the remaining 6 penetrations, 1 or 2 units out of 6-8 units per penetration showed a different BF which caused an higher fractional bandwidth of 1.3-3.8.

Once a unit was isolated, its frequency response area was measured. Then, BIC was iontophoretically applied with increasing ejection currents until an

4 Results

increase in spontaneous or evoked discharge activity was observed, which occurred at 10-40 nA for most units. The increase in discharge rate usually occurred rapidly (within 1-2 minutes) and was stable for several minutes. The ejection current was not increased further to prevent the tissue from being saturated with BIC and to ensure a local application of the drug. BIC was applied continuously during the measurement of the receptive field. In the majority of the units, the recordings were stable for more than one hour, and hence, it was possible to measure recovery from BIC or to additionally investigate the effect of GABA.

BIC increased the spontaneous firing rate in 82% of the units tested at ejection currents between 2 and 60 nA. The mean increase in spontaneous rate of these units amounted to 235% (range 6-3780%; units that showed no or <0.1 spikes/s spontaneous activity before BIC application were excluded from this analysis). In most cortical units, the tone-evoked response consisted of a phasic increase of discharge rate related to stimulus onset. This onset activity, measured in a 20-30-ms time window starting with the first stimulus-evoked spike, was increased in 79% of the units for stimulus levels of up to 80 dB SPL. The mean increase in stimulus-evoked discharge rate of these units amounted to 147%.

4.3 Influence of bicuculline on receptive fields of single and multi units

For 127 units, a tuning curve could be calculated before and during application of BIC. The influence of BIC on frequency tuning curves of a single unit in layer V is shown in Figure 8A. Under control conditions (predrug, *top*) the spontaneous activity was 2.3 spikes/s and increased to 6.1 spikes/s during the application of BIC (*middle*). The maximum onset discharge rate increased from 17 spikes (at 5.8 kHz; 55 dB SPL) to 33 spikes (at 5.2 kHz; 35 dB SPL) during BIC iontophoresis. A broadening of the receptive field toward higher frequencies was observed and $Q_{10\text{dB}}$ and $Q_{40\text{dB}}$ values decreased during BIC application (predrug: 2.3 and 0.9; BIC: 0.85 and 0.35). A recovery from the drug effects was achieved immediately after finishing drug ejection (*bottom*).

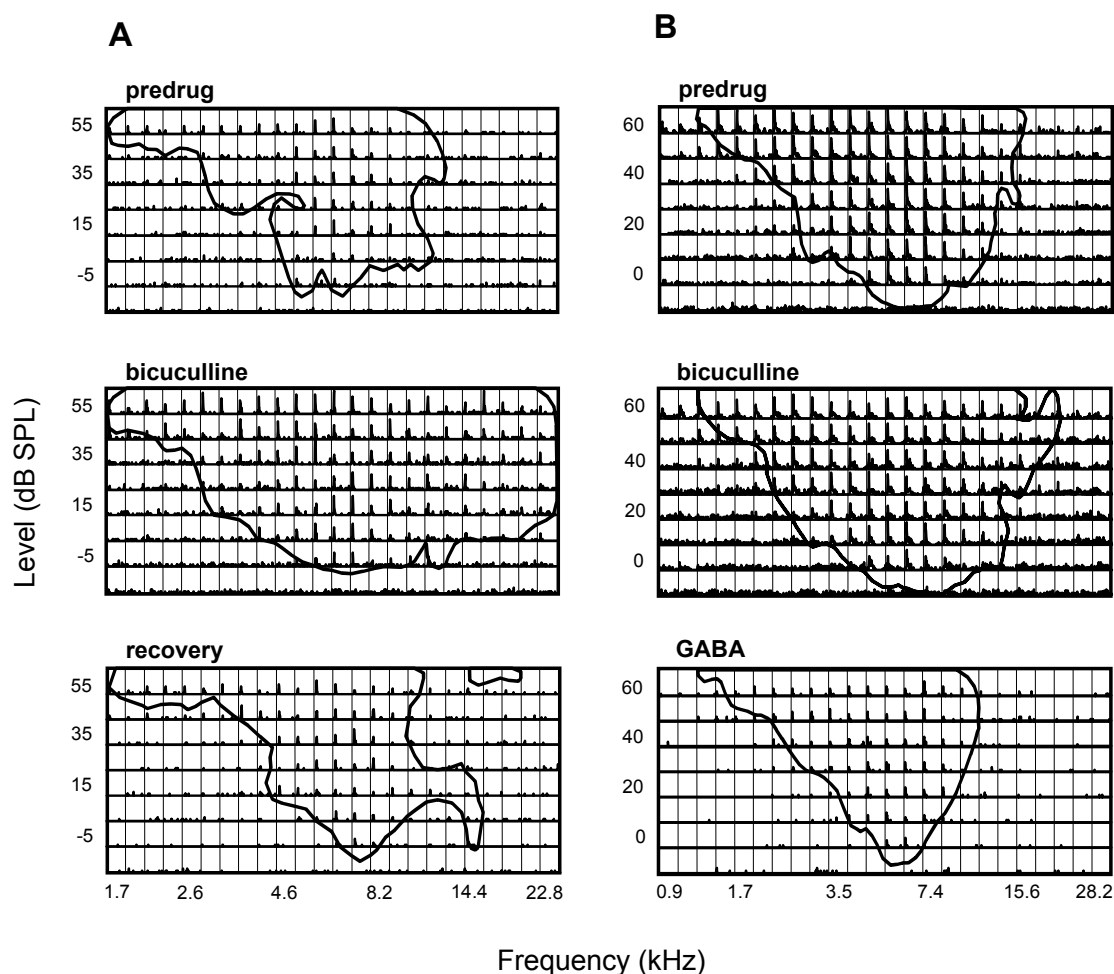


Figure 8 (A) Tuning curves and PSTH-histograms for a single unit in layer V in response to random presentation of a 80-ms pure tone at frequencies from 1.7 to 22.8 kHz and intensities from -25 to 55 dB SPL before (*top*), during (*middle*) and after (*bottom*) the application of bicuculline (5 nA). Each box represents the average of neuronal activity over 10 trials and over 240 ms for each frequency-level combination. PSTH bin width is 4 ms. PSTH y axis is 12 spikes. Threshold criterion for the tuning curves is 20% maximum onset spike rate plus spontaneous activity. (B) Example for a single unit in layer III for which no change of the receptive field was measured during the application of BIC (10-20 nA) despite an increase in spontaneous activity. Application of GABA (20 nA) decreased the spontaneous activity and the receptive field size was reduced slightly. Each box represents the average of neuronal activity over 8 (*top/middle*) and 4 (*bottom*) trials over 240 ms for each frequency-level combination. PSTH bin width is 4 ms. PSTH y axis is 20 spikes (*top/middle*) and 10 spikes (*bottom*).

In general, BIC enlarged the receptive field. The degree and the form of the enlargement were various and complex. Figures 9A and 9B show two further examples of single units in layers V and II for which the application of BIC led to a pronounced broadening of the frequency tuning curve at the low-frequency and the high-frequency side of the tuning curve. This demonstrates intracortical GABAergic inhibition creating inhibitory sidebands that surround the excitatory response area. In addition, the threshold of the neuron shown in Figure 9A

4 Results

decreased during the application of BIC suggesting that inhibition was also present within the excitatory receptive field. The broadening of the tuning curve was often more pronounced at high sound levels than at low levels (e.g., Fig. 9D). To gain an insight into possible unspecific changes of BF over time, I compared the BF of the tuning curves measured before and after BIC application (recovery). In 34% of the investigated units (n=15), a shift of the BF of ≥ 0.2 octave was observed, the maximal individual shift amounted to 0.47 octaves. In the remaining 66% of the units the BF did not shift, as assessed by using the 0.2-octave criterion. During application of BIC, a shift of BF of the units to higher (27%) or lower frequencies (39%) was observed. The remaining 34% of the units showed no apparent change of their BF. For the majority of the units, the shift of BF was below 1 octave, but 10 units shifted their BF by more than 1 octave to lower frequencies (Fig. 9C) and 4 units shifted their BF by more than 1 octave to higher frequencies (maximum shift of 2.5 octaves). The thresholds to tone stimulation of different units varied between -12 and 45 dB SPL prior to drug application. BIC decreased the threshold in 63% of the units (e.g., Figs. 9C and D). The average decrease was 5.5 ± 4.8 dB. I suggest that this decrease of threshold was caused by a release of inhibition since unspecific threshold changes, assessed from the differences measured before and after BIC application (recovery), did not show a systematic decrease and were on average -0.12 ± 5.4 dB (n=15). Eleven units exhibited multi-peaked frequency tuning curves in control conditions; the most extreme case is shown in Figure 9E. This multi unit in layer VI had four clearly separated response areas that were merged during BIC application creating a very broadly tuned tuning curve. Similar effects were also seen in four single units. BIC eliminated receptive field gaps at higher stimulus levels. This demonstrates the involvement of intracortical GABAergic inhibition in the creation of nonmonotonic rate-level functions (Fig. 9F). An example for a single unit for which the receptive field structure changed only slightly during GABA_A blockade, although BIC increased the spontaneous activity from 15 to 40 spikes/s, is shown in Figure 8B. GABA application reduced the spontaneous rate to 1.25 spikes/s and shifted the high-frequency slope of the receptive field downward by about 2 kHz.

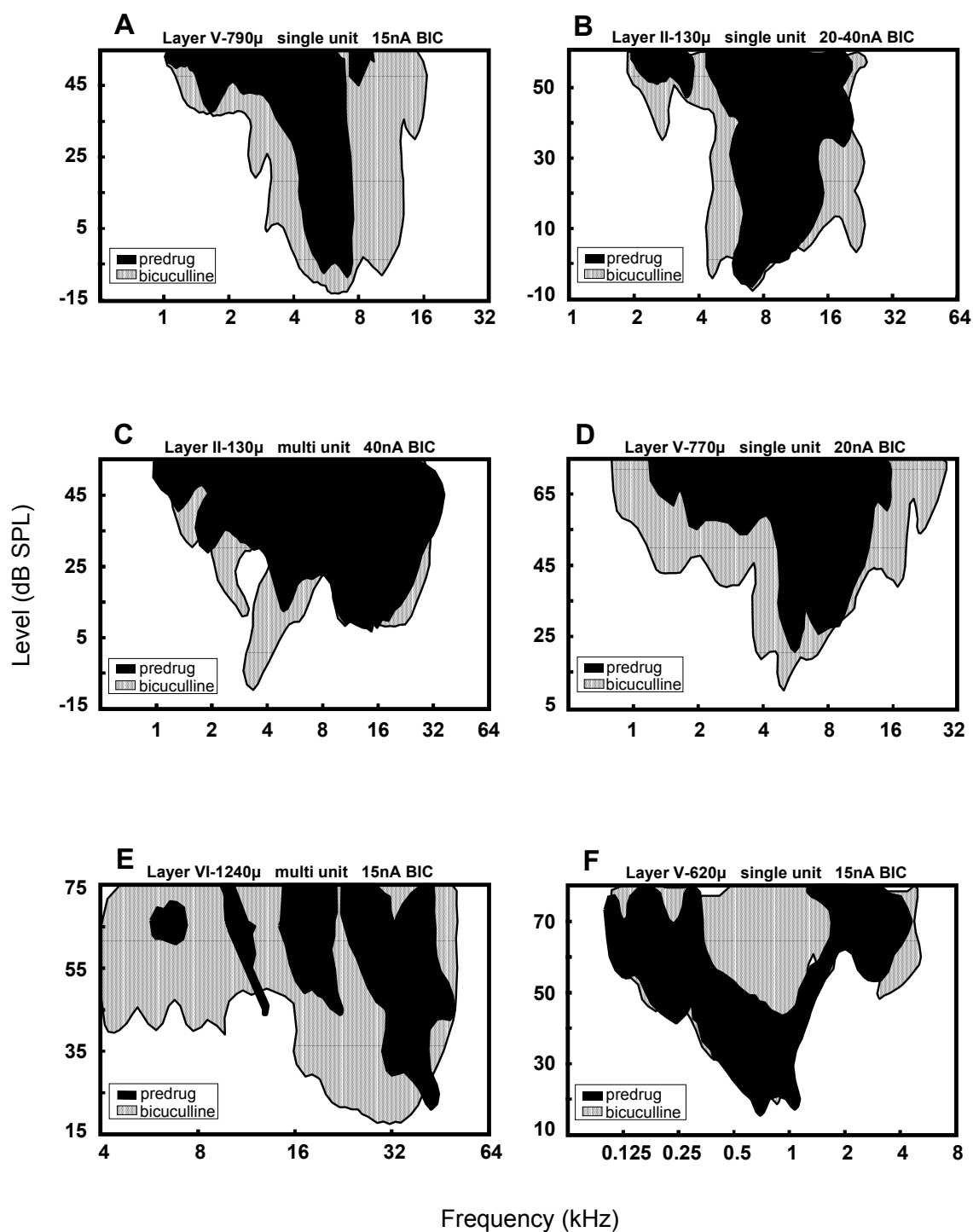


Figure 9 Examples for receptive fields of single and multi units from different layers under predrug condition (black) and during the application of bicuculline (grey).

4.4 GABAergic involvement in two-tone masking

In 10 units, the influence of two-tone masking and GABA_A blockade was compared. In two-tone masking experiments, an excitatory tone (probe) at BF is presented, either prior to or simultaneously with a second tone (masker) of variable frequency and intensity. Masking is present, when the masker tone reduces the response to the probe tone below the response generated by the probe tone alone. Two mechanisms contribute to this masking. First, especially when using a simultaneous masking paradigm, mechanical suppression in the cochlea occurs that is projected into the central auditory system. In addition, neural inhibition originating from all stations of the auditory pathway may be reflected in the cortical response. Figure 10 shows the response area of a single unit in layer III before and during the application of BIC and the result of a two-tone masking experiment for the same unit. The shapes of the tuning curve during GABA_A blockade and during two-tone masking are similar suggesting that, for this neuron, the suppressive effect of the masker tone was mainly mediated by local GABAergic inhibition in the cortex. In the other neurons, the two-tone masking curve was broader than the receptive field size during BIC application indicating that the suppressive effect of the masker tone was mainly mediated by mechanical suppression in the cochlea and/or subcortical neural inhibitory mechanisms.

4.5 Influence of bicuculline on the tuning sharpness

Changes of tuning sharpness as a result of the blockade of GABAergic inhibition were analyzed in all units that showed an increase of spontaneous and/or stimulus-evoked activity during the application of BIC. The correlation of tuning sharpness expressed as Q_{10dB} and Q_{40dB} before and during the application of BIC is plotted for single and multi units (Fig. 11). In the control situation, the mean Q_{10dB} was 2.3 (n=127; range 0.6-5.8) and slightly decreased to 2 during BIC application (range 0.5-7.8). The decrease of Q_{10dB} was significant ($p < 0.01$, paired 2-tailed Wilcoxon test).

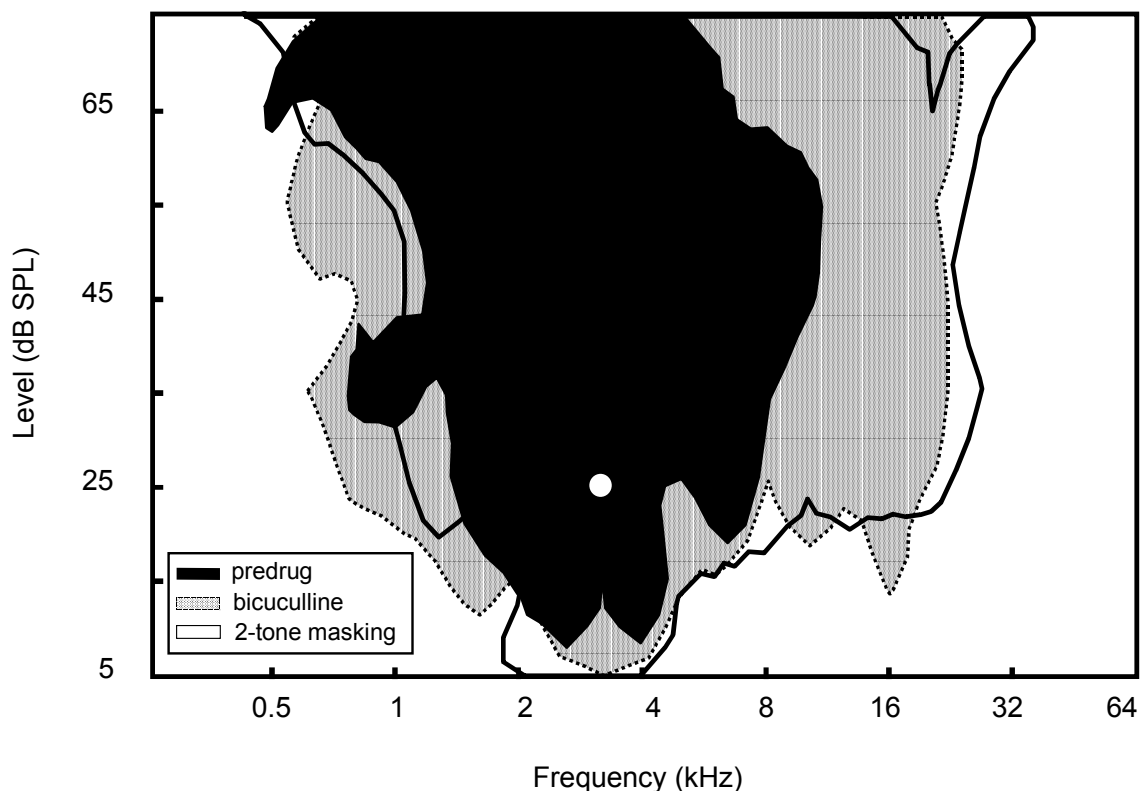


Figure 10 Comparison of tuning curves for a neuron in layer III before (black) and during (grey) the application of bicuculline (30 nA) with a two-tone masking curve (solid line). The shape of the masking tuning curve is similar to the tuning curve during bicuculline application. This indicates that, for this neuron two-tone masking is mediated by intracortical GABAergic inhibition. The white dot represents the probe stimulus (duration 80 ms). The delay from the onset of the masker (duration 50 ms) to the onset of the probe was set at 69 ms. The time interval between trials was 400 ms. To construct the masking curve, a masking criterion of 50% of the control onset discharge rate was used.

If tuning curves were defined as narrow when their $Q_{10\text{dB}}$ value was > 2 (Pelleg-Toiba and Wollberg 1989), then the percentage of narrowly tuned units decreased from 54% before BIC to 41% during BIC application. The mean $Q_{40\text{dB}}$ decreased from 1 (range 0.1-6) during predrug conditions to 0.6 (range 0.1-1.8) during BIC application. The decrease of the $Q_{40\text{dB}}$ was highly significant ($p < 0.001$, paired 2-tailed Wilcoxon test). Before drug application 75% of the units ($n=110$) had values >0.5 compared with 56% during BIC application. The total sample is smaller for the $Q_{40\text{dB}}$ values because in some units threshold was relatively high and I did not measure 40 dB above threshold, or the bandwidth was not clearly defined because the flanks exceeded the frequency boundaries of the measurement.

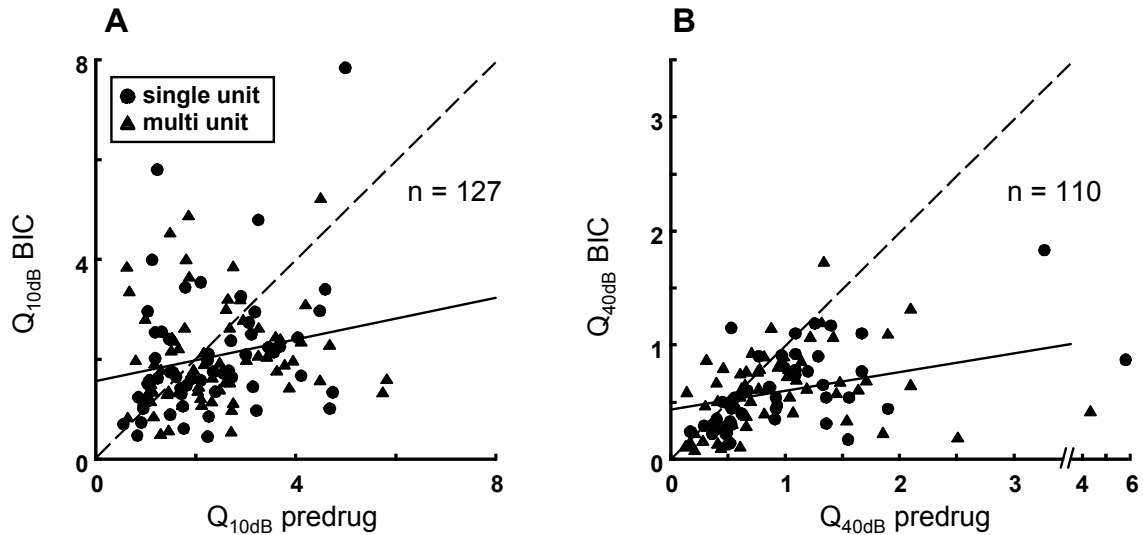


Figure 11 Q values of tuning curves before and during BIC application with regression lines. Equal Q values before and during BIC application result in a point on the dashed line at 45°. The solid lines gives the regression line for (A) the Q_{10dB} (with $y = 0.21x + 1.56$; $r = 0.21$) and (B) the Q_{40dB} (with $y = 0.16x + 0.43$; $r = 0.38$). Both correlations were significant ($p < 0.05$; $p < 0.01$).

4.6 Effects of bicuculline across different cortical layers

By using near-radial penetrations, it was possible to study BIC effects in different cortical layers, defined by the depth of the recording site. General physiological response properties varied among layers, for example, cells in layers II and IV were characterized by low spike amplitudes, whereas in layers III, VI, and in, particularly, layer V, numerous single units with large spike amplitudes were isolated that often showed bursting activity.

Examples for the depth-dependent distribution of the BF are shown in three near-radial penetrations before and during BIC application (Fig. 12). In 13 out of 20 penetrations, the BF remained nearly constant with recording depth (fractional bandwidth ≤ 1) and was similar during BIC application (Fig. 12A). In a penetration that was likely to be at the border between A1 and the anterior auditory field, where units were exceptionally broadly tuned, BIC shifted the BF downward in layers III and IV (Fig. 12B). For the penetration shown in Figure 12C, BIC stabilized the BF at values below the predrug condition for all layers. In the remaining 5 out of 20 penetrations where I could record enough units to analyze a dependence of BF with depth in the predrug situation, the fractional

bandwidth was >1 , indicating that the BF of the units changed with cortical depth. In these units, the BF during BIC application either was similar to the respective BF during predrug conditions, or the BF was changed during BIC application but these changes were not related to cortical depth.

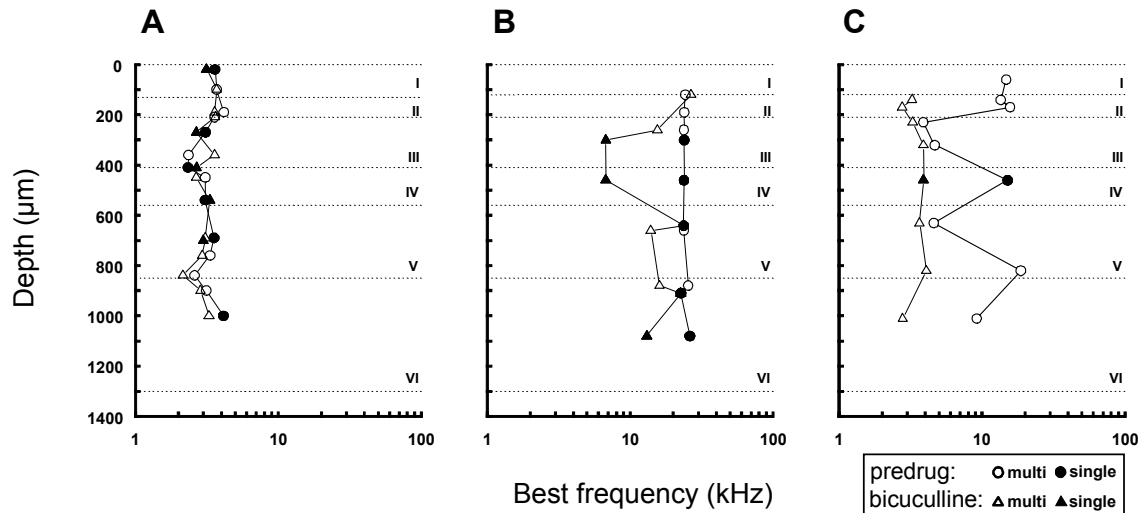


Figure 12 Depth-dependent distribution of the best frequency during three near-radial penetrations in three animals before (circles) and during (triangles) bicuculline application. Open symbols represent multi units; closed symbols represent single units. (A) Similar BF under predrug and drug conditions. (B) BIC shifted the BF downward in layers III and IV. (C) BIC stabilized the BF at values below the predrug condition for all layers.

4.6.1 Latency of single units

The latency of stimulus-evoked first spikes of single units, before and during BIC application, was analyzed for sound pressure levels 10-20 dB above the actual threshold at the BF. The ranges of latencies were between 16 and 40 ms before and between 12 and 41 ms during the application of BIC. The mean latencies were similar across the different layers (Fig. 13). Slightly shorter latencies were found in layer VI, but this difference was not significant (t-test, $p > 0.05$). The change of latency caused by BIC was highly variable between neurons (range -12 to 12 ms, average -0.98 ± 3.9 ms, $n=49$) and was not significantly different across layers ($p > 0.05$, Kruskal-Wallis test).

4 Results

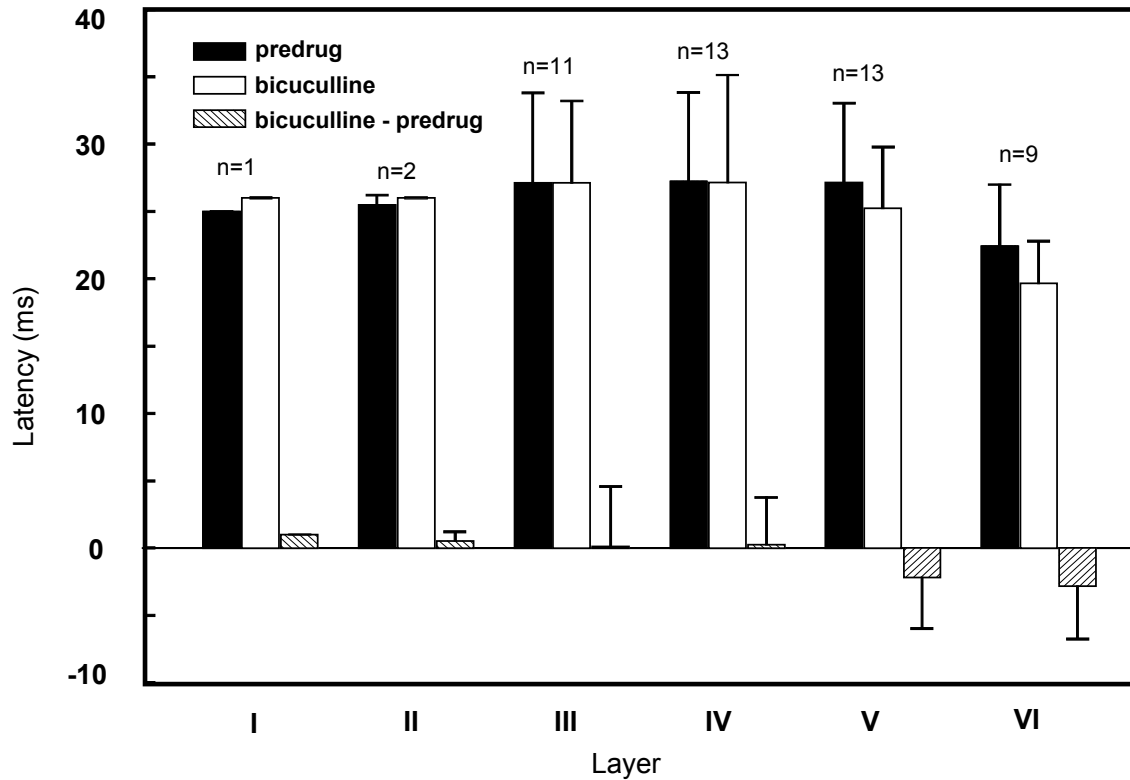


Figure 13 Average response latencies of single units for all layers before (filled boxes) and during (open boxes) the application of bicuculline. Stippled boxes represent the average difference between drug and predrug latencies. Error bars represent standard deviations. Note that for layers I and II there were not enough units to obtain an useful measure of standard deviation.

4.6.2 Change of tuning caused by GABA_A blockade

A possible layer specificity of Q_{10dB} and Q_{40dB} values during control conditions was tested for single units, multi units, and all units grouped together (Table 1). However, no layer specificity ($p > 0.05$, Kruskal-Wallis test) could be detected. To investigate a possible layer-specific strength of inhibition, the changes of the Q_{10dB} and Q_{40dB} values caused by GABA_A blockade were plotted as a function of the cortical depth for single and multi units (Fig. 14A). The criterion that was used to define an increase or a decrease of tuning sharpness was a change of the Q_{10dB} value of at least ± 0.5 or at least ± 0.125 for the Q_{40dB} value. Abolishing GABA_A-receptor mediated inhibition resulted in a decrease of tuning sharpness measured as Q_{10dB} values in 45% ($n=127$) of the units and an increase in 22% of the units. There was no evident layer specificity. A more uniform effect of blocking GABA_A receptors was observed for the Q_{40dB} values: They decreased in 63% of the 110 units for which a Q_{40dB} was definable before and during BIC application and increased in only 10%. The decrease of the

$Q_{40\text{dB}}$, and, hence, the decrease of tuning sharpness, was largest for one unit at the border of layers III and IV and for units in layer VI. However, over the whole population, there was no significant layer-specificity ($p > 0.05$, Kruskal-Wallis test).

Layer	$Q_{10\text{dB}}$			$Q_{40\text{dB}}$		
	Median	1 st Quartile	3 rd Quartile	Median	1 st Quartile	3 rd Quartile
I	1.12	0.87	2.02	0.89	0.64	1.30
II	1.80	1.47	4.15	0.45	0.40	0.88
III	2.28	1.60	3.91	0.65	0.52	1.19
IV	2.23	1.47	3.09	1.03	0.65	1.34
V	2.28	1.31	2.92	0.90	0.51	1.33
VI	2.31	1.53	3.01	0.88	0.49	1.54

Table 1 $Q_{10\text{dB}}$ and $Q_{40\text{dB}}$ of single and multi units per layer

To investigate a possible frequency asymmetry of inhibitory effects, the shifts of the high- and low-frequency slopes of the tuning curves 40 dB above the threshold were measured (Fig. 14B). The shifts were not dependent on the BF of the unit (data not shown). To take into account slight irregularities of the edges of the tuning curves, a criterion of 0.25 octave was used to define a significant shift of the slope. In the pooled data, BIC shifted the low-frequency slope in the majority of units (56%, $n=110$) to lower frequencies (range -3.63 to -0.25 octave) and the high frequency slope to higher frequencies (43%, range 0.26 to 1.68 octaves). A broadening of the tuning curve on both the high-frequency side and the low-frequency side of more than 0.25 octave was observed in 29% of the units. In 26% of the units a pronounced broadening was observed only on the low frequency side. Seventy-two percent of these units shifted their high-frequency slope to higher frequencies, 28% to lower frequencies. In 15% there was a pronounced broadening at only the high-frequency flank; 56% out of these units shifted their low-frequency side to lower frequencies and 44% to higher frequencies. In general, the broadening toward lower frequencies was seen in a higher percentage of the neuronal sample and

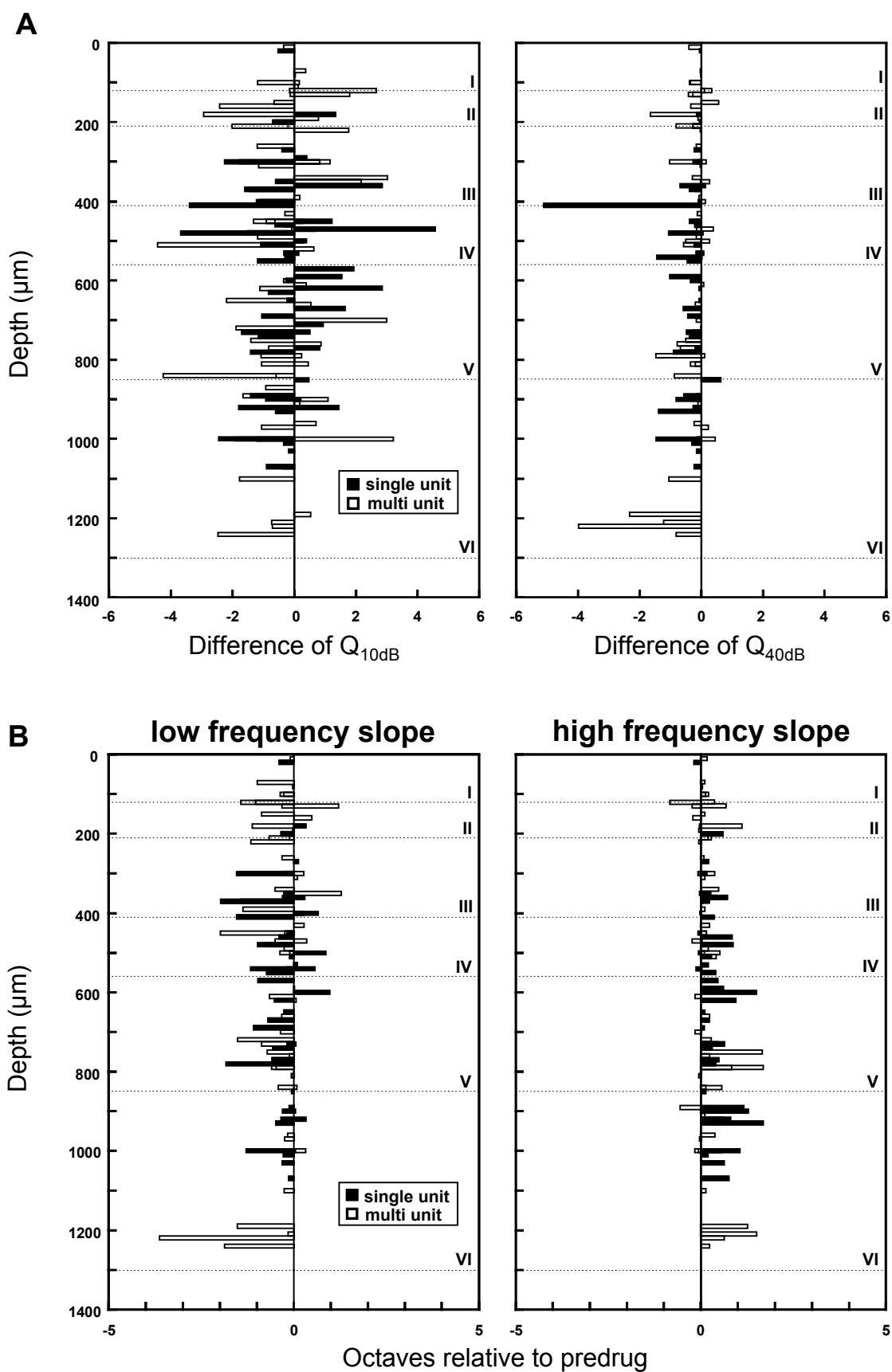
4 Results

it was more pronounced, indicating a more widespread inhibition at the low-frequency side of the tuning curves. There was no significant layer-difference in the effect of BIC on the change of the low-frequency slope ($p > 0.05$, Kruskal-Wallis test) and high-frequency slope (one-way ANOVA with Bonferroni correction).

4.6.3 Paradoxical effects of bicuculline and silent neurons

Two single units and eight multi units were recorded in layer I at a depth of 10-100 μm . Interestingly, for four of ten units in layer I, the application of BIC resulted in an inhibitory effect on both the stimulus-evoked and the spontaneous activity and/or a decrease of receptive field size (Fig. 15). A small network consisting of two inhibitory neurons connected in series and projecting to the recorded unit could be responsible for this effect if BIC preferentially affects the synapses between the two inhibitory neurons. Since neuronal cell bodies are spaced far apart from each other in layer I, it is surprising that multi-unit recordings are possible in this layer. However, spike amplitudes generally were quite small in layer I. Consequently, fluctuations of spike amplitude which led to a classification of the unit as a multi-unit recording could have been due to the low signal to noise ratio. To maintain a similar classification scheme over all recordings, I still defined these units as multi units. Of course, from the anatomical data, it can be suspected that the spike amplitude fluctuations were probably a consequence of the low signal-to-noise ratio and were not due to the presence of neighboring neurons.

Figure 14 (A) Difference of Q values between predrug condition and bicuculline application as a function of cortical depth. Each bar represents one unit. Bars orientated to the left side indicate lower Q values during BIC application and, hence, a decreased tuning sharpness. Bars orientated to the right side indicate higher Q values during BIC application and, hence, an increased tuning sharpness. BIC reduced the $Q_{40\text{dB}}$. **(B)** Frequency shift of the low- and the high-frequency slope of the tuning curves during the application of BIC relative to the corresponding frequency of the tuning curve before drug application. Each bar represents one unit. Bars orientated to the left side indicate a shift of the slope to lower frequencies and bars orientated to the right side indicate a shift of the slope to higher frequencies during BIC application. Measurements were taken 40 dB above threshold.



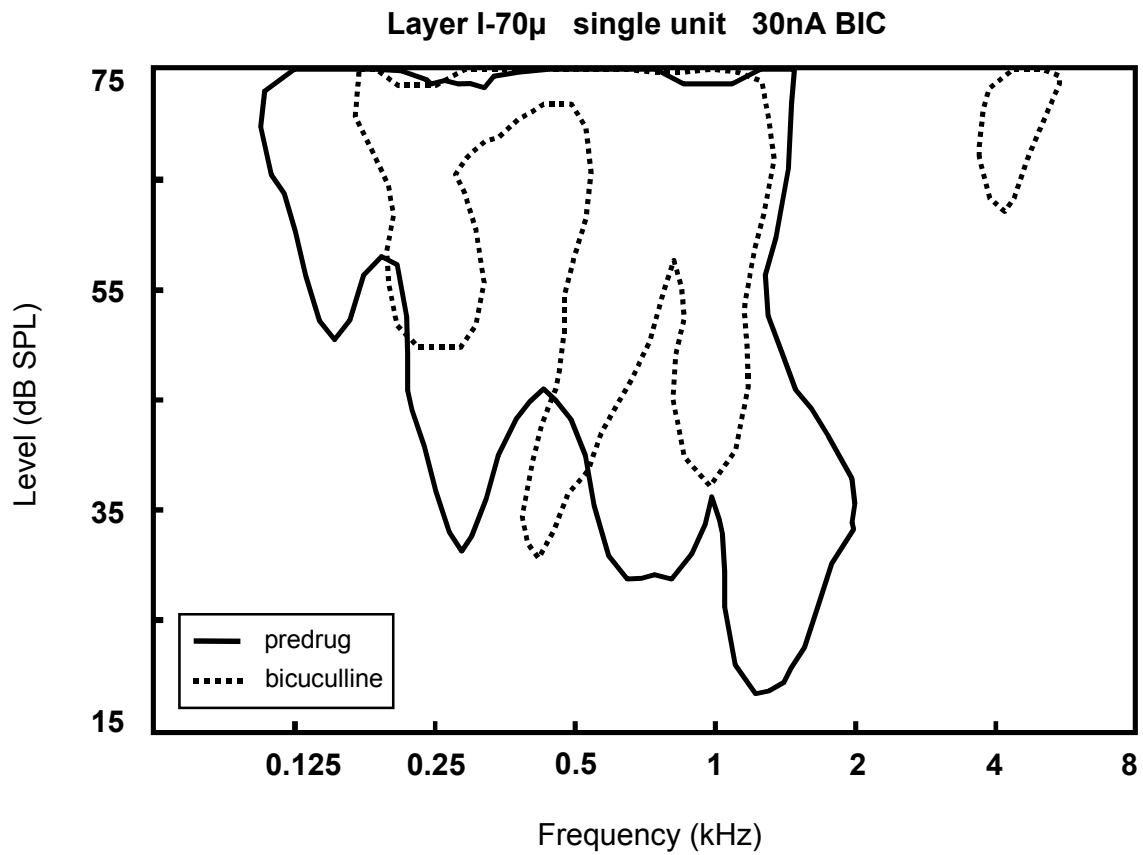


Figure 15 Example for a sharpening of the receptive field during the application of bicuculline (30 nA; dashed line) for a single unit in layer I.

Eight of 33 units recorded in layer VI and one unit at the border of layers II and III could not be driven by stimulation with pure tones under predrug conditions but showed acoustic responses within defined receptive fields during BIC application (Fig. 16). Analogous to recordings from the somatosensory cortex (Dykes et al. 1984), I defined these cells as silent neurons.

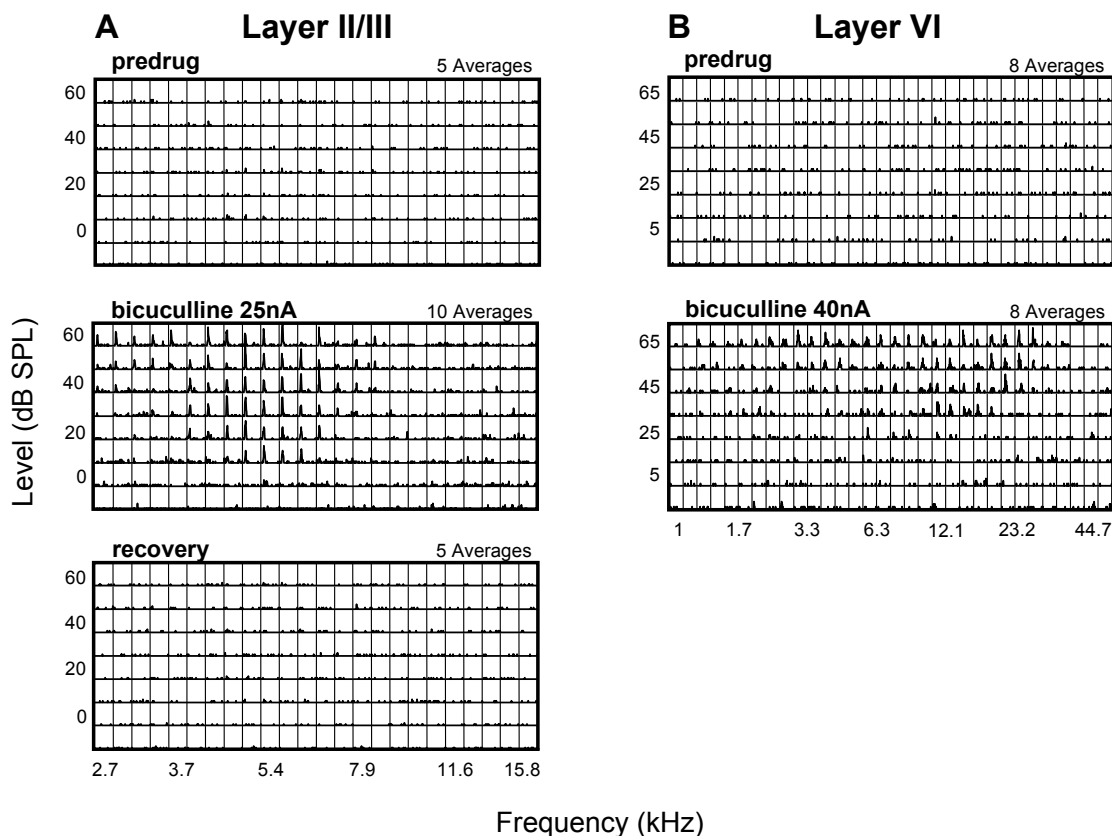
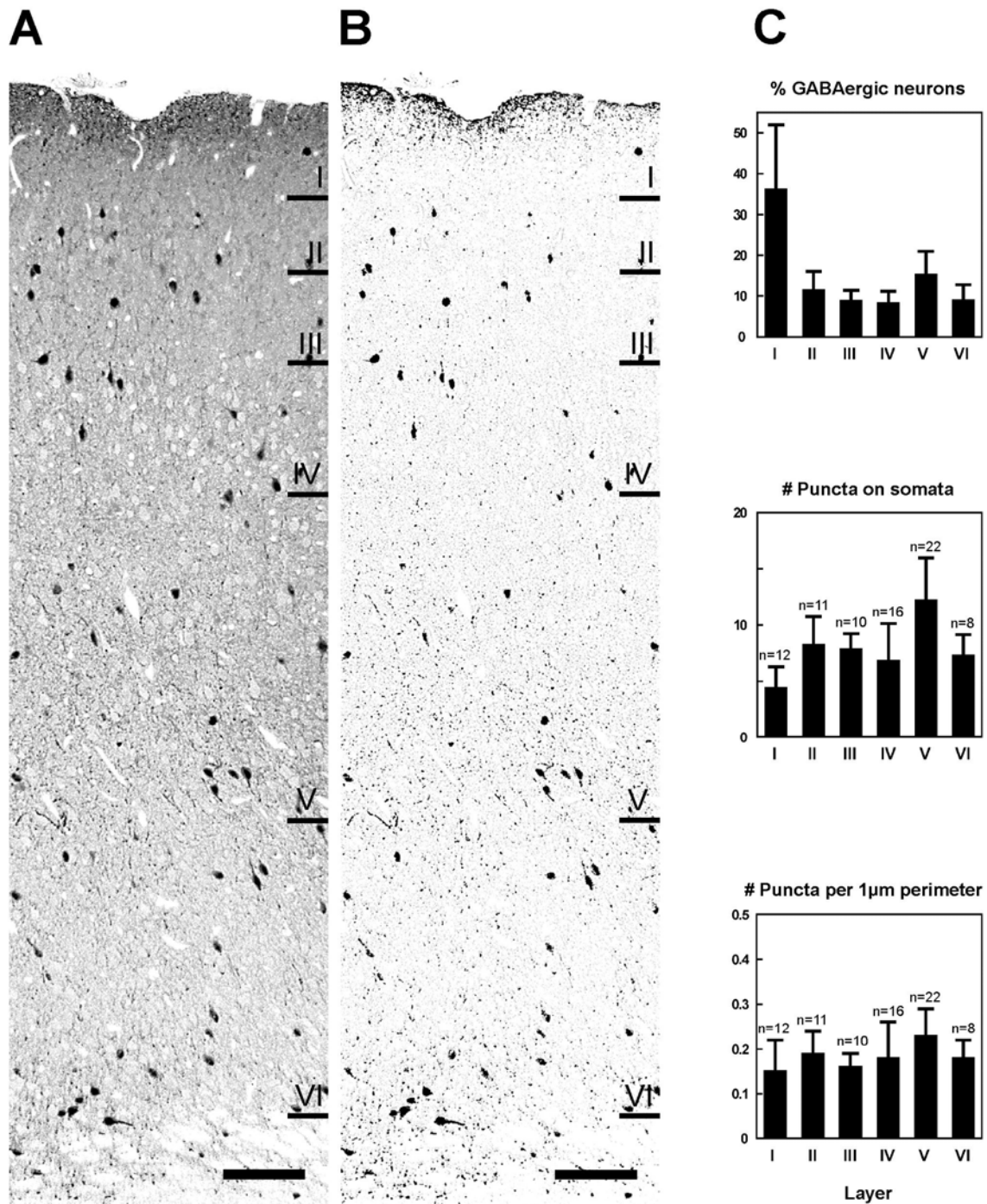


Figure 16 Receptive fields of a single unit in layer II/III (**A**) and a multi unit in layer VI (**B**) composed of single PSTHs. Prior to bicuculline application, there was no obvious response to pure tone stimuli and a receptive field could not be defined. For the neuron in (**B**), a recovery from BIC could not be measured because the neuron was lost after the application of BIC. PSTH bin width is 4 ms. PSTH x axis is 240 ms. PSTH y axis is 15 spikes (**A**) and 10 spikes (**B**).

4.6.4 Immunocytochemistry

To determine the extent of the six cortical layers, the cytoarchitecture of the auditory cortex was light microscopically analyzed in GABA-immunostained sections and adjacent Richardson blue-stained sections. Layer I contained only very few cell bodies. Layer II was composed of small, densely packed cell bodies, mostly small pyramidal cells. In layer III, pyramidal cells predominated, which increased in size from superficial to deep. Layer IV consisted of small, tightly packed somata. In layer V, medium-size and large, loosely arranged pyramidal cells prevailed. Layer VI was composed of densely packed somata of various sizes and shapes. Figures 17A and B show the laminar distribution of GABA-immunoreactive neuronal elements. The same section was plotted twice with different contrasts to illustrate either unstained cell bodies (Fig. 17A) or GABA-immunopositive puncta (axon terminals, Fig. 17B).



Figures 17 (A, B) GABA-immunostained 1-µm-thick section of the auditory cortex, plotted twice with different contrast enhancement (Adobe Photoshop), to show the profiles of immunopositive and immunonegative neurons (**A**) or immunopositive neurons and axon terminals (puncta, **B**). The immunonegative cells were often ringed by immunopositive endings. The density of puncta seemed to be highest in layer V. N.A. 0.7, $\times 40$. Scale bar = 100 µm. (**C**) Numerical analysis of GABAergic neurons and axon terminals. *Top*: Histogram showing the laminar distribution of GABAergic neurons. Error bars represent standard errors of the average of 12 samples from one animal. *Middle*: Histogram showing the numbers of puncta on somata of immunonegative neurons. Error bars represent standard errors. For further explanation see text. *Bottom*: Histogram showing the density of puncta on cell perimeter. Error bars represent standard errors.

GABA-labeled neurons were easily distinguished from background. GABA-labeled cells and puncta (Figs. 17B and 18) were present in all cortical layers. A variety of somatic shapes and sizes (area between 39 and 205 μm^2) was observed for GABA-labeled neurons (Fig. 19). Apart from a separation of pyramidal and nonpyramidal cells, a more detailed classification of cells was not possible because only the most proximal dendritic pattern was visible. GABAergic neurons constituted 14.8% of the neurons located in the auditory cortex. The proportion of GABA-labeled neurons was similar across layers II, III, IV, and VI and was largest in layers I (36.1%) and V (15.3%, Fig. 17C *top*). The density of GABA-labeled axon terminals seemed to be highest in layer V (see Fig. 17B).

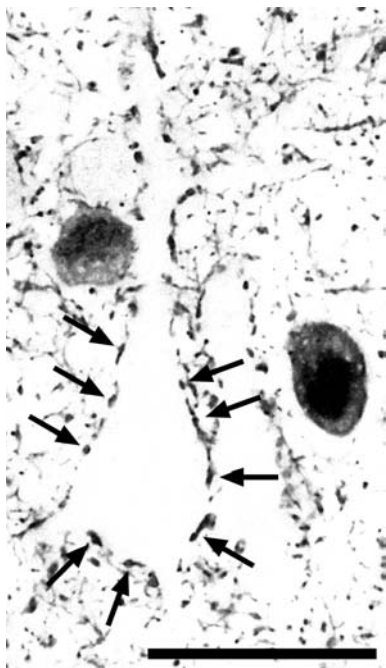


Figure 18 An immunonegative pyramidal cell in layer V whose soma and dendritic trunk received many GABAergic puncta (arrows). N.A. 1.25, $\times 100$, oil immersion. Scale bar = 25 μm .

To examine the laminar distribution of GABA-immunoreactive axosomatic endings, the number of puncta on cells' somata was counted for 8-22 cells per layer. In layers I and IV, immunonegative nonpyramidal cells and in the remaining layers, immunonegative pyramidal cells were investigated. Pyramidal cells in layer V received the highest number of axosomatic endings (average: 12.1 ± 3.7 , Fig. 17C *middle*) which often extended along the proximal dendrites (see Fig. 18). There were no layer-specific differences in the number of puncta per cell perimeter (Fig. 17C *bottom*).

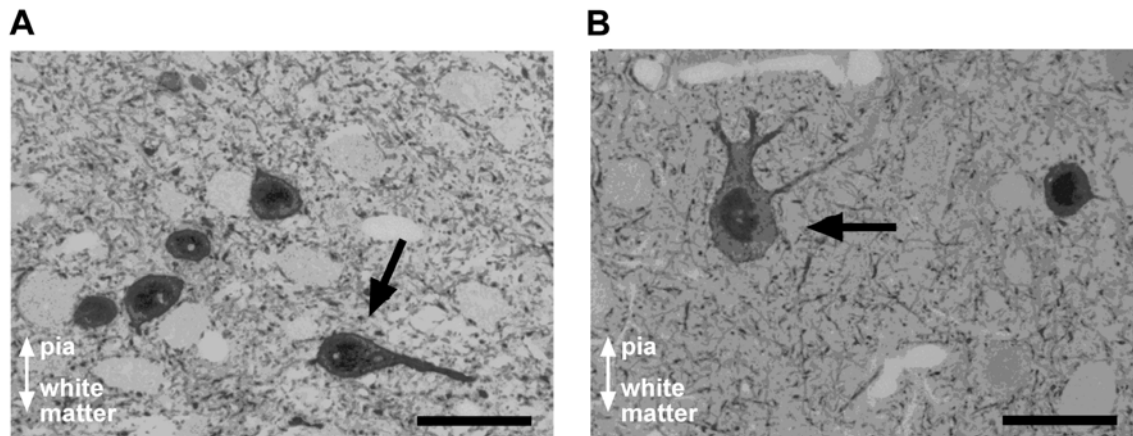


Figure 19 (A) Immunonegative and immunopositive cells in layer VI. One immunopositive cell (arrow) can be classified as horizontal cell by its horizontally orientated dendritic trunk. (B) Immunopositive multipolar cell (arrow) in layer V. N.A. 1.25, $\times 100$, oil immersion. Scale bars = 25 μm

4.7 Blockade of GABA_A receptors induces late responses

Primary auditory cortex neurons respond to pure tone sound either with a phasic pattern related to stimulus onset and/or offset or they respond during the entire stimulus duration (tonic pattern). In some studies, additionally to the short-latency onset response followed by an inhibitory period, a second excitatory response with a latency of 100 ms and more has been reported (Sally and Kelly 1988; Brosch et al. 1999, Fig. 1; Supèr et al. 2001). There are two general mechanisms that could generate the late response. *In vitro* studies of auditory cortex neurons showed a suppression of excitatory postsynaptic potentials by early and late inhibitory postsynaptic potentials mediated by GABA_A and GABA_B receptors, respectively (Cox et al. 1992; Hefti and Smith 2000). Therefore, the late response could be associated with a rebound of inhibition. On the other hand, a long-latency excitatory input could lead to this late activity. In the present study, evidence is given that the late response is not caused by a release of GABA_A-receptor mediated inhibition because the pharmacological blockade of GABA_A receptors enhanced or even elicited late responses.

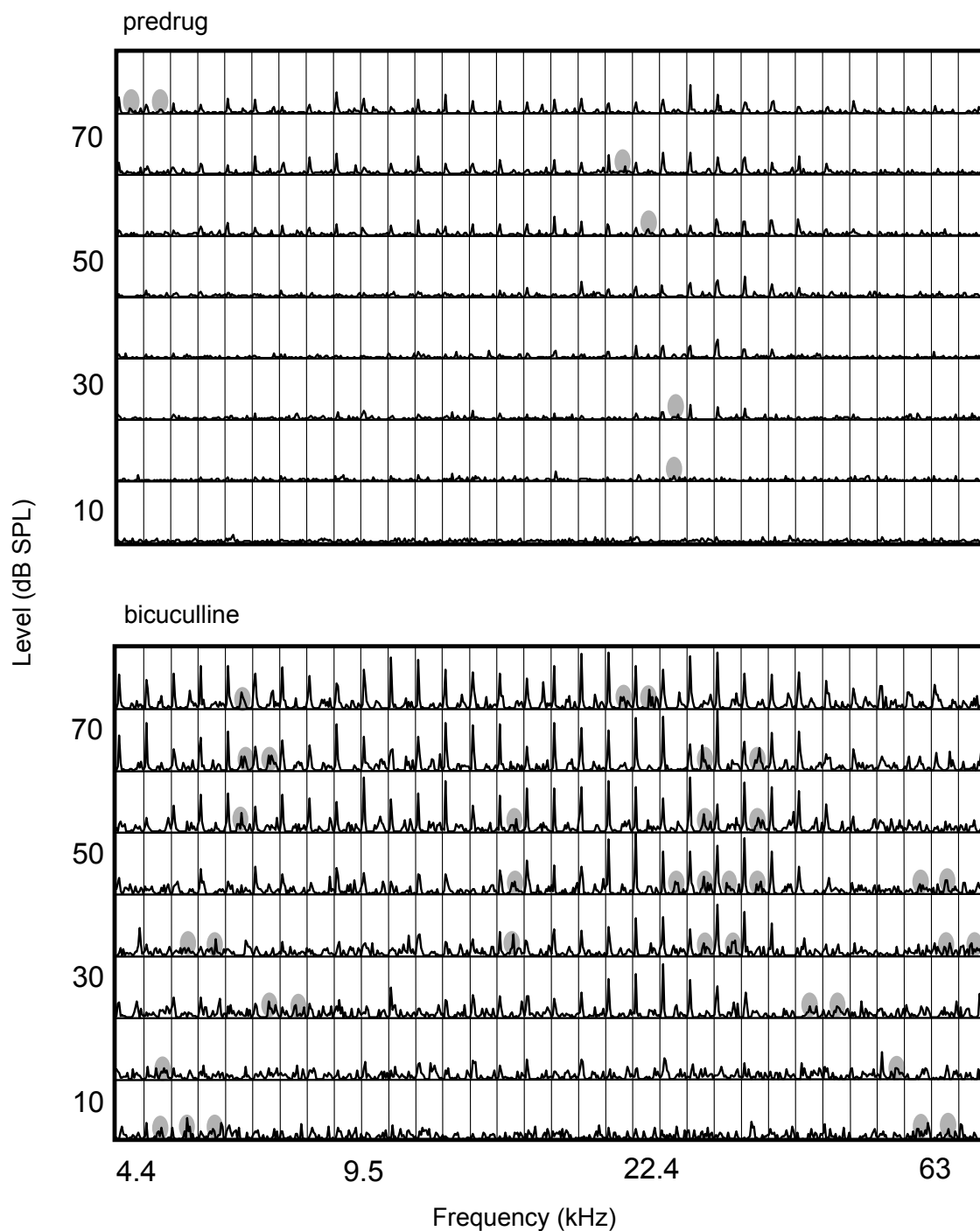


Figure 20 Receptive fields of a multi unit in layer V composed of single PSTHs before (*upper panel*) and during (*lower panel*) the application of bicuculline (10-15 nA). The unit exhibits a significantly elevated activity between 200-300 ms after stimulus onset (indicated by grey ellipses). PSTH bin width is 20 ms. PSTH y axis is 50 spikes. PSTH x axis is 400 ms. Stimulus duration is 50 ms. 10 averages.

The receptive field of a multi unit composed of single PSTHs before and during BIC application is shown in Figure 20. The initial onset response occurred with a latency between 20 and 30 ms and was followed by an inhibitory period (Fig.

4 Results

21). Additionally, a second excitatory, late response occurred with latencies between 200 and 300 ms after tone onset. The duration of the late response ranged between 40 and 120 ms. For the multi unit shown in Figure 20, spike rate was calculated in a time window of 200-300 ms after stimulus onset. The neuronal spike activity was above the mean spontaneous activity plus the standard deviation multiplied by a factor of 2 at several frequency-level combinations (indicated by grey ellipses). During the application of BIC, the late response was elicited at more frequency-level combinations than in the predrug situation, especially in the range of the BF. Late responses were elicited at stimulus levels of 20 to 60 dB above the unit's threshold at BF. The responses at lower stimulus levels were caused by spontaneous burst activity. Similar late responses were found for single units.

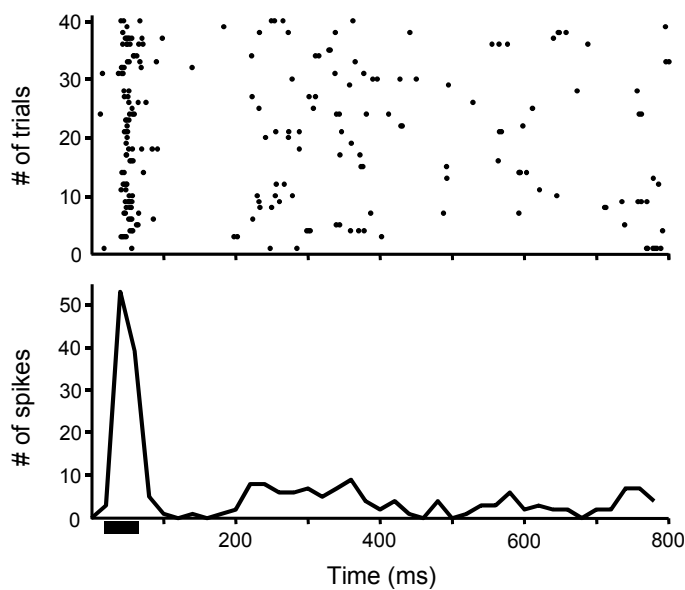


Figure 21 Dot display (A) and PSTH (B) of an unit showing the initial onset response and, after an inhibitory period, a second excitatory response (late response) with a latency of 200 ms and a duration of about 100 ms. (A) Each dot represents the time when an action potential (spike) occurred. (B) PSTH bin width is 20 ms. PSTH x axis is 800 ms. Interpulse interval is 1000 ms. 40 trials. The black bar represents the signal. Same unit as in Figure 20.

To investigate the influence of stimulus duration on the latency and the duration of the late response, I presented a pure tone at a frequency equal to the neuron's BF and at various stimulus intensities (10 to 80 dB SPL) and different stimulus durations (300, 50, and 10 ms; Fig. 22). The late response was independent of the stimulus duration. The response latency was between 200 and 240 ms and the response duration was between 100 and 180 ms. The fact that the timing of the late response was not dependent on the stimulus duration indicates that the late response was correlated with tone onset rather than with

tone offset. The late response was enhanced or induced by blockade of GABA_A-receptor mediated inhibition which clearly shows that it was not caused by a release of inhibition. In units that were tested with a stimulus at BF and an interpulse interval of 1000 ms, a third (Fig. 22, latency of approximately 450-500 ms) and sometimes a fourth response (latency of approximately 620 ms) was observed during the application of BIC. The time interval between the peaks of the excitatory responses ranged between 200 and 300 ms suggesting a rhythmic activity at 3-5 Hz. During predrug condition, most of the units responded with a regular-spiking pattern and changed to generate clusters of high-frequency action potentials (bursts) during the application of BIC.

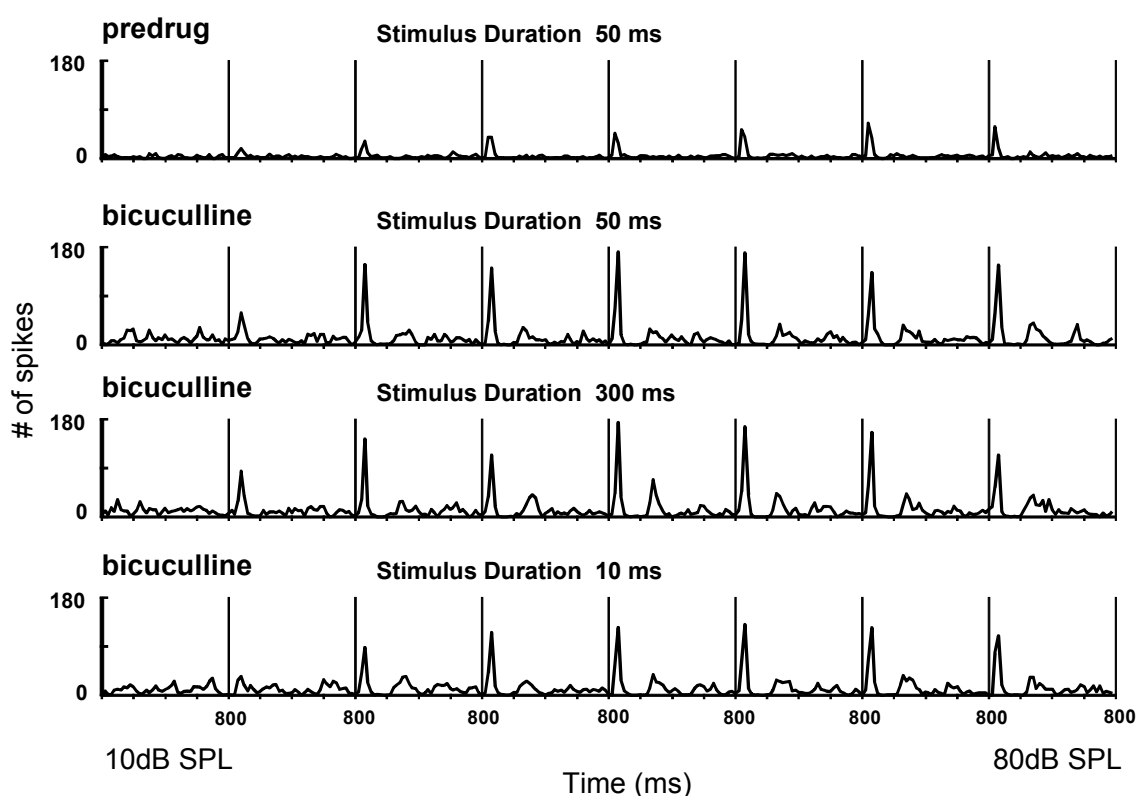


Figure 22 Dependence of the timing of the second excitatory response on the stimulus duration. Each row represents 8 PSTHs recorded with stimulus levels from 10 to 80 dB SPL. The stimulus frequency was at the unit's best frequency. The application of BIC (2nd row) induced a late response ranging between 200 and 400 ms after tone onset. The timing of the late response was not dependent on stimulus duration (3rd and 4th row). PSTH bin width is 20 ms. PSTH x axis is 800 ms. Interpulse interval is 1000 ms. 40 averages.

Interestingly, units that showed a late response during the application of BIC were located in the deep part of layer IV and in layers V and VI. The fact, that

layer V and VI projection neurons are essential for generating thalamocortical and intracortical oscillatory mechanisms and the finding, that multiple late responses could be evoked by GABA_A blockade in these neurons indicate that recurrent excitatory networks can become entrained by small modification of inhibition.

4.8 A neural correlate of comodulation masking release in the auditory cortex of the gerbil

Neurons with best frequencies between 1000 and 4000 Hz were tested for comodulation masking release with combinations of masking stimuli and the test tone (see Fig. 7). A total of 107 single units recorded from A1 were analyzed for this study. Threshold at BF varied between 2 and 30 dB SPL (average: 9.8 dB SPL). The bandwidth of the excitatory tuning curves 10 dB above threshold was 1400 Hz on average (range: 300 - 4600 Hz) and the average Q_{10dB} value was 2.3. For statistical analysis, I randomly selected data of one masker bandwidth for each neuron. Therefore, each neuron was only represented in one of the classes defined by the masker bandwidth to ensure statistical independence.

4.8.1 Responses to unmodulated and comodulated noise

Because masking effects depend critically on excitation caused by the amplitude-modulated masking noise (Mott et al. 1990; Klump and Nieder 2001; Nieder and Klump 2001) responses to the masker alone will be considered first. Maskers had a spectrum level of, on average, 14.8 dB SPL/Hz (5 dB above the average neurons' pure tone threshold). High masker levels of approximately 20-30 dB SPL/Hz above threshold often resulted in a pronounced suppression of the test tone, such that, even at test tone levels of up to 80 dB SPL, a reliable response to the test tone could not be achieved. The activity of single units in response to stimulation of unmodulated respectively comodulated noise did not vary significantly with the bandwidth of the noise ($p > 0.05$, Kruskal-Wallis test; Fig. 23). A pair-wise comparison (Wilcoxon test) revealed that with the

exception of the responses at a noise bandwidth of 200 Hz ($p < 0.05$), there were no significant differences in the units' responses when stimulated with the unmodulated or the comodulated noise ($p > 0.05$).

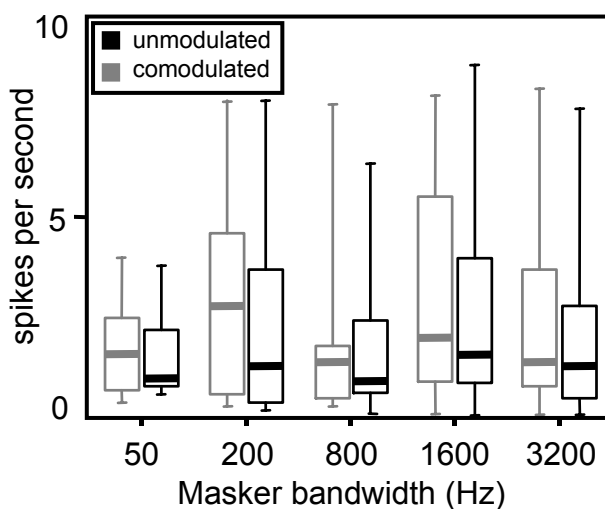


Figure 23 Boxplot showing the median values of the neuronal activity (spikes per second) in response to unmodulated and comodulated noise maskers of different bandwidth. Boxes show the median value and the 25% and 75% percentiles. Whiskers represent 5% and 95% percentiles.

4.8.2 Detection thresholds for test tones masked by unmodulated and comodulated noise

The individual detection threshold of a neuron is positively correlated with the applied spectrum level of the masker. That is, the higher the spectrum level of the masker the higher the expected detection threshold. Because different spectrum levels were applied, it is useful to compute the detection threshold of the tones relative to the spectrum level of the noise masker before averaging detection thresholds of neurons. This ratio is called the “signal to noise ratio”. For the unmodulated noise, the signal to noise ratio increased with increasing masker bandwidth up to a bandwidth of 800 Hz (33.5 dB), remained stable for a masker bandwidth of 1600 Hz (33.7 dB) and then decreased for a masker bandwidth of 3200 Hz (30.1 dB; Fig. 24A). For the comodulated noise, the signal to noise ratio also increased up to a bandwidth of 800 Hz. For bandwidths greater than 800 Hz the signal to noise ratio decreased. To investigate differences in the detection threshold for the test tone between the unmodulated and the comodulated masking condition, pair-wise comparisons (Wilcoxon test) were applied. The masked threshold for detection of the test tone was slightly increased by 1.3 dB (50 Hz) and 0.4 dB (200 Hz) in the comodulated condition versus the unmodulated condition. Therefore, at the two lowest bandwidths

4 Results

tested, a negative release from masking was observed. For maskers of bandwidths of 800, 1600, and 3200 Hz, the detection threshold was improved by 0.35, 5.5, and 6.9 dB, respectively (Fig. 24B), thus showing positive release

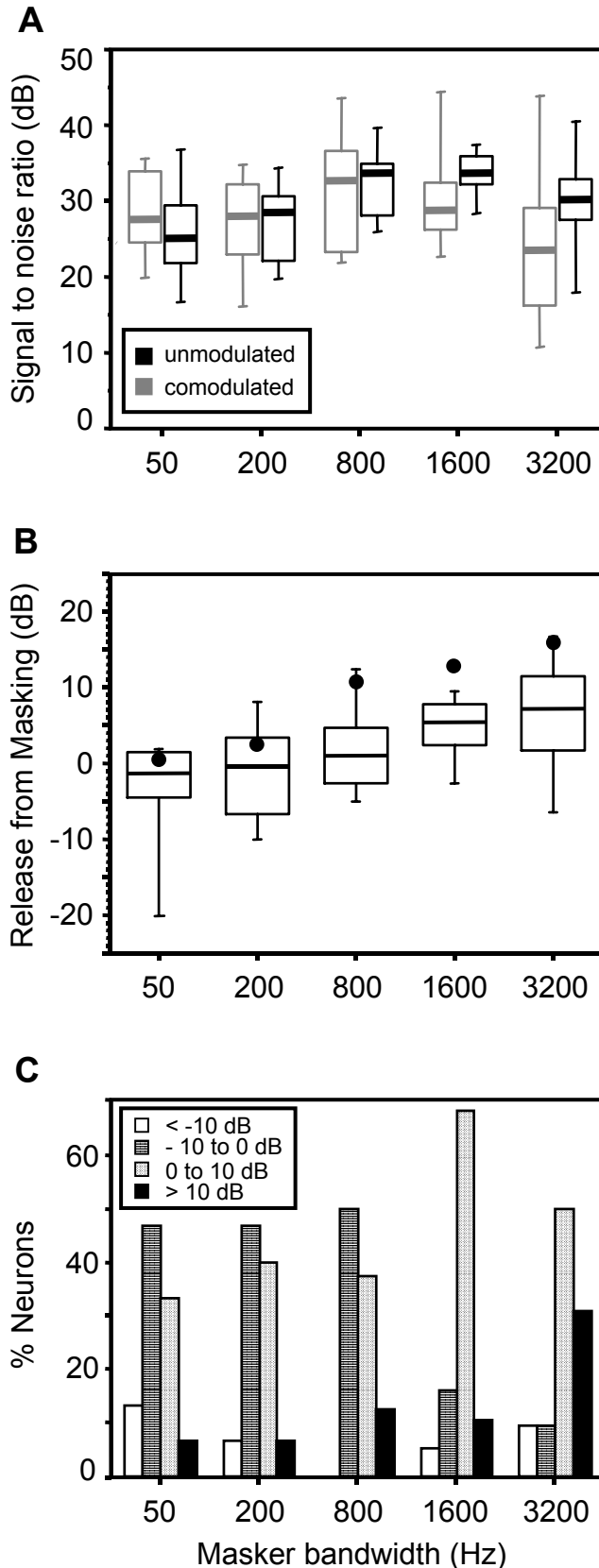


Figure 24 (A) Boxplot showing the median values of the signal to noise ratio (i.e., the signal detection threshold relative to the spectrum level of the masker) as a function of the masker bandwidth for unmodulated and comodulated noise maskers. **(B)** Boxplot showing the median values of masking release as a function of the masker bandwidth. Dots indicate the median values of masking release observed in behavioral experiments (pers. comm., E. Wagner). **(C)** Distributions of the amount of masking release in the randomly drawn sample of neurons when stimulated with different maskers ranging in bandwidths from 50 to 3200 Hz. 3200 Hz: n=42; 1600 Hz: n=19, 800 Hz: n=16; 200 Hz: n=15, 50 Hz: n=15. Boxes show the median value and the 25% and 75% percentiles. Whiskers represent 5% and 95% percentiles.

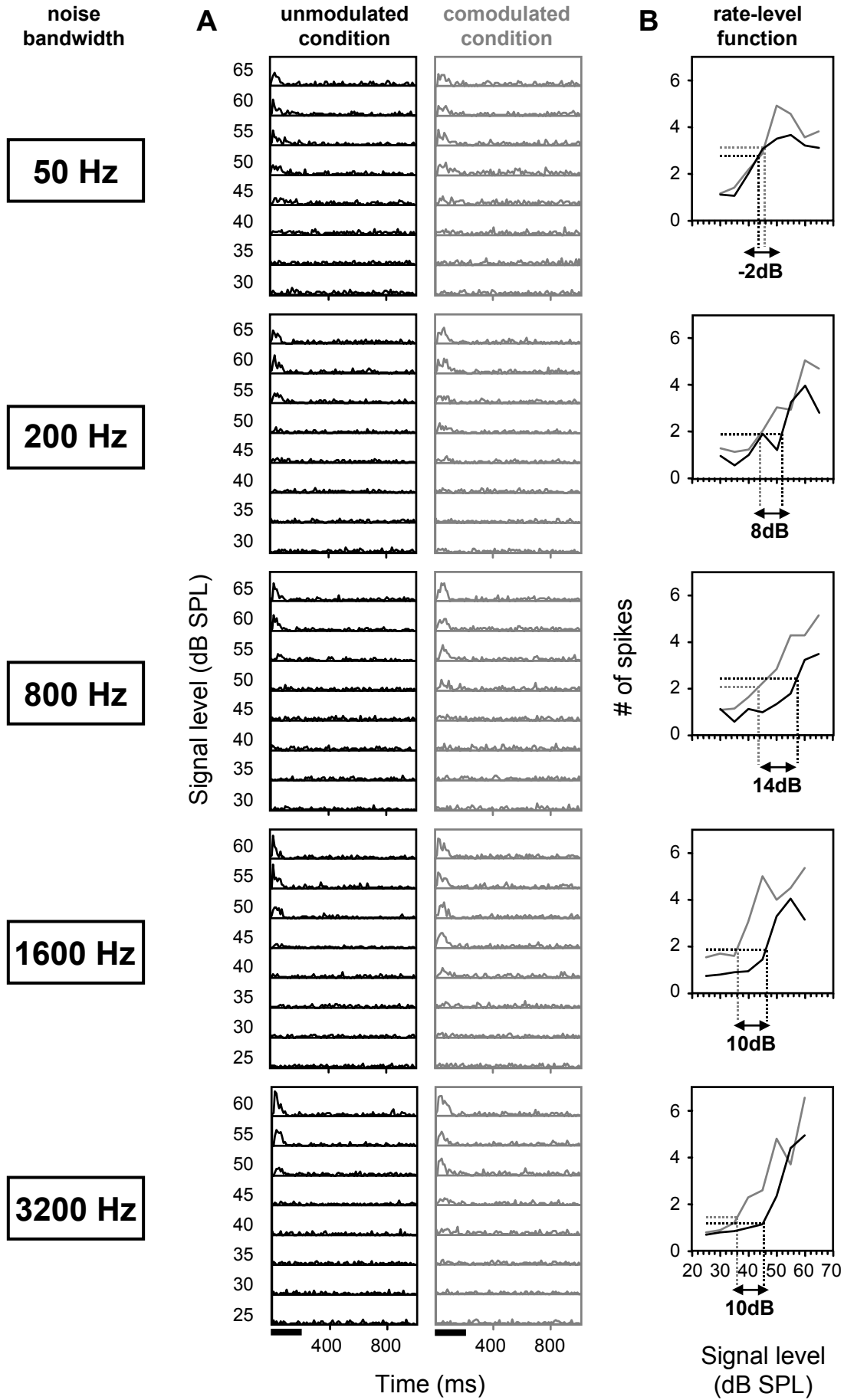
from masking. The detection thresholds for the test tone differed significantly between the unmodulated and the comodulated masking condition for noise bandwidths greater than the auditory filter bandwidth (1400 Hz) of 1600 and 3200 Hz ($p < 0.05$ respectively $p < 0.001$, Wilcoxon test).

There was a significant variation in the neurons' masking release when stimulated with masking noise of different bandwidth ($p < 0.001$; Kruskal-Wallis test). An increase of the amount of masking release with increasing masker bandwidth was observed ($r = 0.41$, $p < 0.0005$, $n=107$). The release from masking was significantly higher at 3200 Hz and 1600 Hz compared to 50 Hz ($p < 0.001$, Mann Whitney U-test) or 200 Hz ($p < 0.01$ respectively $p < 0.05$). The release from masking for a masker of a bandwidth of 800 Hz was not significantly different to release from masking in noise of higher or lower bandwidths.

A similar dependence of the amount of masking release on the masker bandwidth was also observed in individual neurons which could be tested for CMR at several or all masker bandwidths (Fig. 25). In addition, the percentage of units tested for the different bandwidths that showed values of release from masking between -10 and 0 dB decreased with increasing masker bandwidth, and the percentage of units with positive release from masking between 0 and 10 dB or > 10 dB increased with increasing masker bandwidth (Fig. 24C).

On average, the bandwidth of the excitatory tuning curves measured 10 dB above threshold was 1400 Hz. Therefore, maskers of bandwidth of 1600 and, particularly, of 3200 Hz stimulated the signal filter and, additionally, auditory filters remote from the signal filter. The improvement of the detection threshold could be accounted for by comparison across different auditory filters. However, the amount of masking release for maskers of bandwidths of 1600 and 3200 Hz was not correlated with the bandwidth of the tuning curve (i.e. the auditory filter).

4 Results



4.8.3 Release from masking in relation to envelope locking

In a study of the auditory cortex of the cat, Nelken et al. (1999) proposed that neurons which modulate their firing rates coherently with the temporal envelope (a phenomenon called “envelope locking”) represent a neural correlate of CMR. The relevant cue to detect a test tone in noise would be the decrease in the strength of envelope locking when a test tone is added to masking noise. To investigate whether release from masking observed in the present study is correlated with the neurons’ ability to envelope locking, I presented a 10 Hz sinusoidally amplitude-modulated band-pass noise (the unmodulated noise was multiplied by a 10-Hz sinusoidal envelope, modulation depth was 100%) to 10 neurons. Four of these neurons modulated their firing rates coherently with the temporal envelope whereas the remaining 6 neurons did not show envelope locking (Fig. 26). Out of the 10 neurons, 7 neurons showed substantial positive release from masking between 3.7 and 16.7 at a masker bandwidth of 1600 (n=1) and 3200 Hz (n=6). The fraction of these neurons that locked to the envelope (4/7) was approximately equal to the fraction of the neurons that did not lock to the envelope (3/7). A Fisher exact probability test indicates that release from masking as analyzed in this study does not necessarily require envelope locking (two-tailed, $p > 0.05$).

Figure 25 Dependence of the release from masking on the masker bandwidth in an individual neuron. PST-histograms (**A**) and the corresponding rate-level functions (**B**) for signals masked by unmodulated (black) or comodulated (grey) noise. Black bars in (A) represent the signal. PSTH bin width is 10 ms. PSTH y axis is 1.5 spikes. Neuron’s BF was 2.5 kHz. Noise spectrum level is 23 dB SPL/Hz and, hence, 14.1 dB above the neuron’s pure tone threshold (8.9 dB SPL) at BF. Dotted lines in (B) represent detection thresholds in the unmodulated (black) and comodulated (grey) condition.

4 Results

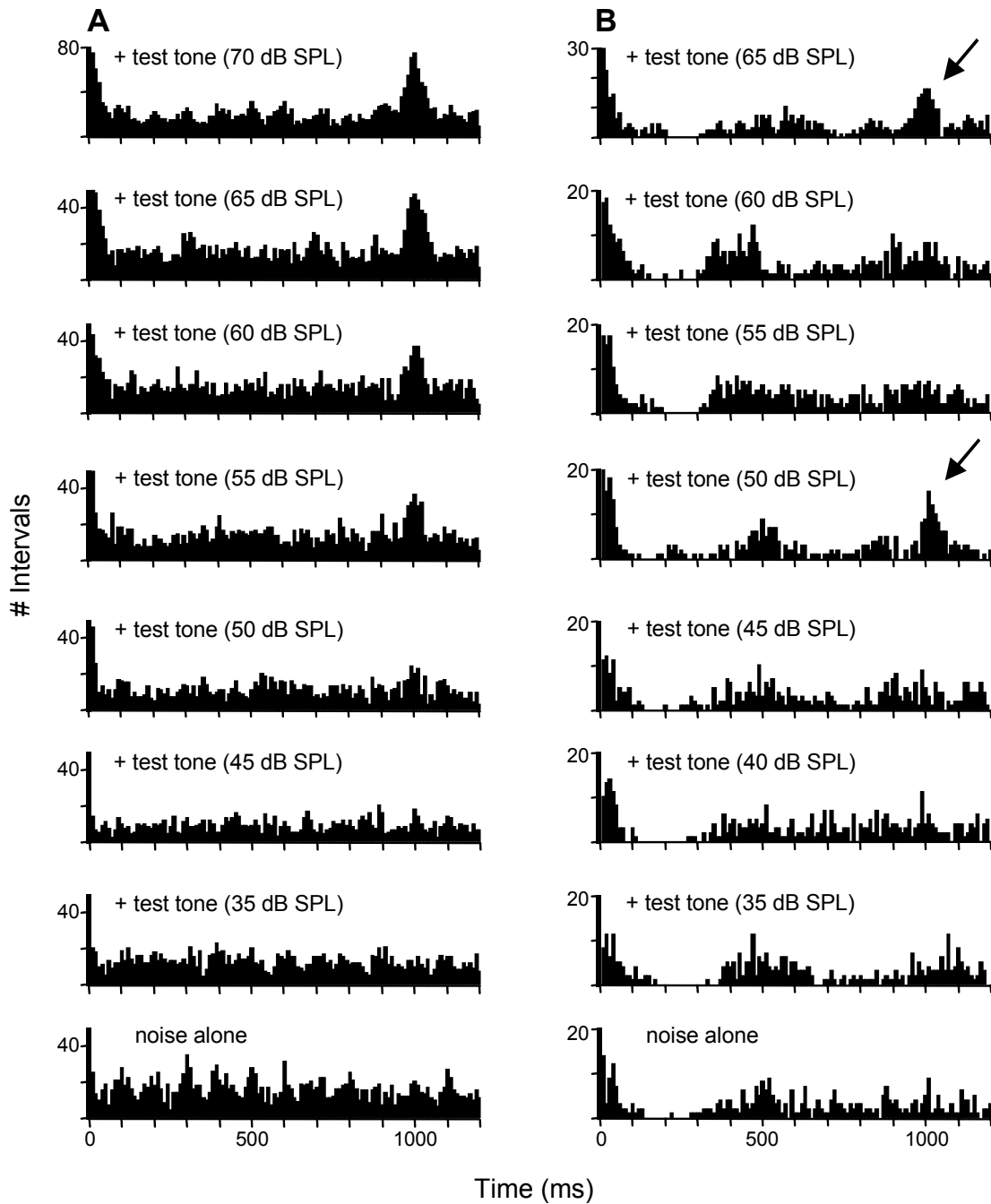


Figure 26 Autocorrelation histograms computed from the activity of two neurons during the response to a 10-Hz sinusoidal modulated noise (bandwidth 3200 Hz) alone or in combination with a test tone at different test tone intensities. The interstimulus interval of the test tone is 1000 ms. Both neurons showed large positive release from masking. Bin width is 10 ms. **(A)** Neuron that locked to the temporal envelope when the masking noise alone was presented. Adding the test tone, envelope locking degraded and a peak at 1000 ms appeared indicating a response to the test tone. This is consistent with the study of Nelken et al. (1999). However, in contrast to Nelken et al. (1999), there was again pronounced envelope locking at a higher test tone intensity (70 dB SPL). Release from masking is 9.5 dB for a masker bandwidth of 3200 Hz. **(B)** Neuron that did not lock to the temporal envelope. Response to the test tone is indicated by the peak in the correlograms at 1000 ms (arrows). Same masking conventions as in (A). Release from masking is 16.2 dB. At an interval of 0 ms, the number of intervals, which is equal to the total number of spikes, exceeds the y axis. For simplicity, the number of intervals in the first bin was restricted to the maximum value of the y axis.

4.8.4 Blockade of GABA_A receptors does not influence the amount of masking release

For 10 units, the release from masking could not be calculated because the rate-level functions of the onset response to the masked signal did not reach the detection threshold either in the unmodulated condition ($n=3$), the comodulated condition ($n=3$) or both ($n=4$) with the experimental paradigm used. I suggest that, in these neurons, masking noise at a high spectrum level completely suppressed the neurons' response to the test tone.

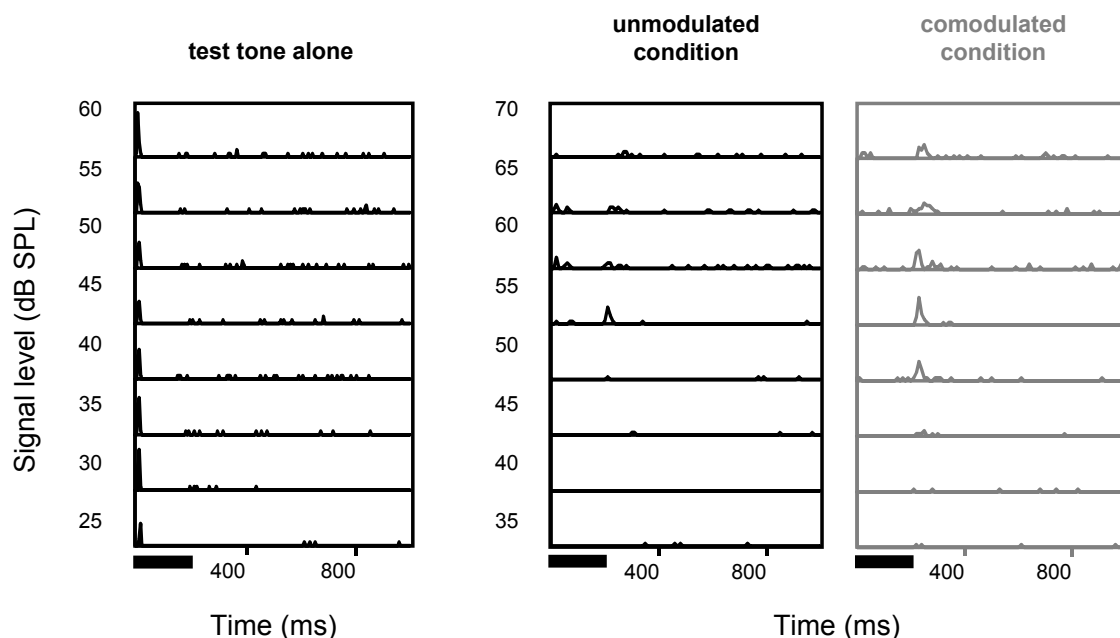


Figure 27 Neuron that showed suppression during simultaneous presentation of masking noise and the signal. PSTHs of the neuron's response to the test tone alone (*left panel*) and to the test tone when masked by unmodulated (*middle panel*) or comodulated (*right panel*) noise. Black bars represent the signal. The neuron's BF and, hence, the signal frequency is 1.8 kHz. Noise bandwidth is 3200 Hz. Noise spectrum level is 13 dB SPL/Hz and, hence, 4.5 dB above the neuron's pure tone threshold at BF (8.5 dB SPL). *Left panel*: PSTH bin width is 5 ms, PSTH y axis is 1.5 spikes. *Middle and right panels*: PSTH bin width is 10 ms, PSTH y axis is 0.5 spike.

This view is supported by the fact that in some units, suppression by simultaneous presentation of masking noise and the test tone as well as an offset response to the test tone was observed (Fig. 27). For 11 neurons a release from masking in response to the offset of the signal could be calculated. Release from masking in response to the offset of the signal ranged from -5.8

4 Results

to 28.6 dB (Fig. 27: 10 dB). Six out of these neurons also showed responses to the onset of the signal, and were included in the statistical analysis. However, because of their low number, neurons for which only offset responses could be calculated were excluded from the statistical analysis.

Similar to psychoacoustic experiments in the gerbil (Kittel et al. 2000), the physiological data show that release from masking increased with increasing masker bandwidth. As shown in the experiments described above, the blockade of GABA_A-receptor mediated inhibition by iontophoretic application of bicuculline resulted in an increase of the bandwidth of tuning curves, implicating existing inhibitory sidebands. One hypothesis is, that maskers extending into the neurons' inhibitory sidebands cause a reduction of the excitatory masker-driven response and, thus, decrease the detection threshold for the test tone. To get an insight into the role of GABAergic inhibition in release from masking, the signal detection for maskers of bandwidths between 50 and 3200 Hz was measured before and during application of BIC in 13 neurons (Fig. 28). Three of these neurons were tested at two masker bandwidths. In 11 neurons, a tuning curve could be measured before and during the application of BIC. In 9 of these neurons, the application of BIC resulted in a broadening of the tuning curve measured 10 dB above threshold. The neurons' response to the comodulated and the unmodulated noise was increased during the application of BIC ($p < 0.01$, Wilcoxon test). As mentioned above, a release from masking could not always be defined because rate-level functions calculated for the onset spike activity did not achieve the threshold criterion. In 3 out of the 13 neurons, a detection threshold could reliably be defined in the unmodulated but not in the comodulated situation. However, the blockade of GABAergic inhibition caused an increase in spike activity, and a signal detection threshold could be defined in both masking conditions (Fig. 28B). In 10 neurons, the release from masking before and during application of BIC could be compared. The amount of masking release increased in 6 neurons by 0.2–29.4 dB and decreased in 4 neurons by 0.6–7.2 dB during the application of BIC (median: 2.1 dB). On average, the amount of masking release was not significantly different before and during the application of BIC ($p > 0.05$, Wilcoxon test). There was no correlation between the change of masking release caused by BIC application

and the broadening of the filter bandwidth or the masker bandwidth ($p > 0.05$, Spearman). For example, the neuron shown in Figure 28A, exhibited substantial release from masking at a masker bandwidth of 3200 Hz. Because the filter bandwidth was 1200 Hz, the masker presumably extended into the neuron's inhibitory sidebands. Indeed, during the application of BIC, the filter bandwidth increased by 600 Hz. However, during the application of BIC, the release from masking was unchanged suggesting that, for this neuron, the extension of the masker into inhibitory sidebands was not essential for masking release.

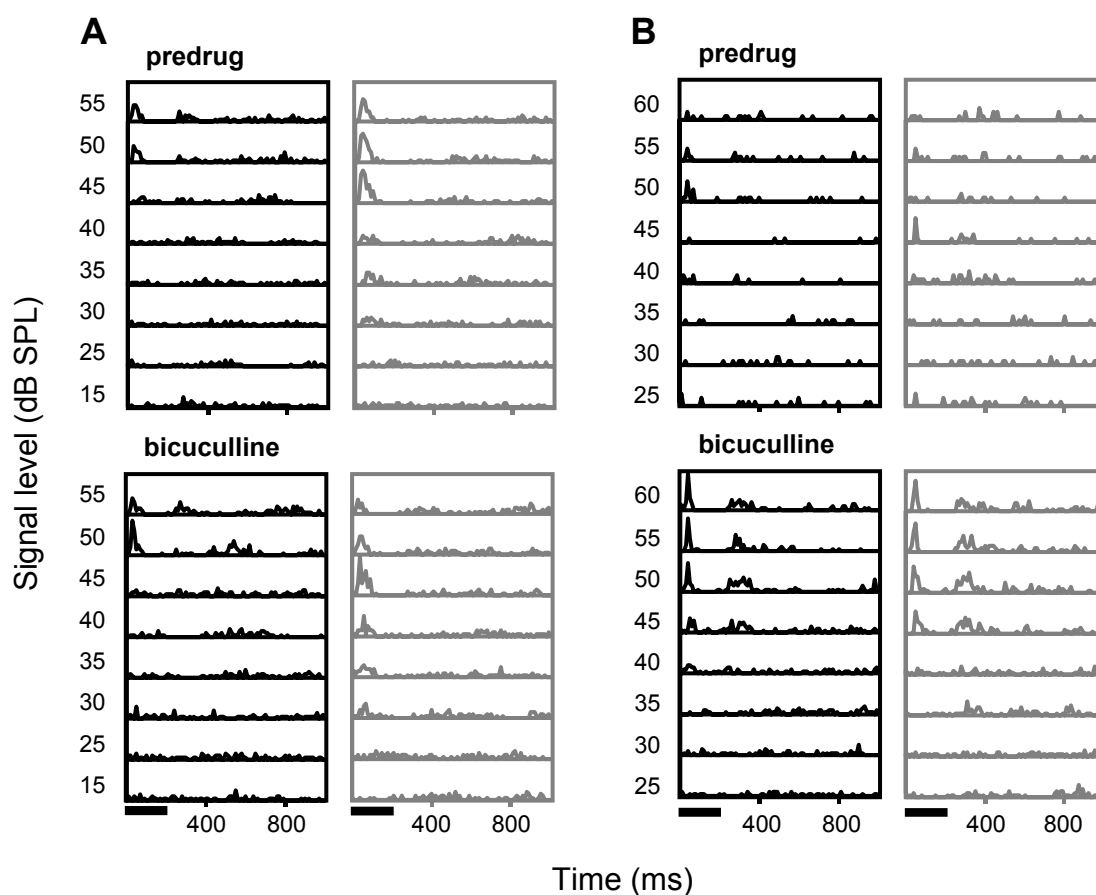


Figure 28 Examples of the effect of bicuculline application on signal detection in background masking noise. **(A)** Neuron that showed a release from masking of 17.2 dB before (*upper panels*) and 16.6 dB during (*lower panels*) the application of bicuculline (25 nA) when masked by noise of 3200 Hz bandwidth. The spike rate during the presentation of the masker alone was slightly increased during BIC application (25% respectively 42% in the unmodulated respectively the comodulated condition). PSTH bin width is 10 ms. PSTH y axis is 1 spike. **(B)** Neuron that showed a weak onset activity in response to the signal when masked by noise of 200 Hz bandwidth (*upper panels*). A release from masking could not reliably be defined. However, the application of BIC (*lower panels*) resulted in a consistent onset and offset activity in response to the signal and a release from masking could be computed (-4 dB). PSTH bin width is 10 ms. PSTH y axis is 0.5 spike (predrug) and 1 spike (bicuculline). Black bars represent the signal.

5 Discussion

5.1 Methodological consideration

Concerning the layer specificity of the effect of bicuculline on frequency tuning it was important to get an insight into the diffusion range of bicuculline. The diffusion range of BIC can extend up to 400 μm . This implies that in those parts of my experiments where larger injection currents were used, BIC could have exceeded laminar boundaries, especially in the upper layers. The resulting effect of BIC application, therefore, can reflect the sum of activity caused by blockade of GABA_A receptors located on neuronal elements near the recording site as well as on neurons situated in layers adjacent to the recording site. Additionally, it has to be kept in mind that neurons in different layers differ in their somatic shape and dendritic tree geometry. Typical pyramidal neurons integrate inhibition from several spatially separated input regions, e.g., they send the apical dendrite to layer I where its terminal tuft receives inhibitory input which can not be assessed by local pharmacological application close to the cell body. Therefore, inhibition might be even more complex than demonstrated in this study. Pharmacological manipulation of inhibition in the different cortical layers while recording from one neuron in a specific layer might reveal the whole extent of inhibitory interactions in a cortical column.

5.2 Comparison of pharmacological blocking of GABA with other studies

The observation that the blockade of GABA_A receptors led to a pronounced increase of neuronal firing, even in the absence of sound, shows that GABA_A receptors were tonically activated by the release of GABA and that these receptors were involved in the regulation of neuronal activity. The change of receptive field size was analyzed for units in which an increase of discharge and/or spontaneous activity was observed. The pharmacologically induced loss of inhibition allowed expression of excitatory inputs from frequencies which

were originally not apparent as part of the excitatory field of a given unit because they were masked by the inhibition.

Sharpening of frequency tuning curves by GABAergic inhibition takes place at different levels in the auditory system as demonstrated in pharmacological studies (e.g., dorsal cochlear nucleus of the rat: Yajima and Hayashi 1990; inferior colliculus of bats: Vater et al. 1992; Yang et al. 1992; Klug and Pollak 2000; medial geniculate body of the mustached bat: Suga et al. 1997; auditory cortex analogue in the bird: Müller and Scheich 1988). Comparable to data of Wang et al. (2000) in A1 of the chinchilla, the present study shows that intracortical GABAergic inhibition was involved in sharpening the receptive field in the majority of the A1 units. In the present data, the effects of BIC on the receptive fields were most obvious in a lowering of the Q_{40dB} values. This indicates that inhibitory mechanisms are mainly effective at moderate or higher stimulus levels. GABA-mediated inhibitory sidebands were present at both the high- and the low-frequency flanks of the excitatory tuning curve in 29% of the units. The higher percentage of neurons in the chinchilla A1 (61% out of 36 neurons) that showed an expansion along both sides of the tuning curves could be related to a generally more narrow tuning in the chinchilla A1. However, direct comparison with the present data is difficult since Wang et al. (2000) did not provide sufficiently detailed information about their threshold criterion. In contrast to the present findings, a study by Schulze and Langner (1999) which investigated the processing of amplitude modulation, did not show a significant expansion of the frequency response range measured 30 dB above threshold during the application of BIC in the gerbil A1. The present data would suggest that, at this stimulus level, inhibitory influence is prominent in many units. The discrepancy between my data and the results of Schulze and Langner (1999) could result from differences in the methodological procedures concerning iontophoresis or reflect a sampling bias since they tested the effect of BIC on receptive fields in only 23 units that were taken exclusively from the low-frequency region of A1.

5.3 Effect of pharmacological blocking of GABA compared with two-tone masking in the auditory cortex

An enlargement of receptive fields of auditory cortex neurons has also been shown in two-tone masking studies (e.g., Shamma and Symmes 1985; Sutter and Schreiner 1991; Shamma et al. 1993; Calford and Semple 1995; Brosch and Schreiner 1997; Sutter et al. 1999). In the present study, the percentage of tuning curves with symmetric inhibitory sidebands is in the range of data from two-tone masking studies where 30% (ferret: Shamma et al. 1993) and 38% (cat: Sutter et al. 1999) of the neurons showed an inhibitory sideband on both the high- and the low-frequency flanks of the tuning curve. In the latter study, the inhibitory areas ranged from a single inhibitory band to more than four inhibitory regions. Cells with the simple two-band inhibitory structure were more common in the ventral part of the cat A1, corresponding to an increased tuning sharpness, the high degree of nonmonotonicity, and a high percentage of GABAergic neurons found in this cortical area (Schreiner and Mendelson 1990; Schreiner et al. 1992; Prieto et al. 1994a; for review: Ehret 1997). Tuning curves with complex structure were more common in the dorsal A1 and related to the higher percentage of multi-peaked and broadly tuned neurons in this cortex region. Information about a similar functional organization in the gerbil is not yet available. From two-tone masking studies, there is evidence that the bands between the excitatory areas are caused by inhibition. In the present study multi-peaked tuning curves could be converted to single-peaked tuning curves by the local application of BIC. This suggests that intracortical GABA_A-mediated inhibition plays an important role in producing these inhibitory bands and, hence, multi-peaked tuning curves.

In the present study, the extent of the expansion of up to 3.6/1.68 octaves at the low-/high-frequency side is basically similar to that reported by Shamma and Symmes (1985) for the squirrel monkey. However, it needs to be kept in mind that two-tone masking measures a net suppressive effect which includes mechanical suppression in the cochlea and inhibitory actions at all levels of the auditory system. Furthermore, the degree of two-tone inhibition strongly

depends on several stimulation parameters, e.g., the timing between the stimuli and the position of the fixed stimulus in respect to the excitatory response area (Calford and Semple 1995; Brosch and Schreiner 1997; Brosch et al. 1999). As shown in Figure 10, a direct comparison of the effect of pharmacological compounds that modify intracortical inhibition with the influence of two-tone masking in individual neurons could elucidate the relative contribution of intracortical and subcortical inhibitory mechanisms in shaping auditory tuning curves. The two-tone masking paradigm showed that frequencies outside the excitatory tuning curve inhibited the response to a frequency within the excitatory tuning curve. However, this is not necessarily the same as showing that the GABA_A-receptor blockade enlarged the tuning curve. To show conclusively that the inhibition which was blocked by BIC is also responsible for the inhibition seen in the two-tone masking paradigm, a comparison of two-tone masking curves before and during BIC application is necessary.

5.4 Is there a layer-specific strength of inhibition?

In the auditory cortex of the gerbil, an increased tuning sharpness in layers III and IV has been reported (Sugimoto et al. 1997). This could have been caused by the specific input from neurons of the ventral division of the medial geniculate body which are known to be sharply tuned, e.g., in the cat (for review: Clarey et al. 1992). The broad tuning in layers I and VI could be caused by diffuse inputs from the medial division of the medial geniculate body (Sugimoto et al. 1997). In the present study, a layer-dependent change of tuning sharpness as quantified by Q_{10dB} and Q_{40dB} values could not be observed. The most likely reason for the discrepancy of these data with that of Sugimoto et al. (1997) could be the methodological difference in defining tuning curves. In contrast to Sugimoto et al. (1997), who defined tuning curves using an audio-visual method, I used random stimulus presentations to measure a detailed response area. From the corresponding response area, the tuning curves were then calculated by a software program which took into account a standardized threshold criterion. The whole procedure yielded tuning curves which, in comparison to those of Sugimoto et al. (1997), were more complex and also slightly broader. Indications that the tuning characteristics are

5 Discussion

independent of cortical depth have also been found for the bat (Chen and Jen 2000), mouse (Shen et al. 1999), and cat auditory cortex (Abeles and Goldstein 1970).

The neurophysiological data showed that the strength of inhibition, as quantified in comparison of several response parameters in predrug conditions and GABA blockade, was not significantly layer-dependent. This is consistent with data of a recent study (Chen and Jen 2000) that showed a similarity of the expanded tuning curves measured during BIC application within an orthogonal penetration in the auditory cortex of a bat species. The high percentage of silent neurons that was found in layer VI suggests that inhibition is strong in the deep layers of A1, which is similar to data from the somatosensory cortex (Dykes et al. 1984).

The percentage of GABAergic neurons found in the gerbil (15%) is between that reported for the cat (24.6%; Prieto et al. 1994a) and the ferret auditory cortex (10.4%; Gao et al. 1999). The proportion of GABAergic neurons appears to be species-specific, since values for sensory cortical areas of the ferret are generally lower than reported for cat neocortex. In cat A1, the percentage of GABAergic neurons peaks in layers I and V, which is comparable to the present data. However, the respective percentages are higher in the cat, especially in layer I. Since most neurophysiological data are from pyramidal cells in layers II, III, V and VI, puncta on pyramidal cells were counted in these layers. The number of puncta was highest for layer V pyramidal cells. However, one has to take into account the larger somatic size of these cells. Indeed, when the number of puncta was related to the cell perimeter, no significant difference was found across layers.

In the neurophysiological data, no layer-specific effects of inhibition were found, except for a high percentage of silent neurons in layer VI. With the method used in this study I mainly measured inhibition mediated by GABAergic synapses on the cell soma and, therefore, could not assess a possible layer-specificity of more distant dendritic inhibitory synapses.

5.5 Potential functional role of silent neurons in the auditory cortex

In some units that did not respond to pure tones under control conditions, BIC elicited auditory responses that were frequency-tuned. These neurons were silent, not because of a lack of excitatory input, but because a tonic GABA_A-receptor mediated inhibition completely suppressed their ability to respond to pure tone stimuli. Silent neurons were also reported in the inferior colliculus of horseshoe bats (Vater et al. 1992), in the bird auditory cortex analogue (Müller and Scheich 1987), and in cat somatosensory cortex (Dykes et al. 1984). One could argue that anaesthesia could lead to a change of response pattern and possibly to a complete suppression of neuronal activity of neurons. However, in the case of the anaesthetic used in this study (ketamine/xylazine), a possible change of the response pattern would most probably not be caused by an influence on GABAergic receptors but, if at all, by a blockade of glutaminergic receptors (NMDA receptors). The strongest argument against the possibility that silent neurons are due to a general effect of anaesthesia is the fact that such neurons were almost exclusively found in the deep layers. This property implies a more specific physiological response characteristic inherent to the neurons. Similar to the present data, Dykes et al. (1984) found silent neurons mainly in superficial and deeper layers. Dykes et al. (1984) routinely applied glutamate to isolate neurons in all layers and to detect silent neurons in the somatosensory cortex of the cat. Usually, I did not apply glutamate to search for neurons and, consequently, in the present study silent neurons might be underrepresented. Therefore, the percentage of silent neurons in layer VI might be even higher suggesting that tonic inhibition is remarkably pronounced in this layer. In the present study, most of these neurons were found in layer VI. Neurons in layer VI mainly project to the contralateral cortex. They represent major output neurons of the cortex, and it may be of functional significance that their activity can be completely switched off by appropriate GABAergic inhibition.

The existence of subthreshold excitatory inputs to neurons that are normally suppressed by inhibition suggests a functional role of silent neurons in plasticity and learning. These units are silent until the appropriate behavioural context or

stimulus properties are present. Once a stimulus gets a behavioral relevance, GABA-mediated inhibition could be abolished and silent neurons participate in information processing in auditory cortex. This could lead to structural changes in neuronal networks which could be involved in the apparent plasticity in the auditory cortex (Jones 1993). For example, training of monkeys at a particular tone frequency resulted in an expansion of the corresponding frequency representation in the auditory cortex of the monkey (Recanzone et al. 1993).

5.6 Late responses

The appearance of multiple responses during BIC application indicates that, by blocking GABA_A-receptor mediated inhibition, recurrent excitatory networks were activated. Neurons exhibiting late responses were found in the deeper cortical layers where projection neurons are located. Pyramidal neurons located in layer V that show bursting activity have been suggested to be part of oscillatory thalamocortical networks in the auditory cortex (Hefti and Smith 2000). It could be possible that the oscillation observed in this study was generated by a thalamocortical network. Such coherent oscillations are known to occur during waking and sleep and could contribute to the strengthening of synaptic contacts. Another possible explanation could be an intracortically generated oscillation. Intracellular studies in the neocortex showed that BIC caused synchronization of neurons, and intrinsically bursting cells have been hypothesized to be involved in the propagation of this synchronization in cortical slices (Chagnac-Amitai and Connors 1989) and might serve as event detectors (Lisman 1997). The rhythmic spike pattern observed in the present study resembles a component of a seizure that was recorded intracellularly and in field potentials in the cat neocortex (for review: Steriade 1999). This seizure consisted of spike-wave and poly-spike wave complexes at 2-4 Hz and faster components at 10-15 Hz occurring spontaneously and electrically induced. This activity pattern is known from some types of epileptic encephalopathy in humans. Evidence for a cortical origin of such seizures is the disappearance after decortication, their survival after thalamectomy (Steriade and Contreras 1998) and the presence of similar types of seizures in isolated cortical slabs (Timofeev et al. 1998). Similar to the present study, Steriade and Contreras

(1998) observed that disinhibition is an additional mechanism in the generation of cortical seizures. Hefti and Smith (2000) reported that bath-applied GABA_A-receptor antagonists at concentrations that totally blocked inhibition caused prolonged epileptiform activity in cortical slices. Systemic application or small amounts of bicuculline leaked into the cortex elicited seizure patterns similar to that in occurring spontaneously or electrically induced paroxysm.

In congenitally deaf cats, that were electrically stimulated with a cochlear implant, a late component in the field potentials of A1 was observed which was not present in naive cats (Klinke et al. 1999). This suggests that late responses reflect a complex cortical information processing that has to be established by auditory experience. Interestingly, a recent study of Supèr et al. (2001) demonstrated a late response in neuronal activity in the primary visual cortex of the monkey that was correlated with the monkey's perceptual awareness of a visual object. The same group of authors previously found that the late response disappeared when the animal was anaesthetized (Lamme et al. 1998). In the present study, the late response was observed in the lightly anaesthetized gerbil and could be enhanced by GABA_A-receptor blockade. This could imply that perceptual awareness in awake animals is related to a decrease of inhibition.

5.7 A neural correlate of comodulation masking release

In the animal kingdom, the separation of acoustic behaviorally relevant signals from background noise is necessary to facilitate communication. The natural situation can be reflected in psychoacoustic experiments that present a signal (usually a pure tone) in masking noise that has to be detected by the human listener or an animal. In psychoacoustics, it has been shown that the detection of an acoustic signal is improved when the masking noise is similar to natural background noise, i.e., when the frequency bands of the masking noise are coherently amplitude-modulated ("comodulated"). Comodulation masking release has been observed in humans and animals and general mechanisms were found.

5.7.1 Comparison of behavioral and neural masking release

Similar to results from a behavioral study in the gerbil (Kittel et al. 2000; E. Wagner, pers. comm.), the release from masking increased with increasing masker bandwidth (Fig. 24B). In contrast to the behavioral study in which a median release from masking of 15.7 dB was observed for maskers of a bandwidth of 3200 Hz, the median neuronal release from masking was 6.9 dB. One explanation for this difference could be that the neural data were derived from anaesthetized animals. Another reason could be that the neural data are based on single neurons whereas a network activity and synchronization of neurons could be essential for an optimal separation of signal and background analogous to object recognition in the visual system (review: Singer and Gray 1995). However, two approaches are commonly used in comparing behavioral and neuronal detection thresholds. Either the neuronal population average predicts the behavior or the behavior is explained by the most sensitive neurons. Psychophysical detection thresholds are often represented by the responses of the most sensitive neurons (Parker and Newsome 1998). For a masker bandwidth of 3200 Hz, 6 out of 45 neurons showed a masking release that was close to the value of the median behavioral masking release of 15.7 dB or even better. Thus, the most sensitive results of this study are in good agreement with behavioral data.

5.7.2 Possible neural mechanisms contributing to CMR in the gerbil primary auditory cortex

It has been proposed that across-channel cues are required to improve the ability to detect a signal in masking noise (e.g., Buus 1985). The signal is presented in one auditory filter and the masking noise covers the signal filter and flanking auditory filters. A comparison of the coherently modulated output of the flanking filters with the output of the signal filter, that shows a changed envelope by adding the signal, could lead to an improved signal detectability in comodulated noise. This would imply that increasing the masker bandwidth beyond the bandwidth of the tuning curve, the amount of CMR would increase. Maskers having a greater bandwidth than the bandwidth of the unit's excitatory

tuning curve extend into inhibitory sidebands. One could suggest that these frequency bands inhibit the neuron's response to the masking frequency bands represented in the excitatory tuning curve and, thus, improve the signal detection. This effect would be more pronounced in the comodulated than in the unmodulated situation which would result in an increased release from masking. With the experimental paradigm used in this study, it was investigated whether cross-channel mechanisms contribute to CMR.

The average filter bandwidth of auditory cortex neurons in the gerbil was 1400 Hz. For masker bandwidth of 50 and 200 Hz, a small negative release of masking was found. At 800 Hz bandwidth, a small positive release of masking was observed that increased when increasing the masker bandwidth to 1600 and 3200 Hz, beyond the auditory filter bandwidth (Fig. 24B). This suggests that cross-channel comparison is contributing to CMR. However, the amount of release from masking was not correlated with the neurons' filter bandwidth. In a recent behavioral study in the gerbil, CMR was investigated using narrow-band maskers (Wagner and Klump 2001). The masker consisted of two narrow-band noise stimuli (bandwidth 25 Hz). One band of noise was centered on the signal frequency (2 kHz). The center frequency of the flanking noise band was between 400 and 3600 Hz. Because the psychoacoustically determined auditory filter bandwidth at 2 kHz is 216 Hz in the gerbil (Kittel et al. 2001), the flanking bands of noise were represented in channels remote from the signal channel. Adding an uncorrelated 25-Hz-wide flanking band of noise did not effect the gerbils' detection threshold for a pure tone. Adding a correlated 25-Hz-wide band of noise improved the detection threshold considerably, thus, indicating CMR. This behavioral experiment showed that the gerbil used cross-channel comparison to improve signal detection.

The present study suggests that even if the gerbil can use cross-channel comparison, this is, at least for some neurons, not necessarily required for CMR. The influence of inhibition on CMR was tested in a preliminary series of measurements and further data still have to be obtained. In the present study, the spectrum level of the masker had to be adjusted to a value of, on average, only 5 dB above the neurons' pure tone threshold to avoid a complete suppression of the signal. This paradigm is not ideal for investigating effects of

5 Discussion

inhibition, because inhibitory sidebands are more pronounced at higher stimulus levels (see chapter 4.6.2). However, in 10 units, the role of inhibition in masked signal detection could be tested before and during bicuculline application. The preliminary data suggest that the effect of bicuculline on the signal detection was not different between the comodulated and the unmodulated condition. Thus, release from masking was independent of the position of the masking noise bands in respect of the neurons' inhibitory sidebands. This implies that within-channel cues are more relevant than across-channel comparison. Recently, the role of sideband inhibition on neural release from masking was tested in the starling's (*Sturnus vulgaris*) auditory forebrain (Klump and Nieder 2001; Nieder and Klump 2001) which is the analogue of the mammalian primary auditory cortex. In contrast to the auditory cortex of mammals, most neurons in the bird's auditory forebrain show clear inhibitory sidebands that are characterized by a significantly lower neural activity than the discharge level in the unit's excitatory tuning curve (Nieder and Klump 1999). Therefore, inhibitory sidebands can be visualized without pharmacological manipulation. Consistent with the present data, inhibitory interactions between different auditory filters did not appear to play a role in release from masking.

The present neurophysiological data are different in one important aspect from that obtained in the auditory cortex of the anaesthetized cat. In the gerbil, it was the increased rate of neuronal discharge that indicated the presence of the test tone in masking noise, and this increase was observed at lower test tone intensities in comodulated maskers. In a study of the auditory cortex of the cat, Nelken et al. (1999) proposed that neurons which show envelope locking represent a neural correlate of CMR. This envelope locking disappeared when a test tone at high tone levels was added and the impairment of envelope locking indicated the presence of the tone. They found that the strength of envelope locking often increased with increasing masker bandwidth and that the difference in the detection threshold of the test tone between comodulated and unmodulated conditions increased with increasing bandwidth. However, this model is limited to a rather small percentage of cortical neurons. First, it requires envelope locking and, secondly, the envelope locking must be labile when adding a tone. This could be shown for only 45% of cat cortical neurons.

In contrast to Nelken et al. (1999), I analyzed the spike rate in response to the test tone and could demonstrate a neural correlate of CMR using this approach. Some neurons that showed a positive value of release from masking were additionally tested for their ability to lock to the temporal envelope by presenting a sinusoidally modulated band-pass masker similar to the masking paradigm of Nelken et al. (1999). The release from masking as analyzed in the present study could be correlated with the neurons' ability to lock to the envelope but did not require envelope locking. In this context, one also needs to keep in mind that envelope locking is strongly dependent on anaesthesia (review: Eggermont 2001). It could be possible that awake animals percept and extract the temporal information in comodulated maskers even at high modulation frequencies whereas single cortical neurons under anaesthesia do not show envelope locking at high modulation frequencies.

When a test tone is added to a comodulated masker, the envelope fluctuations are reduced in the frequency band corresponding to the test tone frequency. In addition, a constant high amplitude is found in this frequency band. This increase in energy in the signal channel could provide a within-channel cue that the neuron can exploit for improving signal detection in comodulated noise.

It is not clear whether the release from masking observed in the present study is generated at the level of the primary auditory cortex. Neuronal CMR has also been reported for neurons of the inferior colliculus of the anaesthetized chinchilla in a preliminary study (Henderson et al. 1999) and for neurons in the cochlear nucleus of anaesthetized guinea-pigs (Pressnitzer et al. 2001). Pressnitzer et al. (2001) observed a small average CMR (median 3.2 dB) mainly in certain types of neurons and proposed a simple neuronal circuit in the cochlear nucleus that could underlie the physiological responses they found. It seemed to be reasonable to search for a neural correlate at the cortical level, because acoustic tasks that are investigated in behavioral experiments require conscious perception of complex acoustic stimulation. Therefore, neural CMR should be represented at the cortical level. Indeed, it could be demonstrated that at the cortical level, the origin of auditory perception, the amount of release from masking is comparable to the behavioral CMR in the same species.

5.8 Outlook and open questions

The present study focused on the role of GABA_A-receptor mediated inhibition in cortical information processing. GABA_A receptors are appropriate to regulate fast components of inhibitory transmission. In addition, long-lasting inhibition mediated by the metabotropic GABA_B receptor could play an essential role in the timing of late responses and in the timing of rhythmic spike activity of neuronal networks. Simultaneous recordings of layer V pyramidal cells and thalamic neurons *in vivo* and *in vitro* before and during GABA_A- and GABA_B-receptor blockade could contribute to our understanding of the role of inhibition in thalamocortical recurrent networks.

It would be interesting to examine the role of silent neurons in cortical information processing. First, it could be investigated whether neurons that responded to pure tones only during blockade of inhibition are responsive to more complex sound, e.g., frequency-modulated sound. Most silent neurons were found in layer VI. Under the assumption that these neurons were pyramidal cells, these neurons are likely to project onto layer III cells of the contralateral A1. Therefore, a functional significance of these silent neurons could be the blockade or weakening of excitatory callosal transmission. It would be interesting to examine whether the application of bicuculline on layer V neurons results in an increase in activity in layer III neurons of the contralateral A1. Further, the physiological conditions under which contralateral projections are disinhibited in awake animals could be analyzed.

In this study, preliminary data suggest that the suppression observed in two-tone masking experiments is partially mediated by intracortical GABAergic inhibition. However, a combination of two-tone masking with simultaneous blockade of GABA receptors is necessary to conclusively test the role of intracortical and subcortical inhibition in masking experiments.

To determine the origin of comodulation masking release in the auditory system, CMR could be studied at different stages in the auditory pathway using identical stimulation paradigms in the same species. The present study demonstrated neural CMR on the basis of single unit analysis. CMR could also be explained by factors related to auditory grouping (Hall and Grose 1990). The

comodulation favors the integration of the masking noise bands into an auditory object that could be represented in the correlated activity of several neurons. This independent auditory object can be separated from the signal. One hypothesis is that neurons show a higher degree of coherent activity when stimulated with comodulated masking noise than with unmodulated masking noise and, thus, improving signal detection in the comodulated situation. This hypothesis could be tested by correlation analysis of simultaneously recorded cells.

6 References

Abeles M, Goldstein MH (1970) *Functional architecture in cat primary auditory cortex: Columnar organization and organization according to depth*. J. Neurophysiol. 33:172-187.

Avoli M, Mattia D, Siniscalchi A, Perreault P, Tomaiuolo F (1994) *Pharmacology and electrophysiology of a synchronous GABA-mediated potential in the human neocortex*. Neuroscience 62:655-666.

Barth DS, Di S (1990) *Three-dimensional analysis of auditory-evoked potentials in rat neocortex*. J. Neurophysiol. 64:1527-1536.

Brosch M, Schreiner CE (1997) *Time course of forward masking tuning curves in cat primary auditory cortex*. J. Neurophysiol. 77:923-943.

Brosch M, Schulz A, Scheich H (1999) *Processing of sound sequences in macaque auditory cortex: response enhancement*. J. Neurophysiol. 82:1542-1559.

Budinger E, Heil P, Scheich H (2000a) *Functional organization of auditory cortex in the Mongolian gerbil (Meriones unguiculatus). III. Anatomical subdivisions and corticocortical connections*. Eur. J. Neurosci. 12:2425-2451.

Budinger E, Heil P, Scheich H (2000b) *Functional organization of auditory cortex in the Mongolian gerbil (Meriones unguiculatus). IV. Connections with anatomically characterized subcortical structures*. Eur. J. Neurosci. 12:2452-2474.

Budinger E, Scheich H (2001) *Frequency-specific connections of Mongolian gerbil primary auditory field A1 revealed by double fluorescence and confocal laser scanning microscopy*. In: Elsner N, Kreutzberg GW (eds) Proceedings of the 4th meeting of the German Neuroscience Society 2001. Vol.2, Thieme, Stuttgart. #427.

Buus S (1985) *Release from masking caused by envelope fluctuations*. J. Acoust. Soc. Am. 78:1958-1965.

- Calford MB, Semple MN (1995) *Monaural inhibition in cat auditory cortex*. J. Neurophysiol. 73:1876-1891.
- Chagnac-Amitai Y, Connors BW (1989) *Horizontal spread of synchronized activity in neocortex and its control by GABA-mediated inhibition*. J. Neurophysiol. 61:747-758.
- Chen QC, Jen PH-S (2000) *Bicuculline application affects discharge patterns, rate-intensity functions, and frequency tuning characteristics of bat auditory cortical neurons*. Hear. Res. 150:161-174.
- Clarey JC, Barone P, Imig TJ (1992) *Physiology of thalamus and cortex*. In: Popper AN and Fay RR (eds) *The mammalian auditory pathway: Neurophysiology*. New York, Springer-Verlag, pp. 232-334.
- Cox CL, Metherate R, Weinberger NM, Ashe JH (1992) *Synaptic potentials and effects of amino acid antagonists in the auditory cortex*. Brain Res. Bull. 28:401-410.
- Crook JM, Kisvarday ZF, Eysel UT (1998) *Evidence for a contribution of lateral inhibition to orientation tuning and direction selectivity in cat visual cortex: reversible inactivation of functionally characterized sites combined with neuroanatomical tracing techniques*. Eur. J. Neurosci. 10:2056-2075.
- Durlach NI (1963) *Equalization and cancellation theory of binaural masking-level differences*. J. Acoust. Soc. Am. 35:1206-1218.
- Dykes RW, Landry P, Metherate R, Hicks TP (1984) *Functional role of GABA in cat primary somatosensory cortex: Shaping receptive fields of cortical neurons*. J. Neurophysiol. 52:1066-1093.
- Eggermont JJ (2001) *Between sound and perception: reviewing the search for a neural code*. Hear. Res. 157:1-42.
- Ehret G (1997) *The auditory cortex*. J. Comp. Physiol. 181:547-557.
- Fastl H (1993) *A masking noise for speech-intelligibility tests*. Proc. Acoust. Soc. Japan, TC Hearing, H93-70:1-6.
- Faulstich M, Kössl M (2000) *Evidence for multiple DPOAE components based upon group delay of the 2f1-f2 distortion in the gerbil*. Hear. Res. 140:99-110.

6 References

Festen J (1993) *Contributions of comodulation masking release and temporal resolution on the speech-reception threshold masked by interfering noise*. J. Acoust. Soc. Am. 94:1295-1300.

Fletcher H (1940) *Auditory patterns*. Rev. Mod. Phys. 12:47-65.

Gao WJ, Newman DE, Wormington AB, Pallas SL (1999) *Development of inhibitory circuitry in visual and auditory cortex of postnatal ferrets: immunocytochemical localization of GABAergic neurons*. J. Comp. Neurol. 409:261-273.

Hall JW and Grose JH (1990) *Comodulation masking release and auditory grouping*. J. Acoust. Soc. Am. 88:119-125.

Hall JW, Haggard MP, Fernandes MA (1984) *Detection in noise by spectro-temporal pattern analysis*. J. Acoust. Soc. Am. 76:50-56.

Havey DC, Caspary DM (1980) *A simple technique for constructing piggy back multibarrel electrodes*. Electroencephalogr. Clin. Neurophysiol. 48:249-251.

Hefti BJ, Smith PH (2000) *Anatomy, physiology, and synaptic response of rat layer V auditory cortical cells and effects of intracellular GABAA blockade*. J. Neurophysiol. 83:2626-2638.

Henderson JA, Hongzhe L, Sinex DG (1999) *Responses of inferior colliculus neurons to tones in comodulated and uncomodulated noise*. Soc. Neurosci. Abstr. 25:396.

Hicks TP (1983) *Antagonism of synaptic transmission in vivo: contributions of microiontophoresis*. Brain Behav. Evol. 22:1-12.

Horikawa J, Hosokawa Y, Kubota M, Nasu M, Taniguchi I (1996) *Optical imaging of spatiotemporal patterns of glutamatergic excitation and GABAergic inhibition in the guinea-pig auditory cortex in vivo*. J. Physiol. 497:629-638.

Imig TJ, Adrian HO (1977) *Binaural columns in the primary field (A1) of cat auditory cortex*. Brain Res. 138:241-257.

Imig TJ, Ruggero MA, Kitzes LM, Javel E, Brugge JF (1977) *Organization of auditory cortex in the owl monkey (Aotus trivirgatus)*. J. Comp. Neurol. 171:111-128.

- Jones EG (1993) *GABAergic neurons and their role in cortical plasticity in primates*. Cereb. Cortex 3:361-372.
- Kemmer M, Vater M (1997) *The distribution of GABA and glycine immunostaining in the cochlear nucleus of the mustached bat (Pteronotus parnellii)*. Cell Tissue Res. 287:487-506.
- Kittel M, Wagner E, Klump GM (2000) *Hearing in the gerbil (Meriones unguiculatus): Comodulation masking release*. Zoology 103 (Suppl. III):68.
- Klinke R, Kral A, Heid S, Tillein J, Hartmann R (1999) *Recruitment of the auditory cortex in congenitally deaf cats by long-term cochlear electrostimulation*. Science 285:1729-1733.
- Klug A, Pollak G (2000) *Responses of many IC neurons to complex stimuli can be predicted based on their excitatory and inhibitory tuning*. Abstracts of the 23th midwinter research meeting, Association for Research in Otolaryngology, # 883.
- Klump GM, Langemann U (1995) *Comodulation masking release in a songbird*. Hear. Res. 87:157-164.
- Klump GM, Nieder A (2001) *Release from masking in fluctuating background noise in a songbird's auditory forebrain*. Neuroreport 12:1-5.
- Kolston J, Osen KK, Hackney CM, Ottersen OP, Storm-Mathisen J (1992) *An atlas of glycine- and GABA-like immunoreactivity and colocalization in the cochlear nuclear complex of the guinea-pig*. Anat. Embryol. 186:443-465.
- Kyriazi HT, Carvell GE, Brumberg JC, Simons DJ (1996) *Quantitative effects of GABA and bicuculline methiodide on receptive field properties of neurons in real and simulated whisker barrels*. J. Neurophysiol. 75:547-560.
- Lamme VAF, Zipser K, Spekreijse H (1998) *Figure-ground activity in primary visual cortex is suppressed by anesthesia*. Proc. Natl. Acad. Sci. 95:3263-3268.
- Langemann U, Klump GM (1994) *Acoustic perception in birds: Can they profit from atmospheric turbulences to improve signal detection?* J. Orn. 135:422.
- Langemann U, Klump GM (2001) *Signal detection in amplitude-modulated maskers. I. Behavioural auditory thresholds in a songbird*. Eur. J. Neurosci. 13:1025-1032.

6 References

- Lisman JE (1997) *Bursts as a unit of neural information: making unreliable synapses reliable*. Trends Neurosci. 20:38-43.
- Liu CJ, Grandes P, Matute C, Cuenod M, Streit P (1989) *Glutamate-like immunoreactivity revealed in rat olfactory bulb, hippocampus and cerebellum by monoclonal antibody and sensitive staining method*. Histochemistry 90:427-445.
- Merzenich MM, Knight PL, Roth GL (1975) *Representation of cochlea within primary auditory cortex in the cat*. J. Neurophysiol. 38:231-249.
- Mitani A, Shimokouchi M, Itoh K, Nomura S, Kudo M, Mizuno N (1985) *Morphology and laminar organization of electrophysiologically identified neurons in the primary auditory cortex in the cat*. J. Comp. Neurol. 235:430-447.
- Moore BCJ (1992) *Across-channel processes in auditory masking*. J. Acoust. Soc Jpn. 13:25-37.
- Mott JB, McDonald LP, Sinex DG (1990) *Neural correlates of psychophysical release from masking*. J. Acoust. Soc. Am. 88:2682-2691.
- Mountcastle VB (1997) *The columnar organization of the neocortex*. Brain 120:701-722.
- Müller CM, Scheich H (1987) *GABAergic inhibition increases the neuronal selectivity to natural sounds in the avian auditory forebrain*. Brain Res. 414:376-380.
- Müller CM, Scheich H (1988) *Contribution of GABAergic inhibition to the response characteristics of auditory units in the avian forebrain*. J. Neurophysiol. 59:1673-1689.
- Nelken E, Rotman Y, Yosef OB (1999) *Responses of auditory cortex neurons to structural features of natural sound*. Nature 397:154-157.
- Nieder A, Klump GM (1999) *Adjustable frequency selectivity of auditory forebrain neurons recorded in a freely moving songbird via radiotelemetry*. Hear. Res. 127:41-54.
- Nieder A, Klump GM (2001) *Signal detection in amplitude-modulated maskers. II. Processing in the songbird's auditory forebrain*. Eur. J. Neurosci. 13:1033-1044.

- Oonishi S, Katsuki Y (1965) *Functional organization and integrative mechanism on the auditory cortex of the cat*. Japan. J. Physiol. 15:342-365.
- Parker AJ, Newsome WT (1998) *Sense and the single neuron: probing the physiology of perception*. Annu. Rev. Neurosci. 21:227-277.
- Pelleg-Toiba R, Wollberg Z (1989) *Tuning properties of auditory cortex cells in the awake squirrel monkey*. Exp. Brain Res. 74:353-364.
- Phillips DP, Irvine DR (1983) *Some features of binaural input to single neurons in physiologically defined area A1 of cat cerebral cortex*. J. Neurophysiol. 49:383-395.
- Pressnitzer D, Meddis R, Delahaye R, Winter IM (2001) *Physiological correlates of comodulation masking release in the mammalian ventral cochlear nucleus*. J. Neurosci. 16:1-10.
- Prieto JJ, Peterson BA, Winer JA (1994a) *Morphology and spatial distribution of GABAergic neurons in cat primary auditory cortex (A1)*. J. Comp. Neurol. 344:349-382.
- Prieto JJ, Peterson BA, Winer JA (1994b) *Laminar distribution and neuronal targets of GABAergic axon terminals in cat primary auditory cortex (A1)*. J. Comp. Neurol. 344:383-402.
- Recanzone GH, Schreiner CE, Merzenich MM (1993) *Plasticity in the frequency representation of primary auditory cortex following discrimination training in adult owl monkeys*. J. Neurosci. 13:87-103.
- Richards DG, Wiley RH (1980) *Reverberations and amplitude fluctuations in the propagation of sound in a forest: Implications for animal communication*. Am. Naturalist 115:381-399.
- Richter K, Hess A, Scheich H (1999) *Functional mapping of transsynaptic effects of local manipulations of inhibition in gerbil auditory cortex*. Brain Res. 831:184-199.
- Ryan AF (1976) *Hearing sensitivity of the mongolian gerbil (Meriones unguiculatus)*. J. Acoust. Soc. Am. 59:1222-1226.

6 References

Sally SL, Kelly JB (1988) *Organization of auditory cortex in the albino rat: Sound frequency*. J. Neurophysiol. 59:1627-1638.

Scheich H, Heil P, Langner G (1993) *Functional organization of auditory cortex in the mongolian gerbil (Meriones unguiculatus). II. Tonotopic 2-deoxyglucose*. Eur. J. Neurosci. 5:898-914.

Schooneveldt GP, Moore BCJ (1987) *Comodulation masking release (CMR): Effects of signal frequency, flanking-band frequency, masker bandwidth, flanking-band level, and monotic versus dichotic presentation of the flanking band*. J. Acoust. Soc. Am. 82:1944-1956.

Schooneveldt GP, Moore BCJ (1989) *Comodulation masking release (CMR) as a function of masker bandwidth, modulator bandwidth, and signal duration*. J. Acoust. Soc. Am. 85:273-281.

Schreiner CE, Mendelson JR (1990) *Functional topography of cat primary auditory cortex: distribution of integrated excitation*. J. Neurophysiol. 64:1442-1459.

Schreiner CE, Mendelson JR, Sutter ML (1992) *Functional topography of cat primary auditory cortex: representation of tone intensity*. Exp. Brain Res. 92:105-122.

Schulze H, Langner G (1999) *Auditory cortical responses to amplitude modulations with spectra above frequency receptive fields: evidence for wide spectral integration*. J. Comp. Physiol. 185:493-508.

Shamma SA, Symmes D (1985) *Patterns of inhibition in auditory cortical cells in awake squirrel monkeys*. Hear. Res. 19:1-13.

Shamma SA, Fleshman JW, Wiser PR, Versnel H (1993) *Organization of response areas in ferret primary auditory cortex*. J. Neurophysiol. 69:367-383.

Shen JX, Xu ZM, Yao YD (1999) *Evidence for columnar organization in the auditory cortex of the mouse*. Hear. Res. 137:174-177.

Sillito AM (1984) *Functional considerations of the operation of GABAergic inhibitory processes in the visual cortex*. In: Jones EG and Peters A (eds) *Cerebral Cortex*. Vol.2, Plenum, New York, pp. 91-114.

- Singer W, Gray CM (1995) *Visual feature integration and the temporal correlation hypothesis*. Annu. Rev. Neurosci. 18:555-586.
- Steriade M (1999) *Coherent oscillations and short-term plasticity in corticothalamic networks*. Trends Neurosci. 22:337-345.
- Steriade M, Contreras D (1998) *Spike-wave complexes and fast components of cortically generated seizures. I. Role of neocortex and thalamus*. J. Neurophysiol. 80:1439-1455.
- Suga N, Jen PHS (1976) *Disproportionate tonotopic representation for processing CF-FM sonar signals in the mustache bat auditory cortex*. Science 194:542-544.
- Suga N, Zhang Y, Yan J (1997) *Sharpening of frequency tuning by inhibition in the thalamic auditory nucleus of the mustached bat*. J. Neurophysiol. 77:2098-2114.
- Sugimoto S, Sakurada M, Horikawa J, Taniguchi I (1997) *The columnar and layer-specific response properties of neurons in the primary auditory cortex of Mongolian gerbils*. Hear. Res. 112:175-185.
- Supèr H, Spekreijse H, Lamme VA (2001) *Two distinct modes of sensory processing observed in monkey primary visual cortex (V1)*. Nat. Neurosci. 4:304-310.
- Sutter ML, Schreiner CE (1991) *Physiology and topography of neurons with multip peaked tuning curves in cat primary auditory cortex*. J. Neurophysiol. 65:1207-1226.
- Sutter ML, Schreiner CE, McLean M, O'Conner KN, Loftus WC (1999) *Organization of inhibitory frequency receptive fields in cat primary auditory cortex*. J. Neurophysiol. 82:2358-2371.
- Tamás G, Buhl EH, Lörincz A, Somogyi P (2000) *Proximally targeted GABAergic synapses and gap junctions synchronize cortical interneurons*. Nat. Neurosci. 3:366-371.
- Thomas H, Tillein J, Heil P, Scheich H (1993) *Functional organization of auditory cortex in the mongolian gerbil (Meriones unguiculatus). I*.

6 References

Electrophysiological mapping of frequency representation and distinction of fields. Eur. J. Neurosci. 5: 882-897.

Timofeev I, Grenier F, Steriade M (1998) *Spike-wave complexes and fast components of cortically generated seizures. IV. Paroxysmal fast runs in cortical and thalamic neurons.* J. Neurophysiol. 80:1495-1513.

Tremere L, Hicks TP, Rasmusson DD (2001) *Expansion of receptive fields in raccoon somatosensory cortex in vivo by GABA_A receptor antagonism: implications for cortical reorganization.* Exp. Brain Res. 135:447-455.

Vater M (1995) *Ultrastructural and immunocytochemical observations on the superior olivary complex of the mustached bat.* J. Comp. Neurol. 358:155-180.

Vater M, Hartmann H, Kössl M, Grothe B (1992) *The functional role of GABA and glycine in monaural and binaural processing in the inferior colliculus of horseshoe bats.* J. Comp. Physiol. 171:541-553.

Volkov IO, Galazjuk AV (1991) *Formation of spike response to sound tones in cat auditory cortex neurons: interaction of excitatory and inhibitory effects.* Neuroscience 43:307-321.

Wagner E, Klump GM (2001) *Comodulation masking release in Mongolian gerbils (Meriones unguiculatus) studied with narrow-band maskers.* In: Elsner N, Kreutzberg GW (eds) Proceedings of the 4th meeting of the German Neuroscience Society 2001. Vol.2, Thieme, Stuttgart. #415.

Wang J, Caspary DM, Salvi RJ (2000) *GABA-A antagonist causes dramatic expansion of tuning in primary auditory cortex.* Neuroreport 11:1137-1140.

Winer JA (1992) *The functional architecture of the medial geniculate body and the primary auditory cortex.* In: Popper AN and Fay RR (eds) *The mammalian auditory pathway: Neuroanatomy.* New York, Springer-Verlag, pp. 222-409.

Yajima Y, Hayashi Y (1990) *GABAergic inhibition upon auditory response properties of neurons in the dorsal cochlear nucleus of the rat.* Exp. Brain Res. 81:581-588.

Yang L, Pollak GD, Resler C (1992) *GABAergic circuits sharpen tuning curves and modify response properties in the mustache bat inferior colliculus.* J. Neurophysiol. 68:1760-1774.

7 Danksagung

Mein besonderer Dank gilt Prof. Manfred Kössl für die Überlassung des Themas und für die fortwährende Unterstützung während der gesamten Arbeit. Herzlichen Dank auch dafür, dass ich außerhalb dieser Arbeit am Kuba-Projekt mitwirken konnte.

Des weiteren gilt mein Dank Prof. Gerhard Neuweiler für hilfreiche Diskussionen innerhalb der Montagsseminare.

Prof. Georg Klump danke ich für die Generierung der akustischen Reize für das CMR-Projekt und für fruchtbare Diskussionen bei der Datenanalyse und der statistischen Auswertung.

Prof. Marianne Vater danke ich für die Einführung in immunocytochemische Techniken und für die Vorschläge zur Analyse der Daten.

Christoph Kapfer danke ich für seine Hilfsbereitschaft bei der computerunterstützten Analyse und Präsentation der immunocytochemischen Daten.

Einen herzlichen Dank an Claudia Schulte, die immer ein offenes Ohr für Freuden und Sorgen hatte und bereitwillig bei den aufreibenden Kleinigkeiten half.

Thomas Fenzl und Rudolph Marsch danke ich für die Durchsicht des Manuskripts.

Der gesamten Arbeitsgruppe danke ich für die hervorragende Arbeitsatmosphäre und für die gemeinsamen Freizeitaktivitäten.

Zuletzt danke ich meiner Familie und meinen FreundInnen, die mich auch in schwierigen Phasen immer unterstützt haben.

8 Lebenslauf

7. August 1972	geboren in München
1979-1983	Besuch der Grundschule in Söcking
1983-1992	Besuch des Gymnasiums Starnberg
1992-1997	Studium der Biologie an der Ludwig-Maximilians-Universität München
1996	Diplomhauptprüfungen in den Fächern Neurobiologie (Hauptfach), Zoologie, Genetik, Psychologie
1997	Diplomarbeit im Labor von Dr. M. Kössl. Thema: Innenohrmechanik bei der Fledermaus <i>Hipposideros lankadiva</i>
Januar 1998	Beginn der Promotion bei Dr. M. Kössl
Juli 1998/Juli 1999	Gastwissenschaftler der Universität von Havanna. Thema: Otoakustische Emissionen bei der Schnurrbartfledermaus
Juli 2000-Juni 2001	Stipendiatin im Rahmen des Dritten Hochschulsonderprogramms

Publikationen

- Foeller E, Kössl M (2000) Mechanical adaptations for echolocation in the cochlea of the bat *Hipposideros lankadiva*. J. Comp. Physiol. A 186:859-870.
- Kössl M, Foeller E, Faulstich M (2000) Otoacoustic emissions and cochlear mechanisms in echolocating bats. In: Thomas JA, Moss C, Vater M, (eds.), "Echolocation in bats and dolphins" Univ. of Chicago Press (im Druck).
- Foeller E, Vater M, Kössl M (2001) Laminar analysis of inhibition in the gerbil primary auditory cortex. JARO 2:279-296.